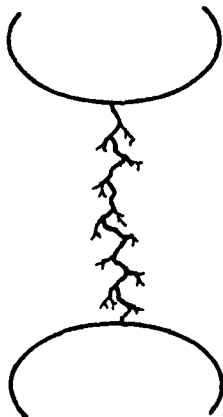


AD-A156 465

2

# AN INTRODUCTION TO ELECTRICAL BREAKDOWN IN DIELECTRICS

DTIC FILE COPY



T.L. Skvaren na

DTIC  
ELECTE  
JUL 12 1985  
S D  
E

This document has been approved  
for public release and sale; its  
distribution is unlimited.

85 06 25 083

## DISCLAIMER

The views and conclusions expressed in this document are those of the author. They are not intended and should not be thought to represent official ideas, attitudes, or policies of any agency of the United States Government. The author has not had special access to official information or ideas and has employed only open-source material available to any writer on this subject.

This document is the property of the United States Government. It is available for distribution to the general public. A loan copy of the document may be obtained from the Air University Interlibrary Loan Service (AUL/LDEX, Maxwell AFB, Alabama, 36112) or the Defense Technical Information Center. Request must include the author's name and complete title of the study.

This document may be reproduced for use in other research reports or educational pursuits contingent upon the following stipulations:

-- Reproduction rights do not extend to any copyrighted material that may be contained in the research report.

-- All reproduced copies must contain the following credit line: "Reprinted by permission of the Air Command and Staff College."

-- All reproduced copies must contain the name(s) of the report's author(s).

-- If format modification is necessary to better serve the user's needs, adjustments may be made to this report--this authorization does not extend to copyrighted information or material. The following statement must accompany the modified document: "Adapted from Air Command and Staff Research Report \_\_\_\_\_ (number) \_\_\_\_\_ (title) by \_\_\_\_\_ (author) \_\_\_\_\_."

-- This notice must be included with any reproduced or adapted portions of this document.



**REPORT NUMBER** 85-2470

**TITLE** AN INTRODUCTION TO ELECTRICAL BREAKDOWN  
IN DIELECTRICS

**AUTHOR(S)** MAJOR TIMOTHY L. SKVARENINA, USAF

**FACULTY ADVISOR** MAJOR ALLAN K. BEAN, ACSC/EDOWD

**SPONSOR** DR. ROBERT E. FONTANA, AFIT/ENG

Submitted to the faculty in partial fulfillment of  
requirements for graduation.

**AIR COMMAND AND STAFF COLLEGE**  
**AIR UNIVERSITY**  
**MAXWELL AFB, AL 36112**

This document has been approved  
for public release and sales in  
distribution is unlimited.

UNCLASSIFIED

SECURITY CLASSIFICATION OF THIS PAGE

## REPORT DOCUMENTATION PAGE

1a. REPORT SECURITY CLASSIFICATION <b>UNCLASSIFIED</b>		1b. RESTRICTIVE MARKINGS	
2a. SECURITY CLASSIFICATION AUTHORITY		3. DISTRIBUTION/AVAILABILITY OF REPORT	
2b. DECLASSIFICATION/DOWNGRADING SCHEDULE			
4. PERFORMING ORGANIZATION REPORT NUMBER(S) <b>85-2470</b>		5. MONITORING ORGANIZATION REPORT NUMBER(S)	
6a. NAME OF PERFORMING ORGANIZATION <b>ACSC/EDCC</b>	6b. OFFICE SYMBOL (If applicable)	7a. NAME OF MONITORING ORGANIZATION	
6c. ADDRESS (City, State and ZIP Code) <b>Maxwell AFB AL 36112</b>		7b. ADDRESS (City, State and ZIP Code)	
8a. NAME OF FUNDING/SPONSORING ORGANIZATION	8b. OFFICE SYMBOL (If applicable)	9. PROCUREMENT INSTRUMENT IDENTIFICATION NUMBER	
8c. ADDRESS (City, State and ZIP Code)		10. SOURCE OF FUNDING NOS	
11. TITLE (Include Security Classification) <b>AN INTRODUCTION TO ELECTRICAL</b>		PROGRAM ELEMENT NO.	PROJECT NO.
		TASK NO.	WORK UNIT NO.
12. PERSONAL AUTHOR(S) <b>Skvarenina, Timothy L., Major, USAF</b>			
13a. TYPE OF REPORT	13b. TIME COVERED FROM _____ TO _____	14. DATE OF REPORT (Yr., Mo., Day) <b>1985 April</b>	15. PAGE COUNT <b>282</b>
16. SUPPLEMENTARY NOTATION  <b>ITEM 11: BREAKDOWN IN DIELECTRICS</b>			
17. COSATI CODES		18. SUBJECT TERMS (Continue on reverse if necessary and identify by block number)	
FIELD	GROUP	SUB GR.	
19. ABSTRACT (Continue on reverse if necessary and identify by block number)			
<p>This report was written to serve as a text for an introductory graduate course in high voltage engineering at the Air Force Institute of Technology. However, anyone with an undergraduate electrical engineering or physics degree should be able to understand it, if they so desire. The material presented falls into three sections. The first part discusses the basics of kinetic theory of gases, atomic structure, ionization, mobility, diffusion, and electron emission. The second portion covers gas breakdown and the characteristics of the glow, corona, and arc discharges. The final portion provides a very brief introduction to breakdown in vacuum, liquids, and solids. Numerous references to the literature are provided.</p>			
20. DISTRIBUTION/AVAILABILITY OF ABSTRACT <b>UNCLASSIFIED/UNLIMITED</b> <input type="checkbox"/> SAME AS RPT <input checked="" type="checkbox"/> DTIC USERS <input type="checkbox"/>		21. ABSTRACT SECURITY CLASSIFICATION <b>UNCLASSIFIED</b>	
22a. NAME OF RESPONSIBLE INDIVIDUAL <b>ACSC/EDCC Maxwell AFB AL 36112</b>		22b. TELEPHONE NUMBER (Include Area Code) <b>(205) 293-2483</b>	22c. OFFICE SYMBOL



## PREFACE

This book is the result of my experiences during three years of teaching the Pulsed Power curriculum in the Graduate Electrical Engineering Program at the Air Force Institute of Technology (AFIT). While teaching a course in high voltage engineering, I was continually faced with a lack of a suitable textbook which would remain in print or not be too expensive for the student. I hope this text will fill that void not only for future classes at AFIT, but also for individuals who find themselves working in the area without the benefit of formal coursework.

Although the title of the course was High Voltage Engineering, I titled this work, "An Introduction to Electrical Breakdown Phenomena," because breakdown may occur at low voltages when spacecraft systems are considered. I have included those aspects of breakdown which I believe provide the student with a background for a study of the various types of switches encountered in pulsed power systems. Others such as power system engineers should find the book useful as well. Since the book is written by an engineer, and intended to be read by engineers, much of the basic physics, underlying the phenomena of interest, has been omitted or presented in somewhat simplistic terms. Each chapter of this book has been the subject of numerous journal articles and texts, and, as much as possible, I have referenced them.

The material presented falls into three sections. Chapters two through five discuss the basics of kinetic theory of gases, atomic structure, ionization, mobility, diffusion, and electron emission, all of which are essential to understanding the different types of gas discharges. I have found students often consider this material to be somewhat tedious because it requires them to recall a great deal of their early chemistry and physics. However, this material is important, and I have tried to point out the importance of the topics by referencing the later chapters. Another difficulty with this material is the subject of units. Much of the early work was done in CGS, some in MKS, and some in mixed units. I have used the units which seem to be most common in the literature and have tried to be explicit as to what the units are. An appendix includes many useful constants and conversion factors.

The second portion of the text includes chapters six through nine and covers breakdown in gases and the characteristics of the different types of discharges. The glow and arc discharges occur in some of the most important types of switches, while corona is a problem which must always be considered when working with high voltage systems. Generally, I have found that students find this material more interesting than the first section

The remainder of the text, chapters 10 - 12, considers breakdown phenomena in dielectrics other than gas; that is, vacuum, liquid, and solid. Each of these type media finds use in pulsed power systems, not only in switches but also as insulation. Thus, it is desirable to understand how to keep them from breaking down.

The amount of time spent covering the material in this text is, of course, a function of how much detail the instructor desires to go into. Most of the material was covered in approximately twenty, standard fifty minute class periods; however, there is enough to build a four quarter hour or three semester hour course.

Accession For	
NTIS GRA&I	<input checked="" type="checkbox"/>
DTIC TAB	<input type="checkbox"/>
Unannounced	<input type="checkbox"/>
Justification	
By	
Distribution/	
Availability Codes	
Dist	Avail and/or Special
A-1	



## CONTENTS

Preface . . . . .	iii
Figures . . . . .	ix
Tables. . . . .	.xiii

### CHAPTER 1 - INTRODUCTION

1.1 Historical Overview . . . . .	1
1.2 Technical Overview. . . . .	5
1.2.1 Energy . . . . .	5
1.2.2 Power. . . . .	7
1.2.3 Pulsed Power . . . . .	9
1.2.3.1 Systems Using Capacitive Energy Storage . . . . .	10
1.2.3.2 System Using Inductive Energy Storage . . . . .	12
1.3 Summary . . . . .	14
References . . . . .	15

### CHAPTER 2 - FUNDAMENTALS

2.1 Electromagnetic Fields. . . . .	17
2.1.1 Field Enhancement Factors. . . . .	18
2.2.2 Space Charge Effects . . . . .	22
2.2.3 Multiple dielectrics . . . . .	23
2.2 Kinetic Theory of Gases . . . . .	26
2.2.1 Nature of an Ideal Gas . . . . .	26
2.2.2 Maxwell-Boltzmann Speed Distribution . . . . .	27
2.2.2.1 Particle Density. . . . .	28
2.2.2.2 Velocity Density. . . . .	28
2.2.2.3 Temperature . . . . .	33
2.2.2.4 Pressure. . . . .	33
2.3 Atomic Structure and Radiation. . . . .	35
2.3.1 The Bohr Model of the Hydrogen Atom. . . . .	36
2.3.2 Absorption and Emission of Energy. . . . .	37
References . . . . .	41

### CHAPTER 3 - EXCITATION AND IONIZATION PROCESSES

3.1 Introduction. . . . .	43
3.2 Collisions. . . . .	45
3.2.1 Electron-Gas Molecule Collisions . . . . .	45
3.2.1.1 Collision Parameters. . . . .	47
3.2.1.2 Excitation and Ionization of Gas Molecules . . . . .	54
3.2.1.3 Electron Attachment . . . . .	58

## CONTENTS

3.2.2 Collisions between Gas Molecules . . . . .	59
3.3 Thermal Ionization. . . . .	61
3.4 Photoionization . . . . .	62
3.5 Deionization. . . . .	66
3.6 Summary . . . . .	67
References . . . . .	67

## CHAPTER 4 - MOTION OF PARTICLES

4.1 Introduction. . . . .	69
4.2 Mobility. . . . .	69
4.3 Diffusion . . . . .	75
4.4 Ambipolar Diffusion . . . . .	77
4.5 Summary . . . . .	78
References . . . . .	79

## CHAPTER 5 - ELECTRON EMISSION FROM SOLIDS

5.1 Introduction. . . . .	81
5.2 The Theory of Electrons in Metals . . . . .	82
5.2.1 Fermi-Dirac Statistics . . . . .	83
5.2.2 Electron Band Theory . . . . .	85
5.2.3 A Metal-Vacuum Boundary. . . . .	88
5.3 Thermionic Emission . . . . .	91
5.4 Schottky Emission . . . . .	92
5.5 Field Emission. . . . .	94
5.6 Photoelectric Emission. . . . .	95
5.7 Emission by Particle Bombardment. . . . .	98
5.7.1 Emission by Electron Bombardment . . . . .	99
5.7.2 Emission by Positive Ion Bombardment . . . . .	101
5.8 Summary . . . . .	102
References . . . . .	103

## CHAPTER 6 - BREAKDOWN IN GASES

6.1 Introduction. . . . .	105
6.2 Townsend's First Ionization Coefficient . . . . .	108
6.3 Townsend's Second Ionization Coefficient. . . . .	115
6.4 Sparking Voltage - Paschen's Law. . . . .	120
6.5 Alternate Theories of Breakdown . . . . .	126
6.5.1 Time Lags for Breakdown. . . . .	126
6.5.2 The Streamer Theory. . . . .	128
6.5.3 Statistical Nature of Electrical Breakdown . . . . .	132
6.6 Non-Uniform Field Breakdown . . . . .	133
6.7 Surface Flashover . . . . .	136
6.8 Summary . . . . .	139
References . . . . .	139

## CONTENTS

### CHAPTER 7 - THE GLOW DISCHARGE

7.1	Introduction. . . . .	141
7.2	Phenomena . . . . .	143
7.2.1	The Visual Phenomena . . . . .	145
7.2.2	Variation of Pressure or Tube Length . . . . .	148
7.2.3	Normal and Abnormal Glow . . . . .	150
7.3	Grid Control of Glow Discharges . . . . .	153
7.4	Summary . . . . .	156
	References . . . . .	156

### CHAPTER 8 - CORONA

8.1	Introduction. . . . .	157
8.2	Negative Point Corona . . . . .	159
8.2.1	Theory of the Trichel Pulse. . . . .	161
8.2.2	Physical Appearance of Negative Corona . . . . .	165
8.3	Positive Point Corona . . . . .	166
8.3.1	Theory of Positive Corona. . . . .	170
8.3.2	Appearance of Positive Point Corona. . . . .	172
8.4	Detection and Control of Corona . . . . .	173
8.5	Partial Discharge in Solids and Liquids . . . . .	174
8.6	Summary . . . . .	175
	References . . . . .	176

### CHAPTER 9 - THE ARC DISCHARGE

9.1	Introduction. . . . .	177
9.2	General Characteristics . . . . .	179
9.3	The Regions of the Arc. . . . .	182
9.3.1	Cathode. . . . .	182
9.3.2	Positive Column. . . . .	185
9.3.3	Anode. . . . .	186
9.4	Oscillations in DC Arcs . . . . .	188
9.5	AC Arcs . . . . .	190
9.6	Summary . . . . .	192
	References . . . . .	193

### CHAPTER 10 - BREAKDOWN IN VACUUM

10.1	Introduction . . . . .	195
10.2	Pre-Breakdown Conduction . . . . .	197
10.3	Factors Affecting the Breakdown Voltage. . . . .	199
10.3.1	Electrode Separation . . . . .	200
10.3.2	Electrode Material, Finish, and Conditioning . . . . .	201
10.3.3	Electrode Area . . . . .	205
10.3.4	Time Effects . . . . .	206

## CONTENTS

10.4	Breakdown Hypotheses . . . . .	212
10.4.1	Particle Exchange. . . . .	212
10.4.2	Electron Beam. . . . .	213
10.4.3	Clump. . . . .	214
10.5	Summary. . . . .	216
	References . . . . .	217
CHAPTER 11 - BREAKDOWN IN LIQUIDS		
11.1	Introduction . . . . .	219
11.2	Conduction in Liquids. . . . .	220
11.3	Breakdown Theories . . . . .	222
11.3.1	Bubble Breakdown . . . . .	223
11.3.2	Liquid Globule Breakdown . . . . .	224
11.3.3	Solid Particle Breakdown . . . . .	224
11.3.4	Electronic Breakdown . . . . .	225
11.4	Summary. . . . .	225
	References . . . . .	226
CHAPTER 12 - BREAKDOWN IN SOLIDS		
12.1	Introduction . . . . .	227
12.2	Breakdown Mechanisms . . . . .	231
12.3.1	Intrinsic Breakdown. . . . .	231
12.3.2	Electromechanical Breakdown. . . . .	232
12.3.3	Avalanche or Streamer Breakdown. . . . .	233
12.3.4	Thermal Breakdown. . . . .	234
12.3.5	Erosion Breakdown. . . . .	235
12.3	Factors Affecting Breakdown. . . . .	235
12.4	Summary. . . . .	236
	References . . . . .	236
APPENDIX - Useful Constants and Conversion Factors. . . . .		237
INDEX . . . . .		239

## FIGURES

Figure 1-1:	Generic pulsed power system. . . . .	9
Figure 1-2:	Basic pulse generator using capacitive energy storage. . . . .	11
Figure 1-3:	Basic pulse generator using inductive energy storage. . . . .	13
Figure 2-1:	Simple point to plane electrode system . . . . .	18
Figure 2-2:	Microprojection on an Electrode Surface. . . . .	22
Figure 2-3:	Effect of space charge on the electric field . . . . .	23
Figure 2-4:	Two dielectric insulation (a) and the equivalent circuit (b) . . . . .	24
Figure 2-5:	Molecular position space . . . . .	29
Figure 2-6:	Molecular velocity space . . . . .	29
Figure 2-7:	Typical shape of Maxwell-Boltzmann speed distribution . . . . .	31
Figure 2-8:	Maxwell-Boltzmann speed distributions for conditions as shown. . . . .	32
Figure 2-9:	Calculation of gas pressure by momentum transfer to the container walls. . . . .	34
Figure 2-10:	Illustration of the spectral series of the hydrogen atom . . . . .	38
Figure 2-11:	Energy states for the hydrogen atom . . . . .	39
Figure 3-1:	The collision volume of an electron moving through a gas. . . . .	48
Figure 3-2:	Probabilities of collision for several gases (after Brode, 1933). . . . .	50
Figure 3-3:	Distribution of electron free paths. . . . .	52
Figure 3-4:	Cross section for excitation of helium as a function of electron energy (after VonEngel, 1965,p.47) . . . . .	56
Figure 3-5:	Probability of ionization for helium (after VonEngel, 1965, p.63). . . . .	56
Figure 3-6:	Probabilities of single and multiple ionization for mercury (after Bleakney, 1930, p.139). . . . .	57
Figure 3-7:	Curves showing the ionization of a gas, as predicted by Saha's equation for various values of pressure and ionization potential . . . . .	63
Figure 3-8:	Photoabsorption cross sections for (a) helium and (b) argon. . . . .	65
Figure 4-1:	An electron subjected to an electric field . . . . .	70
Figure 4-2:	A swarm of electrons between two electrodes. . . . .	72
Figure 4-3:	Electron drift velocities for several gases (after Christophorou and Hunter, 1983) . . . . .	74
Figure 5-1:	The Fermi-Dirac distribution for $T=0^{\circ}\text{K}$ and $T=300^{\circ}\text{K}$ . . . . .	84
Figure 5-2:	Sketch showing how energy levels split as the inter-atomic separation decreases: (a) an insulator and (b) a metal (after Azaroff and Brophy, 1963, p.180) . . . . .	87
Figure 5-3:	Potential energy diagram at a metal-vacuum interface for several conditions. . . . .	89

## FIGURES

Figure 5-4:	Curves showing the form of the Richardson-Dushman equation. (a) saturation current (b) temperature saturation . . . . .	93
Figure 5-5:	Curve showing thermionic current as a function of the electric field for fixed temperature. Dotted line shows field saturation. Solid line shows enhancement due to Schottky effect . . . .	94
Figure 5-6:	Typical photoelectric yield as a function of wavelength . . . . .	98
Figure 5-7:	Secondary electron yield as a function of primary electron energy. . . . .	100
Figure 5-8:	Distribution of secondary electron energies. . .	100
Figure 6-1:	A uniform field, two electrode system. . . . .	106
Figure 6-2:	Current-voltage characteristic for the system of figure 6-1. . . . .	106
Figure 6-3:	Generation of an electron avalanche. . . . .	109
Figure 6-4:	Relative densities of electrons and positive ions in a gap (after VonEngel, 1965, p.173). . .	111
Figure 6-5:	Curves of $\ln[I(d)/I_0]$ vs $d$ for air for various values of $E/p$ (after Llewellyn-Jones and Parker, 1952). . . . .	112
Figure 6-6:	Curves of $\ln[I(d)/I_0]$ vs $d$ for nitrogen for various values of $E/p$ (after Dutton, et al, 1952) .	112
Figure 6-7:	Diagram illustrating secondary emission. . . . .	118
Figure 6-8:	Breakdown voltage between parallel plates for several gases (after Dunbar, 1966, p.40) . . . .	121
Figure 6-9:	Sparking voltage for hydrogen in the vicinity of the Paschen minimum for various cathodes. . .	124
Figure 6-10:	Paschen curves for neon-argon gas mixtures (after Penning, 1931) . . . . .	125
Figure 6-11:	Development of a cathode directed streamer. . .	129
Figure 6-12:	Development of an anode directed streamer . . .	131
Figure 6-13:	Schematic breakdown curves for a point to plane gap . . . . .	134
Figure 6-14:	RMS breakdown voltage between planes, rods, and points in nitrogen (after Dunbar, 1966, p. 86). . . . .	135
Figure 6-15:	Edge treatment of a parallel plate transmission line to eliminate flashover . . . . .	137
Figure 7-1:	A discharge tube and the voltage as a function of current over several orders of magnitude of current . . . . .	142
Figure 7-2:	Characteristics of the glow discharge: (a) visual appearance; (b) light intensity; (c) voltage; (d) electric field; (e) net charge density; (f) positive and negative charge densities; (g) electron and positive ion current densities. . . . .	144
Figure 7-3:	Paschen type breakdown curve for the system of figure 7-1. . . . .	152
Figure 7-4:	Three electrode, gas filled tube . . . . .	154



## FIGURES

Figure 8-1:	Characteristic shape of Trichel pulse and variation of frequency with voltage (after Trichel, 1938) . . . . .	160
Figure 8-2:	Variation of pulse frequency with point diameter (after Trichel, 1938) . . . . .	160
Figure 8-3:	Variation of pulse frequency with gas pressure (after Trichel, 1938). . . . .	161
Figure 8-4:	Negative point corona modes as a function of voltage and pressure-distance product (after Loeb, 1965, p. 393). . . . .	162
Figure 8-5:	Schematic illustration of the movement of space charges in negative point corona: (a) early in the Trichel pulse; (b) late in the pulse (after Trichel, 1938). . . . .	163
Figure 8-6:	Physical appearance of negative point corona (after Loeb, 1948) . . . . .	166
Figure 8-7:	Voltage-current characteristic for positive point corona (after Kip, 1938) . . . . .	167
Figure 8-8:	Forms of positive point corona observed by Kip with an oscilloscope: (a) two bursts; (b) a streamer followed by a short burst; (c) streamer followed by a long burst. The decay of the streamers was dragged out by the oscilloscope time constant (Loeb, 1965, p.80) . . . . .	169
Figure 8-9:	Positive point corona modes as a function of voltage and electrode separation (after Loeb, 1965, p. 94) . . . . .	169
Figure 8-10:	Physical appearance of pre-onset streamers in positive point corona. Dimensions are for 760 torr (after Loeb, 1948) . . . . .	172
Figure 9-1:	Variation of voltage and current for a sudden application of a voltage above the breakdown voltage. . . . .	178
Figure 9-2:	Temperature variation with pressure of the positive column plasma components. . . . .	181
Figure 9-3:	Regions of the arc discharge: (a) typical visual appearance; (b) potential distribution. . . . .	181
Figure 9-4:	Schematic illustration of the variation of arc voltage with current . . . . .	183
Figure 9-5:	Retrograde motion of the cathode spot due to a transverse magnetic field. . . . .	186
Figure 9-6:	Variation of temperature, illumination, and current density across the diameter of the positive column (after Brown, 1966, p.241) . . . . .	187
Figure 9-7:	Illustration of the dynamic characteristics of a DC arc subjected to sinusoidal perturbations of varying frequencies (after Cobine, 1957, p. 345). . . . .	189
Figure 9-8:	Current and voltage waveforms for the positive half-cycle of an AC arc (after Cobine, 1957, p. 348). . . . .	191

## FIGURES

Figure 9-9:	Voltage-current characteristic of an AC arc (after Cobine, 1957, p. 349) . . . . .	191
Figure 10-1:	Sketch of a cathode whisker formed by a high electric field at the cathode surface . . . . .	198
Figure 10-2:	Current and voltage waveforms for a 1.0 mm vacuum gap between steel electrodes (after Mulcahy and Bolin, 1971, p. 3-6). . . . .	199
Figure 10-3:	Vacuum breakdown voltage as a function of gap length for copper and aluminum electrodes (after Meek and Craggs, 1978, p.130). . . . .	201
Figure 10-4:	Variation of breakdown voltage with the number of breakdowns (Mulcahy and Bolin, 1971, p.4-14) . . . . .	202
Figure 10-5:	Effect of surface contamination on vacuum breakdown voltage (after Denholm, et al, 1973 p. 363) . . . . .	205
Figure 10-6:	Breakdown Voltage vs Electrode Area . . . . .	206
Figure 10-7:	Vacuum breakdown voltage as a function of gap length for AC, DC, and 1.2/50 impulse voltages (after Denholm, 1958) . . . . .	207
Figure 10-8:	Time required for a 7.5 mm vacuum gap to breakdown for a range of applied voltages (after Mulcahy and Bolin, 1971, p. 4-20). . . . .	207
Figure 10-9:	Particle exchange mechanism of vacuum breakdown (after Alston, 1968, p. 76) . . . . .	213
Figure 10-10:	Electron beam theory of vacuum breakdown (a) vaporization at the anode (b) vaporization at the cathode (after Alston, 1968 pgs. 77-81). . . . .	214
Figure 10-11:	Clump hypothesis of vacuum breakdown (a) clump in the anode surface (b) clump flying across the gap (c) clump exploding at cathode surface (after Alston, 1968, p. 82). . . . .	215
Figure 11-1:	Schematic illustration of the increase in current with electric field for a liquid (after Alston, 1968, p. 115). . . . .	221
Figure 12-1:	Schematic illustration of the variation . . . . . of the breakdown strength of a solid as a function of the time the voltage is applied (after Kuffel and Abdullah, 1971 p.79)	232

## TABLES

Table 1-1:	Comparison of Energy Storage Techniques. . . .	8
Table 2-1:	Field Enhancement Factors for Several Geometries . . . . .	21
Table 2-2:	Ionization Potentials of Several Elements (Gray, 1957, p.7-14) . . . . .	40
Table 3-1:	Differential Ionization Constant for Electrons (Cobine, 1957, p. 80). . . . .	57
Table 3-2:	Typical Molecular Diameters and Mean Free Paths. . . . .	60
Table 5-1:	Emission Constants of Materials. . . . .	86
Table 5-2:	Common Logarithms of Field Emission Current Density (Dolan, 1953). . . . .	96
Table 6-1:	Values of the Coefficients A AND B for Various Gases (VonEngel, 1965, p. 181) . . . . .	115
Table 6-2:	Minimum Sparking Voltage Between Steel Parallel Plate Electrodes for Several Gases (Dunbar, 1966, pgs. 40-41) . . . . .	123
Table 7-1:	Characteristic Glow Discharge Colors for a Number of Gases (Brown, 1966, p. 214). . . . .	149
Table 10-1:	Vacuum Breakdown Voltages for Several Electrode Materials (Anderson, 1935) . . . . .	203
Table 10-2:	Breakdown Voltage for Different Surface Finishes (Denholm, et al, 1973, p. 365). . . . .	204
Table 10-3:	Factors and Effects in Vacuum Insulation (after Mulcahy and Bolin, 1971 p. 4-36). . . . .	209
Table 12-1:	Properties of interest for solid insulation (after Denholm, et al, 1973, p.301). . . . .	228
Table 12-2:	Factors Affecting The Breakdown Voltage of Solids (Denholm, 1973, p.317). . . . .	235

# CHAPTER 1

## INTRODUCTION

In some ways the understanding of electrical breakdown of dielectrics is very mature, but in other ways it is not. Many of the fundamental phenomena were first observed over a century ago, and theories were developed as long as 40-100 years ago. However, during the last 20 years, as measuring equipment and computational facilities improved, additional observations were made and the theories refined. This chapter provides the reader with a brief historical perspective and an introduction to pulsed power.

### 1.1 Historical Overview

Since the dawn of time, man has observed and marveled at electrical discharges through the atmosphere in the forms of lightning and the Auroras Borealis and Australis (Northern and Southern Lights). Today scientists recognize these as very different forms of gas discharges. Lightning is essentially an arc discharge at one atmosphere pressure, while the Auroras are glow-like discharges occurring at very low pressure in the upper atmosphere. (Penning, 1957, p.1)

The road to understanding electrical breakdown in dielectrics has been a long one--one which is intertwined with many

important advances in atomic physics. The ancient Greeks (600 B.C.) were aware that a rubbed piece of amber would attract bits of straw, but it was Sir William Gilbert in 1600 who first introduced the term electricity. By 1733, French researchers recognized two types of electricity. Benjamin Franklin defined the electricity on a glass rod rubbed with silk as positive and that on a hard rubber rod rubbed with fur as negative. In 1745, the Leyden jar was invented, and transient sparks could be obtained. Franklin deduced that lightning was essentially the same as the Leyden jar spark, and proved it with his famous kite experiment in 1752. Around the turn of the 1800s, the low voltage arc was discovered by Humphrey Davy using a voltaic pile. Despite these early successes, few measurements could be taken and relatively little fundamental knowledge resulted. The more productive experiments were to be those which operated in the low pressure regime. (Hirsh and Oskam, 1978, pgs.1-18)

In the 1830s, Faraday discovered the characteristic striations of the glow discharge (see Figure 7-2a, p.144), and in 1878 de la Rue and Muller published photographic studies of the low pressure discharge. Pluckner discovered "cathode rays" in 1858 which became the subject of intense research. In 1879, Sir William Crookes stated his belief that cathode rays constituted a "fourth state of matter" and prophesized they would help solve "the greatest scientific problems of the future." His prophecy proved correct as much of the theory of modern physics resulted from gas discharge experiments. (Von Engel, 1965, p.2)

In 1885, Balmer discovered the spectral lines of the hydrogen discharge and deduced a formula to predict them. Later, Bohr used the information to develop his atomic model. In 1883, the photoelectric effect was discovered, and Roentgen "accidentally" discovered x-rays in 1895 while working with discharge experiments. However, despite the advances made using the discharges, it was not until the first quarter of this century that considerable progress was made in understanding the actual discharges. (Penning, 1957, p.2)

J.J. Thomson and, later, one of his students, John Townsend, became the leaders in gas discharge research, and much experimental data became available. By the late 1920s, however, equipment sensitivity reached the point that contamination of the gases and electrode surfaces began to mask the results, making correlation of experiments and theories impossible. During the 1930s and 1940s, several reference books (Loeb, 1939; Cobine, 1941; and Thomson and Thomson, 1932) were published. Even today, they serve as excellent introductions to the subject area. Loeb and his students continued the investigation of the various discharges, resulting in a thorough cataloging (Loeb, 1955, 1960, 1965) of their physical phenomena. Eventually technology improved, and today's physicists are attempting to match their theories with experimental results. (Hirsch and Oskam, 1978, P.1-18)

The primary goal of this book is for the reader to understand the fundamental phenomena and theories of electrical break-

down necessary to work with pulsed power. Therefore, it is appropriate to again backup and consider how pulsed power came about. Readers whose interest lies in high voltage for electric power distribution may wish to skip to section 1.3 on page 14.

Pulsed power had its genesis in World War II. The development of radar shortly before and during the war required new types of power supplies. These power supplies were required to supply pulses of high voltage and/or current with very short pulse widths and at high repetition rates. The power supplies were given the name "pulse generators" and their output eventually became known as "pulsed power."

Following the war, the Radiation Laboratory of MIT prepared a series of volumes describing the technologies developed by various U.S. and British laboratories in support of the radar effort. Volume V (Glasoe and Lebacqz, 1948) of the series was entitled "Pulse Generators," and it is still considered "the bible" for pulsed power. For several years, radar was the principle application of pulsed power, but eventually other applications were found.

Today, pulsed power engineers are called upon to provide still shorter, higher rep-rate pulses in support of such applications as: particle accelerators, nuclear weapon effects simulation, electromagnetic propulsion, laser pumping, and fusion reactor research. Two conferences are devoted to current applications of pulsed power. The first is the Power Modulator Symposium (originally called the Hydrogen Thyratron Symposium) which

began in 1950 and is now held in even numbered years. The second is the International Pulsed Power Conference which began in 1976 and is now held in odd numbered years. The bibliography to this chapter contains a listing of the Proceedings of both conferences.

The next section provides a brief introduction to pulsed power and highlights why an understanding of electrical breakdown is important to the pulsed power engineer. For further details, the reader should consult Glasoe and Lebacqz.

## 1.2 Technical Overview

This section introduces the concepts of energy, power, and pulsed power; then, two types of pulsed power systems are examined to illustrate some of the applications of electrical breakdown theory in pulsed power engineering.

### 1.2 1 Energy

Energy is defined as the capacity of a system to do work. Energy may be kinetic--a truck traveling down the highway has kinetic energy--or it may be potential--a pond of water on top of a hill. Potential energy is the most important aspect of energy for our concern since it can be stored for use when needed. The pond of water could be drained through a turbine at the bottom of the hill which in turn could drive a generator to produce electricity. The kinetic energy of the truck, on the other hand, is generally not very useful; although, in the case of an electrically driven truck, one might recharge the batteries as the vehicle decelerated.



A second important point about energy is it exists in many forms and can be changed from one form to another. Forms of energy include heat, light, mechanical, electric field, magnetic field, and chemical. Various pulsed power systems have used the last four types, which will be discussed in more detail after consideration is given to units.

The unit assigned to represent energy is different in each system. Examples include BTUs, calories, ergs in the CGS system, joules in the MKS system, and even oil barrel equivalents. The only unit which will be used in this text is the joule, abbreviated "J", or its multiples--kilojoule ( $1\text{KJ} = 10^3\text{J}$ ) and megajoule ( $1\text{MJ} = 10^6\text{J}$ ). The megajoule is a commonly encountered quantity, and it is enlightening to consider several examples. One MJ is approximately the kinetic energy of a 5000 lb truck traveling 60 miles per hour. It is also the energy required to boil away a quart of room temperature water, and it is the energy contained in 1/2 lb of high explosive.

As will be seen later, energy storage is a key component of all pulsed power systems. Electric fields (capacitive energy storage) and magnetic fields (inductive energy storage) are by far the most commonly used types of energy storage; however, some systems have used rotating mass (flywheel) or chemical energy storage. In a capacitor, energy is stored in the electric field in the dielectric and is given by  $CV^2/2$  where C is the capacitance in farads and V the voltage in volts. Similarly, in an inductor, energy is stored in the magnetic field and is given

by  $LI^2/2$  where  $L$  is the inductance in henries and  $I$  the current in amps. Chemical energy storage can be in the form of a battery where the chemical reaction produces electricity directly, or it may be in the form of explosives. In the latter case, the explosive energy is usually converted to kinetic energy of a conductor which is then converted to electricity. Finally, a fly-wheel stores kinetic energy which can be converted to electricity and is given by  $J\omega^2/2$  where  $J$  is the inertia constant and  $\omega$  is the angular velocity of rotation.

One factor which is important in choosing the type of energy storage is the energy density, i.e. how much energy can be stored per unit mass or volume. Table 1-1 (Kristiansen and Schoenbach, 1982) shows a comparison of energy densities for the four types of energy storage. From the table, it may be noted capacitive storage offers the lowest densities; however, capacitive storage is the most frequently used. Clearly, other factors must influence the selection. One such other factor, the time to deliver the energy, is shown in the table and will be discussed in the Section 1.2.3. Other components in the system may also affect the choice of energy storage technique and will also be discussed in Section 1.2.3. Before considering a typical pulsed power system, we should consider what we mean by power.

#### 1.2.2 Power

Power is defined as the rate at which energy is consumed. In other words, the total energy delivered to a load, divided by the time required to deliver it, yields the average power.

Table 1-1: Comparison of Energy Storage Techniques

Type	Energy/Volume (MJ/m <sup>3</sup> )	Energy/Weight (J/Kg)	Timescale to Deliver to Load
Capacitors	0.01-1.0	300-500	$\mu$ sec
Inductors			
Conventional	3.0-5.0	$10^2$ - $10^3$	$\mu$ sec-msec
Cryogenic	10-30	"	"
Superconducting	20-40	"	"
Chemical			
Batteries	2000	$10^6$	minutes
Explosives	6000	$5 \times 10^6$	$\mu$ sec
Inertial	400	$10^4$ - $10^5$	seconds

As with energy, there are a variety of units such as horsepower and watts (W). Sticking with the MKS system, 1 watt could represent 1 joule delivered in a 1 sec pulse. However, if that same joule was delivered in 1  $\mu$ sec, the average power during the pulse would be 1 MW. Finally, if 1 MJ was delivered in 1  $\mu$ sec, the power during the pulse would be 1 terrawatt (1 TW =  $10^{12}$ W).

At this point, the reader is probably wondering, "What is the meaning of 1 TW?" To put it in perspective, the total electrical generating capability in the United States in 1982 was nearly 600 gigawatts (GW) or 0.6 TW (Elgerd, 1982). Clearly, it would be impossible to "plug in" a load requiring 1 TW. Realistically, it wouldn't be feasible to directly connect even a 1 GW load. Several of the previously mentioned applications require

power levels on the order of terrawatts. Since they can't be fed directly, other types of power supplies must be used.

### 1.2.3 Pulsed Power

From the previous two sections, the reader may already have an idea of what a pulsed power system does. In general, the goal of pulsed power is to use energy storage and switching techniques to deliver power levels to a load which might not be achieved directly. Figure 1-1 shows a generic pulsed power system.

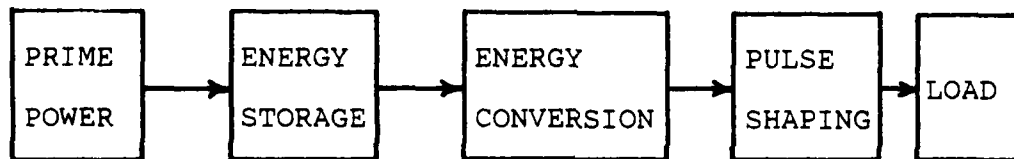


Figure 1-1: Generic pulsed power system.

Energy is provided to some type of storage device from a prime power source (electric utility, generator, etc.). This is normally done over a time which is much longer than the pulse-length required by the load in order to keep the prime power supply size to a minimum. Once the required energy has been stored, it can be converted to electrical form and discharged to the load. Generally, this requires some type of switching and pulse shaping. Briefly stated then, the objective of a pulse generator is to achieve power multiplication by storing energy over a rela-

tively long time and delivering it in the form of a very short pulse. Two things should be noted. First, if the pulselength is a microsecond, then a millisecond is a relatively long time. Second, it is entirely possible, and often necessary, to use two or more stages of energy storage and power compression.

Having established the potential power level, we should consider what it means in terms of voltage and current. Recall that instantaneous electric power is defined as the product of voltage and current. Obviously, if the power is in the GW or TW range, the voltage or current (probably both) must be very high. In most pulsed power supplies, high voltage presents a real problem which requires careful design and construction to avoid breakdown where it is not desired. Also the switches used to deliver the energy to the load must undergo a transition from a non-conducting state to a conducting state, or vice-versa. To understand how these high power switches operate, one must be familiar with electrical breakdown and discharges. This aspect will be examined in more detail in the next two sections.

#### 1.2.3.1 Systems Using Capacitive Energy Storage

Capacitors are the most commonly used energy storage devices for pulsed power systems for two reasons. First, they can deliver their energy very quickly, yielding high peak powers. This is shown in the last column of table 1-1. Second, the switches used are much further advanced than those required for inductive energy

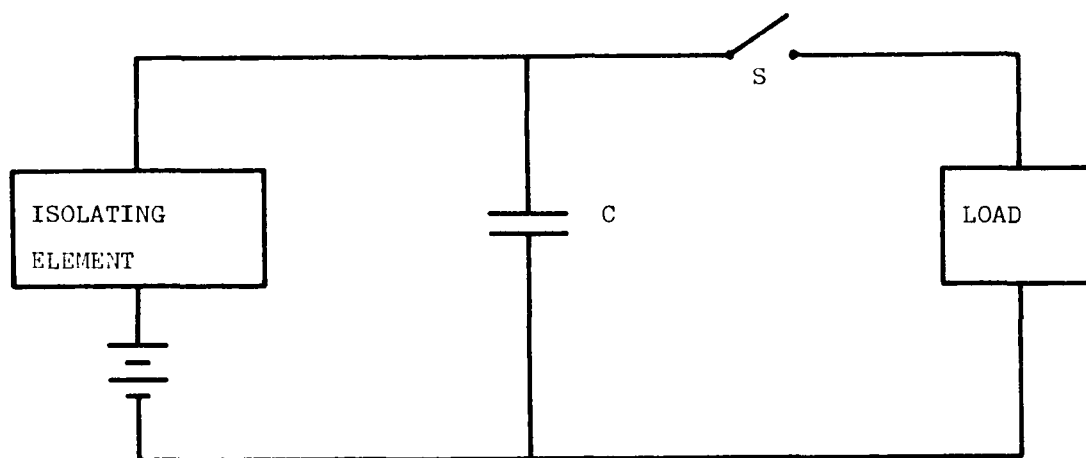


Figure 1-2: Basic pulse generator using capacitive energy storage.

storage. Figure 1-2 shows a basic system. The capacitor<sup>1</sup> is charged from a power supply through an isolating element. The isolating element may be simply a resistor or an inductor and diode. Its purpose is twofold. First, the isolating element controls the rate at which the capacitor is charged; that is, it limits the size of the prime power supply. If a resistor,  $R$ , is used, the capacitor is said to be resistively charged, and the time constant for charging is  $RC$ . Likewise, if the capacitor is inductively charged through an inductor,  $L$ , the time constant is  $(LC)^{0.5}$ . Increasing  $R$  or  $L$  increases the charging time and reduces the peak power drawn from the supply.

---

<sup>1</sup>The capacitor may in fact be a bank of capacitors connected in parallel-series combinations

The second purpose of the isolating element is to isolate the prime power supply from the discharge circuit. The time constant of the discharge circuit will be much smaller than that of the charging circuit in order to obtain the desired power multiplication. Thus, the discharge will be over before the charging current changes very much.

When the capacitor is charged, its energy is delivered to the load by closing switch S. When the switch is in the open state, it must hold off the entire capacitor bank voltage (possibly 100s of KV). When closed, it must carry the current to the load (possibly many KAs) with a minimum voltage drop across the switch. These requirements lead to highly specialized switches. Unlike the wall switches we are all familiar with, most pulsed power switches are capable of opening or closing, but not both. Most conduct current through some type of electric discharge; hence, an understanding of electrical breakdown is crucial to the pulsed power engineer. Excellent reviews of switching capabilities in the Free World and the Soviet Union are given in Burkes, et al, 1978 and Burkes, et al, 1984, respectively.

#### 1.2.3.2 Systems Using Inductive Energy Storage

Inductive energy storage is very attractive because of the immense energy densities which are possible (Table 1-1). Unfortunately, as will be seen, switching presents a formidable problem. Figure 1-3 shows a basic system.

In this case, the inductor is charged from the power supply through switch S1. The resistance, R, may only be the stray

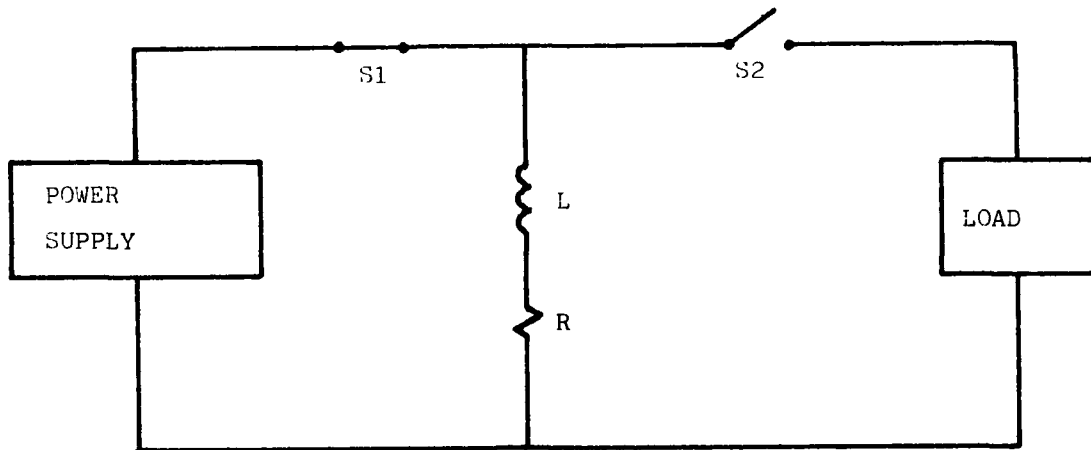


Figure 1-3: Basic pulse generator using inductive energy storage.

resistance in the circuit, and the time constant is  $L/R$ . Once the inductor is charged, the energy is delivered to the load by opening switch  $S1$  and simultaneously closing  $S2$ . Note that as the current is diverted into the load, any inductance in the load circuit will cause a large  $L(di/dt)$  voltage which will appear across  $S1$ . This voltage will try to reclose the switch. Unfortunately, at present, the only opening switches capable of carrying more than a few KAs are single shot devices. For this reason, inductive storage systems have not been used extensively. Because of the potential of inductive storage to achieve very high energy densities, researchers are actively pursuing a rep-rated opening switch (Kristiansen and Schoenbach, 1981, 1982)



1.3 Summary

Although electrical breakdown has been actively investigated for over two hundred years, it is by no means a dead issue. Physicists today are actively studying the various discharges, attempting to correlate experimental results with theory. Engineers face new challenges as they build systems to operate at higher and higher power and voltage levels. This chapter has presented a brief historical overview and an introduction to pulsed power, which is one application of electrical breakdown theory.

**REFERENCES :**

- Burkes, T.R., et al (1978). A Critical Analysis and Assessment of High Power Switches. US Naval Surface Weapons Center Report No. NP30/78, Dahlgren, VA 22448.
- Burkes, T.R., et al (1984). Switches for Directed Energy Weapons. An Assessment of Switching Technology in the USSR. US Army Foreign Science and Technology Center Contract No. DAAK21-82-C-0111, Charlottesville, VA.
- Cobine, J.D. (1941). Gaseous Conductors. McGraw-Hill, New York.
- Elgerd, O.I. (1982). Electric Energy Systems Theory (2nd ed.). McGraw-Hill, New York.
- Glasoe, G.N. and Lebacqz, J.V. (ed) (1948). Pulse Generators. McGraw-Hill, New York. Also reprinted by Dover Publications, 1965, New York.
- Hirsh M.N. and Oskam, H.J. (ed) (1978). Gaseous Electronics. Academic Press, New York.
- Kristiansen, M. and Schoenbach, K. (ed) (1981). Workshop on Repetitive Opening Switches. Tamarron, CO, 28-30 Jan. DTIC AD # A110770.

Kristiansen, M. and Schoenbach, K. (ed) (1981). Workshop on Diffuse Discharge Opening Switches. Tamarron, CO, 13-15 Jan, DTIC AD # A115883.

Loeb, L.B. (1939). Fundamental Processes of Electrical Discharges in Gases. John Wiley & Sons, New York.

Loeb, L.B. (1955). Basic Processes of Gaseous Electronics. University of California Press, Berkeley.

Loeb, L.B. (1960). Basic Processes of Gaseous Electronics (2nd edition). University of California Press, Berkeley.

Loeb, L.B. (1965). Electrical Coronas. University of California Press, Berkeley.

Penning, F.M. (1957). Electrical Discharges in Gases. Mac Millan, New York

Thomson, J.J. and Thomson, G.P. (1932). The Conduction of Electricity through Gases (2 vols). Cambridge University Press, Cambridge.

VonEngel, A. (1965). Ionized Gases. Clarendon Press, Oxford.

## OTHER SOURCES :

The thyatron and modulator symposiums were originally sponsored by the US Army Signal R&D Laboratory (now known as the Electronics R&D Command). Since 1973, the symposiums have been sponsored by the IEEE in cooperation with the DOD Advisory Group on Electron Devices. Some of the proceedings are available as follows:

Proc. of the 5th Symp. on Hydrogen Thyratrons and Modulators (1958) DTIC AD # 650899.

Proc. of the 6th Symp. on Hydrogen Thyratrons and Modulators (1960) DTIC AD # 254102.

Proc. of the 7th Symp. on Hydrogen Thyratrons and Modulators (1962) DTIC AD # 296002.

Proc. of the 8th Symp. on Hydrogen Thyratrons and Modulators (1964) DTIC AD # 454991.

Proc. of the 9th Modulator Symposium (1966) DTIC AD # 651694.

Proc. of the 10th Modulator Symposium (1968) DTIC AD #676854.

Conf. Record of the 1973 11th Power Modulator Symposium. IEEE 73 CH 0773-2 ED.

Conf. Record of the 1976 12th Power Modulator Symposium. IEEE 76 CH 1045-4 ED.

Conf. Record of the 1978 13th Power Modulator Symposium. IEEE 78 CH 1371-4 ED.

Conf. Record of the 1980 14th Pulse Power Modulator Symposium IEEE 80 CH 1573-5 ED. Also DTIC AD #A119663.

Conf. Record of the 1982 15th Power Modulator Symposium. IEEE 82 CH 1785-5. Also DTIC AD #A119664.

Conf. Record of the 1984 16th Power Modulator Symposium. IEEE 84 CH 2056-0.

The International Pulsed Power Conference was begun in 1976 by Texas Tech University under the sponsorship of the IEEE. The first two were held in Lubbock, Texas. The last two were in Albuquerque, and the next one will be in Washington DC in June 1985.

Proc. IEEE Intern. Pulsed Power Conf., 1976, IEEE 76CH1147-8.

Dig. of Tech. Papers, 2nd IEEE Pulsed Power Conf., 1979, IEEE 79 CH 1505-7.

Dig. of Tech. Papers, 3rd IEEE Pulsed Power Conf., 1981, IEEE 81 CH 1662-6.

Dig. of Tech. Papers, 4th IEEE Pulsed Power Conf., 1983, IEEE 83 CH 1908-3.

## CHAPTER 2

### FUNDAMENTALS

The study of electrical breakdown requires knowledge of a wide range of topics in physics, chemistry, and electrical engineering. This chapter begins with a brief introduction to several aspects of electromagnetic field theory which are particularly important in determining breakdown voltages. Then, elements of the kinetic theory of gases, atomic structure, and emission and absorption of radiation are briefly reviewed. These topics are important in understanding the actual mechanisms of electrical breakdown in gases.

#### 2.1 Electromagnetic Fields

An understanding of basic electromagnetic field theory is an essential prerequisite to the study of electrical breakdown. Therefore, it is assumed the reader is familiar with Maxwell's equations in their integral and differential forms. However, there are several concepts of electromagnetic field theory which are especially important in determining when a dielectric will breakdown. These include local field enhancement, space charge effects, and the effects of multiple dielectrics. Since these concepts are so important, they will be covered in this section.

## 2.1.1 Field Enhancement Factors (Denholm, et al, 1972, pgs.6-17)

Many factors enter into the determination of the breakdown voltage of a dielectric material or system. Included among these are the type(s) of material(s), the shape and length of the voltage pulse, the rep-rate, and electric field geometry. The last is particularly important since breakdown is dependent on the maximum electrical stress rather than the average. For example, Figure 2-1 shows a simple point to plane gap with an applied voltage of 5 KV and a gap length of 1 cm. The average electric field can be defined as the potential difference between the electrodes, divided by the minimum separation between them--in this case 5 KV/cm or 500KV/m. We will see in Chapter 6 that this would normally not be enough to breakdown atmospheric air; however, depending on the "sharpness" of the point, the local field may be substantially higher than the average. This

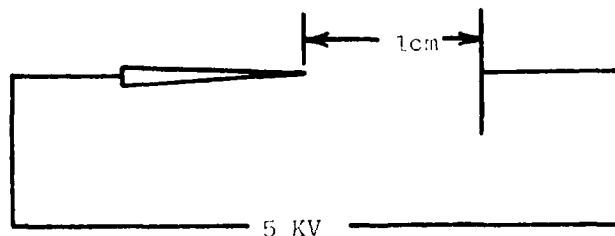


Figure 2-1: Simple point to plane electrode system.

intensification of the local field may cause corona (see Chapter 8) or an arc (Chapter 9) to form. To prevent breakdown where it is not wanted, the field must be graded as uniformly as possible. Two quantities, known as field enhancement factors, give an indication of how uniform the field is.

For a general two electrode structure, the first field enhancement factor,  $F_1$ , is defined as the maximum field strength divided by the average field strength. The average field strength is defined as previously indicated. The maximum field strength normally occurs on the electrode with the smallest radius of curvature (the point in Figure 2-1). The factor,  $F_1$ , gives an indication of how much stronger the peak electric field strength is than it would be for parallel plates with the same voltage and separation. As an example, consider a two electrode system consisting of two coaxial cylinders of radius  $r$  and  $R$  where  $R > r$ . If a voltage,  $V$ , is applied to the electrodes, the average field,  $E_{avg}$ , will be  $V/(R-r)$ . It is left as an exercise for the reader to show the maximum electric field,  $E_{max}$ , is given by  $V/r[\ln(R/r)]$ . Thus  $F_1$  is given by

$$F_1 = \frac{R-r}{r \ln \frac{R}{r}} = \frac{\frac{R}{r} - 1}{\ln \frac{R}{r}} \quad (2.1)$$

The expression for  $F_1$  tells us the field is non-uniform, but it does not say what to do. A second factor,  $F_2$ , can be derived from  $F_1$  and can be used to reduce the non-uniformity.

The factor  $F_2$  is defined as the product  $pF_1$ , where  $p$  is the ratio of the maximum system dimension to the minimum electrode separation. This factor essentially normalizes  $F_1$  to the overall system size, and it always has a minimum value. At this minimum, the maximum field strength has its lowest possible value for the particular geometry, voltage, and overall system size.

For the coaxial electrodes,  $p$  is equal to  $R/(R-r)$ . Then  $F_2$  is given by

$$F_2 = \frac{R}{R-r} \frac{R-r}{r \ln(R/r)} = \frac{R/r}{\ln(R/r)} = \frac{x}{\ln(x)} \quad (2.2)$$

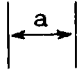
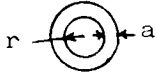
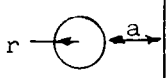
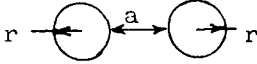
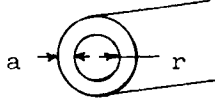

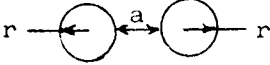
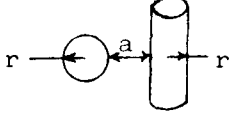
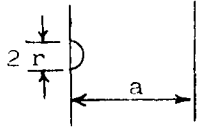
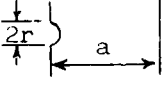
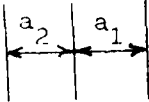
The minimum value for  $F_2$  can be found by differentiating it with respect to  $x$ , setting the derivative equal to zero, and solving for  $x$ . Doing this yields

$$x = R/r = e = 2.718... \quad (2.3)$$

This means the maximum field will have its lowest possible value when the ratio of conductor radii is  $e$ .

While the coaxial cylinder case is easy to calculate, other fairly simple geometries require the use of obscure coordinate systems. Table 2-1 (Denholm, et al, 1972, p.7) gives approximate formulas for  $F_1$  for several cases. Many real life electrode configurations can be approximated in terms of them. Microprojections on electrodes (see Figure 2-2) are often very important in determining when a set of electrodes will breakdown. It has been shown that  $F_1$  may reach values in excess of 1000 depending on the dimensions of the projection (Alston, 1968, p.101). It will be seen in later chapters that the surface condition of the electrodes may significantly affect the breakdown voltage.

Table 2-1: Field Enhancement Factors for Several Geometries

Configuration		Formula for $F_1$
Two parallel plane plates		1
Two concentric spheres		$(r+a)/r$
Sphere and plane plate		$0.9(r+a)/r$
Two spherical electrodes		$0.45(2r+a)/r$
Two coaxial cylinders		$a/[r \ln(r+a)/r]$
Cylinder parallel to plane plate		$0.9a/[r \ln(r+a)/r]$
Two parallel cylinders		$0.45a/[r \ln(2r+a)/2r]$
Two perpendicular cylinders		$0.45a/[r \ln(2r+a)/2r]$
Hemisphere on one parallel plate		3 ; $(a \gg r)$
Semicylinder on one parallel plate		2 ; $(a \gg r)$
Two dielectrics between parallel plates ( $a_1 > a_2$ )		$a\epsilon_1/(a_1\epsilon_2 + a_2\epsilon_1)$



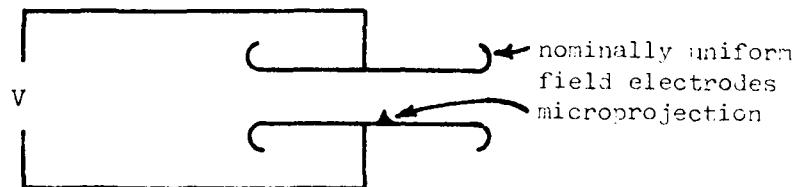


Figure 2-2: Microprojection on an Electrode Surface.

### 2.1.2 Space Charge Effects

The presence of space charge may also significantly affect the breakdown voltage because it distorts the electric field. Figure 2-3a shows a set of parallel plate electrodes with a voltage applied. Figure 2-3b shows the uniform electric field which exists between the electrodes assuming no space charge is present. If a space charge is present between the electrodes, the electric field will be distorted. Figure 2-3c shows a positive space charge in the vicinity of the cathode. This space charge causes the field, shown in Figure 2-3d, to be intensified at the cathode and weakened at the anode. The exact effect depends, of course, on the amount and distribution of the space charge.

Space charge effects are extremely important both in the initiation of breakdown and in determining the effects observed during the discharge. In particular, ionization and electron emission are affected by space charge, as are the phenomena associated with the glow, arc, and corona discharges.

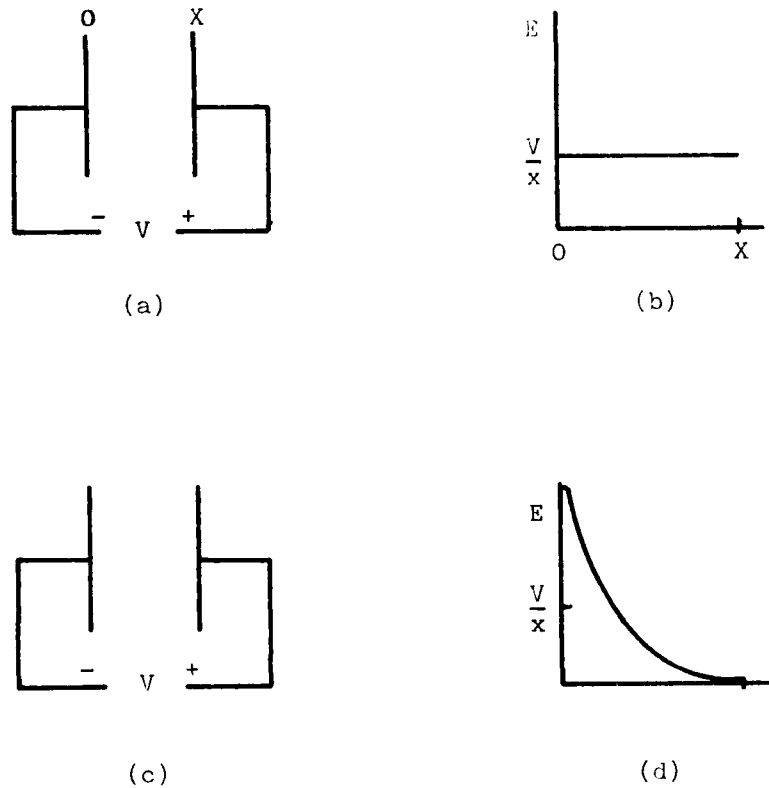


Figure 2-3: Effect of space charge on the electric field.

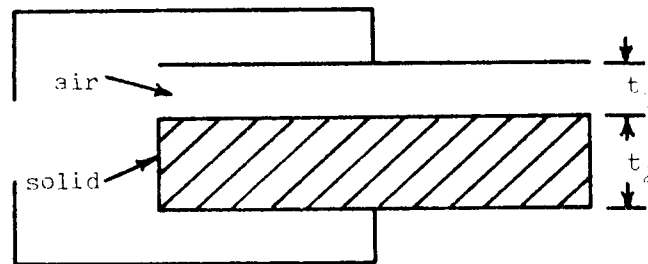
### 2.1.3 Multiple Dielectrics

Quite often the insulation between two conductors or electrodes consists of more than one type of insulation, each having a different dielectric strength. Examples include the insulation in parallel plate transmission lines, the dielectrics in high voltage capacitors, and transformer bushings. This can cause a problem, because the electric field will be higher in the material with the lower dielectric strength.

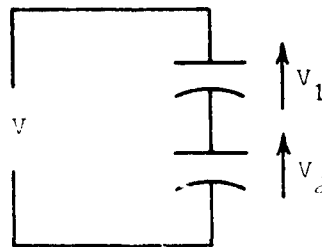
Consider the system, shown in Figure 2-4a, consisting of two electrodes, a solid dielectric, and an airgap. Such a system could represent a solid dielectric capacitor, with the airgap representing any imperfections. More importantly, it will illustrate the difficulty which may arise.

The system could be represented by two capacitors in series, as shown in Figure 2-4b. If  $V_1$  is the voltage across the solid dielectric and  $V_2$  that across the airgap, then the voltage between the two electrodes is

$$V = V_1 + V_2 \quad (2.4)$$



(a)



(b)

Figure 2-4: Two dielectric insulation (a) and the equivalent circuit (b)

The electric fields in the two sections are then given by

$$E_1 = V_1/t_1 \text{ and } E_2 = V_2/t_2 \quad (2.5)$$

From field theory

$$E_1 \epsilon_1 = E_2 \epsilon_2 \quad (2.6)$$

where  $\epsilon_1$  and  $\epsilon_2$  are the relative dielectric constants. Substitution of (2.5) and (2.6) into (2.4) yields

$$V = E_2 \left( t_1 \frac{\epsilon_2}{\epsilon_1} + t_2 \right)$$

or

$$V = V_2 \left( \frac{\epsilon_2 t_1}{\epsilon_1 t_2} + 1 \right) \quad (2.7)$$

If the relative dielectric constant,  $\epsilon_2$ , is 1.0 then

$$V_2 = \frac{V}{\frac{t_1}{t_2 \epsilon_1} + 1} \quad (2.8)$$

Equation 2.8 says that if  $\epsilon_1$  is large, then a substantial portion of the voltage appears across the airgap (Dunbar, 1965, pgs 9-13). This conclusion is extremely important for high voltage equipment. If the airgap represents a small air bubble in a dielectric, it is possible for the bubble to be over stressed and to breakdown. This phenomena is known as partial discharge (corona) and will be discussed in Chapter 8.

An understanding of electrical breakdown requires an understanding of the magnitude of the electric field. Often, the dielectric is a gas, and the kinetic theory of gases becomes very important to the breakdown process.

## 2.2 Kinetic Theory of Gases

The conduction of electricity through gases is extremely important to pulsed power engineers and to electric power system engineers. The overwhelming majority of switches used in pulsed power systems are gas filled, and power system engineers are largely concerned with atmospheric breakdown. As a result, the majority of this text is concerned with gas discharges. In order to understand what determines the type of discharge and the characteristics of the different discharges, one must have a basic understanding of the behavior of the gas.

It is assumed the reader has been exposed to the kinetic theory of gases; however, since that exposure is part of the distant past for most engineers, this section will review some of the basics. Chapters 3 and 4 will cover collisions within the gas and motion through the gas respectively.

### 2.2.1 Nature of an Ideal Gas (Cobine, 1957, p.1)

The classical kinetic theory of gases makes several assumptions about the nature of a gas. A gas is a state of matter in which the density of molecules is sufficiently low that the molecules can move freely within the container holding the gas. The molecules are idealized as small, elastic spheres in continual random motion. As a result of their motion, the molecules collide with one another and the walls of the container. These collisions are assumed to be elastic; that is, momentum and kinetic energy are conserved. It is further assumed the dimensions of the molecule are negligible compared to the distance traveled

between collisions and the molecule is not subject to any force during its travel.

These assumptions work rather well for the noble gases which have essentially spherical molecules, but are somewhat less exact for non-symmetrical molecules (any polyatomic one for example). Similarly, not all collisions are elastic. In some collisions, kinetic energy is converted into internal energy of the molecule, resulting in excitation or ionization. These collisions will be described in Chapter 3.

For now, we need to have a way to describe the state of the gas, one which does not require us to know the location and velocity of every molecule. This is vital because there are  $2.687 \times 10^{19}$  molecules/cm<sup>3</sup> in any gas at 1 atmosphere pressure and 0°C. The way to do this, of course, is to treat the gas statistically.

### 2.2.2 Maxwell-Boltzmann Speed Distribution

As molecules collide, their velocities change in accordance with conservation of energy and momentum. Physically, it is reasonable that, at any given instant, some molecules will be essentially stationary, while others will have very high speeds. However, we would expect most velocities to be somewhere in between the extremes. Maxwell and Boltzmann independently determined the distribution of velocities using very different techniques. The result is given the name "Maxwell-Boltzmann distribution function." Cobine, (1957, p.9) provides Maxwell's derivation

which is considerably simpler than Boltzmann's. We will limit our discussion to the essential concepts.

#### 2.2.2.1 Particle Density

Consider a gas composed of  $N_0$  molecules in a container. At time  $t$ , each molecule has a position given by its coordinates,  $x_1$ ,  $x_2$ , and  $x_3$  (see Figure 2-5). The particle density is defined as the number of molecules per cubic meter, and may be a function of position and time. It is denoted as  $N(\tilde{x}, t)$  where  $\tilde{x}$  is the position at which we are measuring the density. The density will be constant over an incremental distance,  $dx$ . Therefore, if an incremental volume, denoted  $dx^3$ , is chosen at position  $\tilde{x}$ , then the total number of particles in the incremental volume is  $Ndx^3$ . The total number of molecules is found by integrating the density over the entire volume

$$N_0 = \iiint N(\tilde{x}, t) dx^3 \quad (2.9)$$

#### 2.2.2.2 Velocity Distribution (Delcroix, 1960, pgs 25-27)

For the particle density, we assigned each molecule to a location in position space. We can do the same thing for velocities. That is, we can define a three dimensional velocity space and assign each molecule, from some incremental volume, to a location given by its velocity components,  $v_1$ ,  $v_2$ , and  $v_3$ , as shown in Figure 2-6. Note the vector from the origin to point "p" has a magnitude "c" which is the scalar speed of the molecule.<sup>1</sup> All of the molecules having speeds between  $c$  and  $c+dc$  will lie within

---

<sup>1</sup>Unfortunately, "c" is commonly used in the literature for speed. It should not be confused with the speed of light.

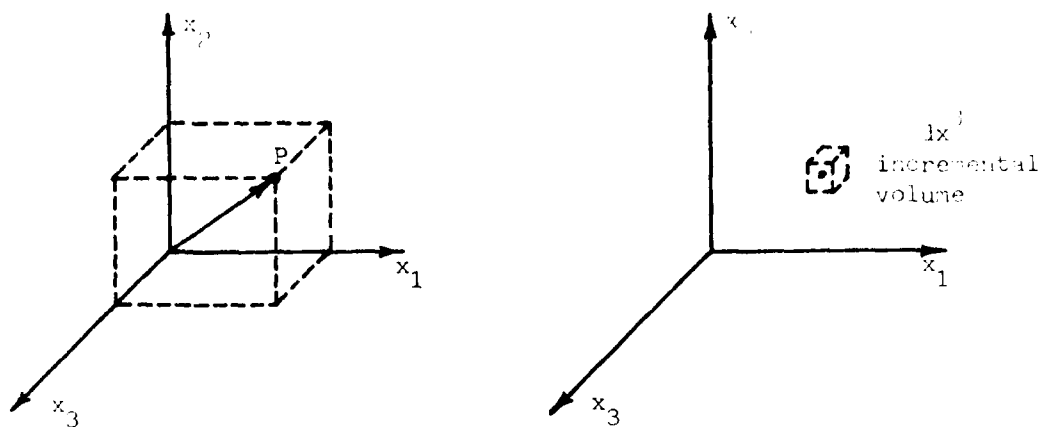


Figure 2-5: Molecular position space.

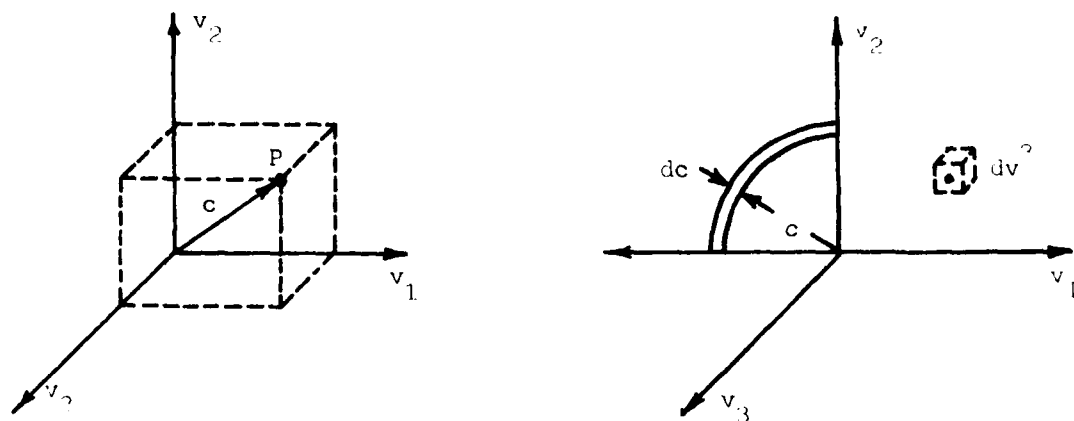


Figure 2-6: Molecular velocity space.



a thin spherical shell, shown in the third quadrant of the  $x_1x_2$  plane in Figure 2-6. The "velocity density" will be a function not only of  $\tilde{v}$  and time, but also of position, and is designated  $f(\tilde{x}, \tilde{v}, t)$ . The number of molecules in an incremental velocity space volume,  $dv^3$ , is

$$dN = f(\tilde{x}, \tilde{v}, t) dv^3 \quad (2.10)$$

The density at the position  $\tilde{x}$  may then be recovered by integrating 2.10 over all velocity space

$$N(\tilde{x}, t) = \iiint f(\tilde{x}, \tilde{v}, t) dv^3 \quad (2.11)$$

If the velocity density is a function of position, the gas is said to be inhomogeneous. The velocity density is said to be isotropic, if it is a function only of the scalar speed; that is, if it is constant throughout the spherical shell of Figure 2-6. If the velocity density varies throughout the shell, it is called anisotropic. If a gas is initially inhomogeneous or anisotropic, the collisions of the molecules will tend to make it become homogeneous and isotropic. The Maxwell-Boltzmann speed distribution applies to gases which are homogeneous and isotropic.

The Maxwell-Boltzmann (M-B) speed distribution is given by

$$f_c(c) = (4N/\sqrt{\pi})(m/2kT)^{3/2} c^2 \exp(-mc^2/2kT) \quad (2.12)$$

where  $N$  is the particle density,  $m$  is the molecular mass,  $k$  is the Boltzmann constant, and  $T$  is the temperature in  $^{\circ}\text{K}$ . This distribution gives the number of molecules contained in the

spherical shell of Figure 2-6; that is, the number having velocities between  $c$  and  $c+dc$ . Figure 2-7 shows the characteristic shape of the M-B distribution. Integrating the curve between  $c_1$  and  $c_2$  yields the total number of molecules/ $m^3$  having velocities between  $c_1$  and  $c_2$ . Figure 2-8 shows two M-B curves for a gas at different temperature and pressure conditions. Three important velocities are associated with the M-B curve.

The first characteristic speed is the most probable speed which occurs at the peak of the curve. It is denoted by  $c_0$  and can be found by differentiating  $f_c(c)$  with respect to  $c$  and setting the result equal to zero. Solving for  $c_0$ , yields

$$c_0 = (2kT/m)^{0.5} \quad (2.13)$$

The second characteristic speed is the average speed,  $\langle c \rangle$ , given by

$$\langle c \rangle = 2c_0/\sqrt{\pi} = 1.128c_0 \quad (2.14)$$

Again, this is the average of the scalar speed. The average of the velocity, for an isotropic system, is zero, which means all directions of travel are equally probable.

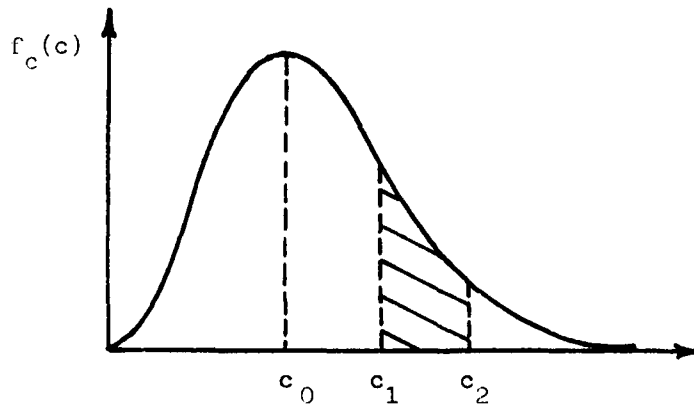


Figure 2-7: Typical shape of Maxwell-Boltzmann speed distribution.

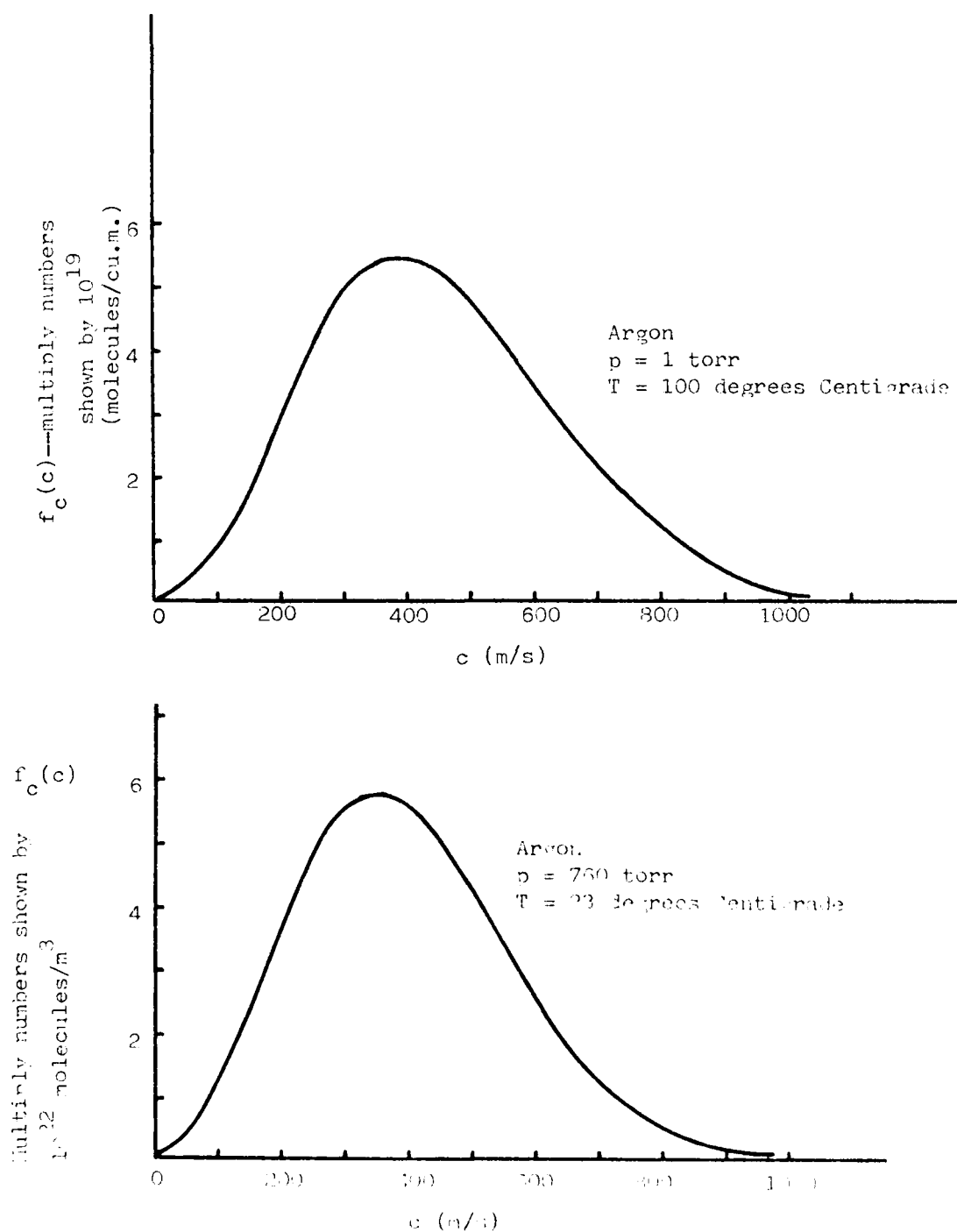


Figure 2-8: Maxwell-Boltzmann speed distributions for conditions as shown.

The third characteristic speed is the effective or RMS speed,  $\langle c^2 \rangle^{0.5}$ , given by

$$\langle c^2 \rangle = 1.5c_0^2 = 3kT/m \quad (2.15)$$

or

$$\langle c^2 \rangle^{0.5} = 1.22c_0 \quad (2.16)$$

#### 2.2.2.3 Temperature

From equation 2.13 we can define temperature in terms of the kinetic energy of a molecule having the most probable velocity; that is

$$mc_0^2/2 = kT \quad (2.17)$$

This concept will be very useful when we study the arc discharge in which the "temperatures" of electrons and ions may be very different.

#### 2.2.2.4 Pressure (Weidner and Sells, 1960, p.25)

The pressure of the gas is the force per unit area exerted by the molecules on the walls of the container. It can be found in terms of the temperature by considering the effect of the individual collisions of molecules with the walls. Figure 2-9 shows a container, whose sides are parallel to the planes of a cartesian coordinate system. Consider a molecule which has a velocity with components,  $v_x$ ,  $v_y$ , and  $v_z$ . Now, assume the molecule collides with the wall located at  $x_0$ , that the collision is elastic, and the wall is immovable.

Since the collision is elastic, conservation of energy requires the molecule to rebound with a component of velocity,  $-v_x$ . Before the collision, the momentum of the molecule in the

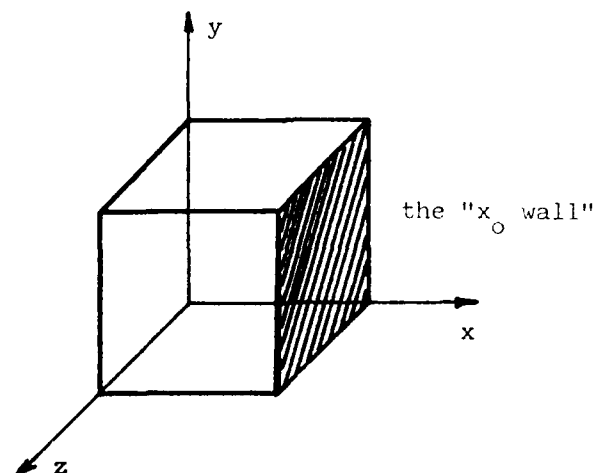


Figure 2-9: Calculation of gas pressure by momentum transfer to the container walls

x direction was  $mv_x$ , and afterward it is  $-mv_x$ . Conservation of momentum requires the momentum imparted to the walls to be  $2mv_x$ .

After rebounding, the molecule must travel back to the y-z plane where it will collide and return to the wall at  $x_0$ . Thus, it must travel a distance of  $2x_0$  in the x direction between collisions with the  $x_0$  wall. The time between collisions of the molecule and the  $x_0$  wall will be  $2x_0/v_x$ , and the number of collisions per second will be  $v_x/2x_0$ . The momentum transferred to the wall per second is the product of the momentum/collision and the # collisions/second:

$$\text{Momentum transfer to wall} = 2mv_x(v_x/2x_0) = mv_x^2/x_0 \quad (2.18)$$

which has the units of force. Since pressure is force/unit area

$$P = mv_x^2/x_0 y_0 z_0 = mv_x^2/V \quad (2.19)$$

where  $V$  is the volume of the container. This is the pressure

due to one molecule. Actually, there are  $NV$  molecules for a homogeneous gas, and

$$P = NVm\langle v_x^2 \rangle / V = Nm\langle v_x^2 \rangle \quad (2.20)$$

where  $\langle v_x^2 \rangle$  is the average of the velocity squared in the  $x$  direction. We can relate the pressure to the RMS speed by noting

$$\langle c^2 \rangle = \langle v_x^2 \rangle + \langle v_y^2 \rangle + \langle v_z^2 \rangle \quad (2.21)$$

For an isotropic gas, the average of the velocity squared will be the same in all directions, so  $\langle v_x^2 \rangle = \langle c^2 \rangle / 3$ . Thus

$$P = Nm\langle c^2 \rangle / 3 \quad (2.22)$$

Finally, substituting 2.15 into 2.22 yields the ideal gas law

$$P = NkT \quad (2.23)$$

In later chapters, we will see that pressure and temperature have a strong influence on the type of electrical discharge which forms in a gas.

### 2.3 Atomic Structure and Radiation

The discharge path of a gas discharge is usually luminous; indeed, the light is often the most striking feature of the discharge. This light occurs only at certain wavelengths, which depend on the type of gas in the discharge path. Some basic atomic characteristics are required to understand this behavior. This section will present a brief review of the Bohr model of the hydrogen atom and a discussion of emission and absorption of radiation by atoms.

## 2.3.1 The Bohr Model of the Hydrogen Atom (Beiser, 1967, p.101)

Bohr developed his model of the hydrogen atom in 1913.

While it does not fully account for the wave nature of matter, it does explain the phenomena we are interested in. As Rutherford had done before him, Bohr postulated that the hydrogen atom consisted of a single proton with a single electron orbiting around it. There are two forces acting on the electron--the centripetal force and the electric field force due to the attraction of the opposite charges. For the electron to remain in orbit, the forces must be equal and opposite.

The centripetal force is given by  $m_e v^2/r$  where  $r$  is the radius of the orbit,  $m_e$  is the mass of the electron, and  $v$  is the tangential velocity. Since  $v = \omega r$ , where  $\omega$  is the angular velocity, the centripetal force can be written as  $m_e r \omega^2$ .

The electric field force is given by  $q_e^2/4\pi\epsilon_0 r^2$ , where  $q_e$  is the charge of the electron and  $\epsilon_0$  is the dielectric constant of free space.

Equating the two forces yields

$$m_e r \omega^2 = q_e^2/4\pi\epsilon_0 r^2 \quad (2.24)$$

Previously, Rutherford had assumed that  $r$  could take on essentially any value. Bohr, however, invoked the Plank-Einstein assumption that angular momentum exists only in quantized values:

$$m_e v r = m_e r^2 \omega = nh/2\pi \quad (2.25)$$

where  $n$  is the principal quantum number (1,2,3,...) and  $h$  is Plank's constant.

From 2.24 and 2.25, the radii of the allowable orbits are found to be:

$$r_n = n^2 h^2 \epsilon_0 / \pi m_e q_e^2 \quad (2.26)$$

and the kinetic energy of the electron in an orbit is:

$$W_n = -m_e q_e^4 / 8 \epsilon_0^2 h^2 n^2 \quad (2.27)$$

That is, each quantum number corresponds to a particular orbit and a particular energy level. For an electron to change orbits, its energy must change. This means the electron must absorb or emit a finite amount of energy.

### 2.3.2 Absorption and Emission of Energy

In 1885, Balmer first noted the hydrogen discharge gave off light consisting only of certain wavelengths. Using his model, Bohr postulated that the change of electron orbit was accompanied by a quantum change in energy which was absorbed or emitted in the form of a photon of light; that is

$$W = h\nu \quad (2.28)$$

In particular, the atom absorbs a photon when an electron moves to a higher orbit and emits a photon when an electron moves to a lower orbit. For the hydrogen atom, several series of spectral lines have been identified and named. These are shown in Figure 2-10. Each series is characterized by a transition to a certain inner orbit. The Lyman series appears when electrons fall to the first orbit from higher numbered orbits; its radiation is in the ultra-violet. The Balmer series is in the visible, and involves transitions from outer orbits to the second orbit. Similarly, the Paschen, Brackett, and Pfund series



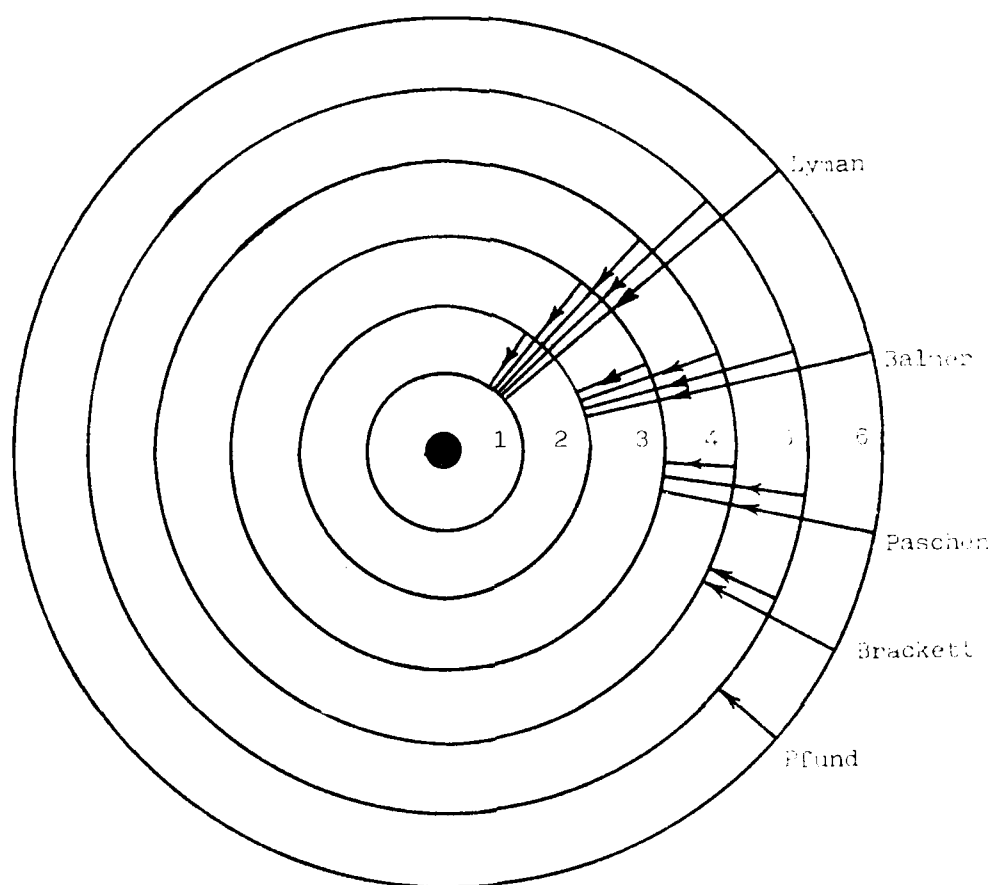


Figure 2-10: Illustration of the spectral series of the hydrogen atom.

involve transitions from outer orbits to the 3rd, 4th, and 5th orbits, respectively. The radiation from these is in the infra-red and beyond. Figure 2-11 shows the energy states and radii for several orbits and the wavelengths associated with the transitions. Note, the energy required to remove an electron from the first orbit to an infinite distance away is called the

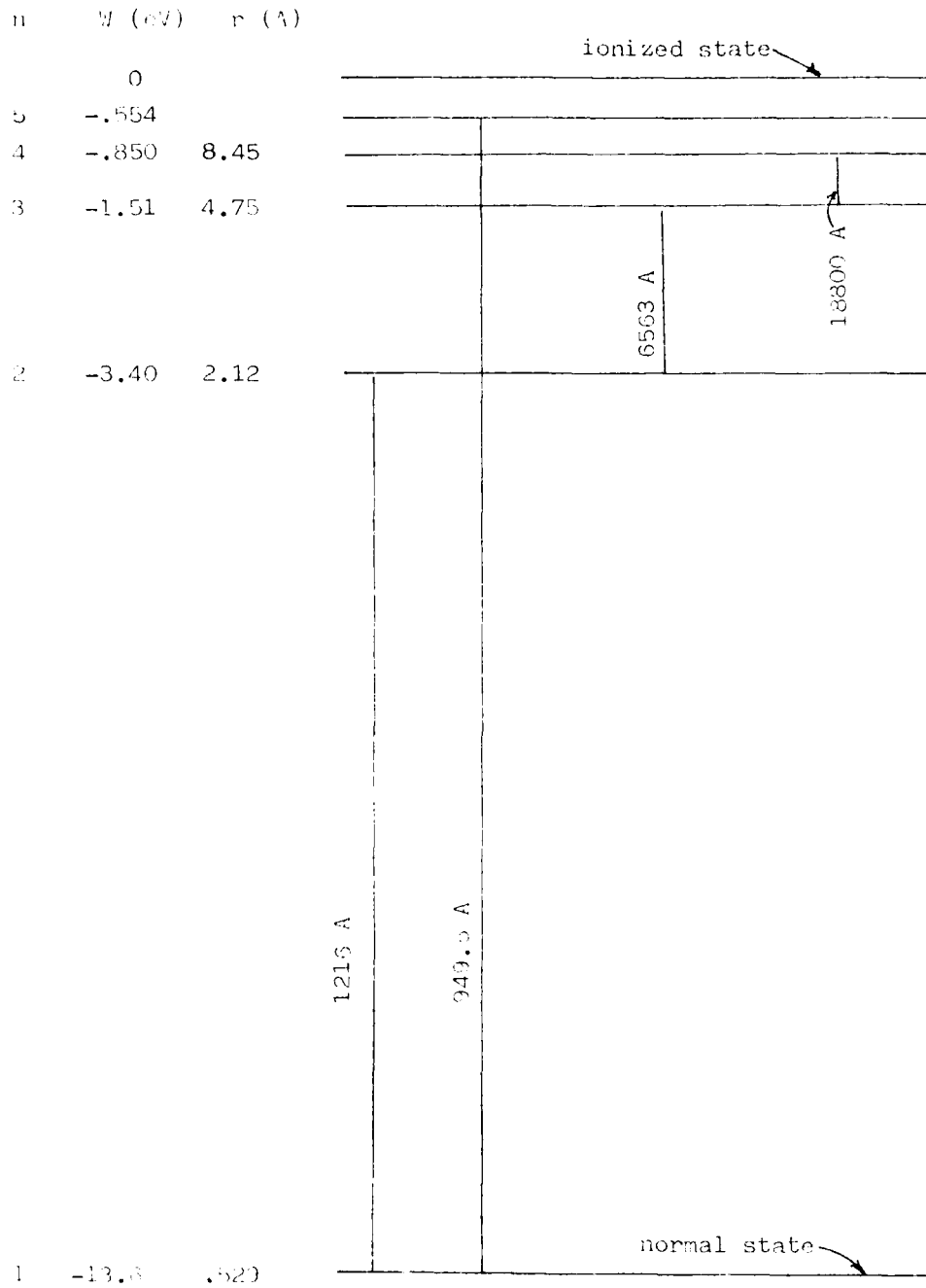


Figure 2-11: Energy states for the hydrogen atom.

Table 2-2: Ionization Potentials of Several Elements  
(Gray, 1957, p.7-14)

Symbol	Atomic Number	Ionization Potential (eV)
H	1	13.595
He	2	24.580
Li	3	5.390
Be	4	9.320
C	6	11.264
N	7	14.54
O	8	13.614
Ne	10	21.559
Na	11	5.138
Mg	12	7.644
Al	13	5.984
A	18	15.755
K	19	4.339
Mn	25	7.432
Fe	26	7.90
Ni	28	7.633
Cu	29	7.724
Kr	36	13.996
Mo	42	7.131
Ag	47	7.574
Xe	54	12.127
Cs	55	3.893
W	74	7.98
Hg	80	10.434
Pb	82	7.415

ionization energy. The term ionization potential is also used; it is the voltage through which an electron must be accelerated to ionize the atom. The ionization energy, in eV, and the ionization potential in volts are numerically equal. Table 2-2 shows the ionization energy for several elements.

#### REFERENCES :

- Alston, L.L. (ed.) (1968). High-Voltage Technology. Oxford University Press, London.
- Beiser, A. (1967). Concepts of Modern Physics. McGraw-Hill, New York.
- Cobine, J.D. (1957). Gaseous Conductors. Dover Publications, New York.
- Delcroix, J.L. (1960). Introduction to the Theory of Ionized Gases. Interscience Publications, New York.
- Denholm, A.S., et al (1973). Review of Dielectrics and Switching. US Air Force Weapons Laboratory Technical Report 72-88, Kirtland AFB, NM 87117. DTIC AD# 907739L.
- Dunbar, W.G. (1966). Corona Onset Voltage of Insulated and Bare Electrodes in Rarefied Air and Other Gases. US Air Force Aero-Propulsion Laboratory Technical Report 65-122, Wright-Patterson AFB, OH 45433. DTIC AD# 483820.
- Gray, D.E. (ed.) (1957). American Institute of Physics Handbook. McGraw-Hill, New York.
- Weidner, R.T. and Sells, R.L. (1960). Elementary Modern Physics. Allyn and Bacon, Boston.

THIS PAGE INTENTIONALLY BLANK

## CHAPTER 3

### EXCITATION AND IONIZATION PHENOMENA

#### 3.1 Introduction

Conducting electricity through a gas is very different than conducting it through a metal. Metals are generally good conductors of electricity in which the voltage and current are related by an almost constant resistance (i.e. Ohm's Law). One can visualize the metal as a lattice-like array of positive ions surrounded by a sea of electrons (at least one per ion). These electrons are relatively free to move about, and if an electric field is applied, they are accelerated toward the positive terminal. As the electrons move through the metal, they may interact with the ion lattice, yielding some of their energy. This energy eventually appears as heat, which is accounted for by the resistance loss ( $I^2R$ ) of the conductor.

Unlike metals, gases are almost perfect insulators at room temperature and atmospheric pressure, consisting of a large number ( $2.69 \times 10^{25}/\text{m}^3$  at 760 torr,  $0^\circ\text{C}$ ) of electrically neutral molecules<sup>1</sup>. Each gas molecule includes a number of positive protons in the nuclei and an equal number of negative electrons

---

<sup>1</sup>The term molecule will be used in its general sense; that is, to include monatomic as well as polyatomic gas particles

which are tightly bound to the nuclei. Thus, there are no charge carriers available<sup>2</sup>, and applying an electric field does not result in a measurable current.

Gas is frequently used as an insulator; for example, the phases of a high voltage transmission line are insulated by the air between them. However, if the proper conditions (electric field strength, pressure, temperature, and electrode separation and geometry) are introduced, the gas can become an excellent conductor. This transition may take place quite suddenly, and will be discussed in Chapter 6. In this chapter, we will be interested in the phenomena which cause the transition.

To become a conductor, a large number of electrons or ions must be present in the gas to carry the current. If they are present, applying an electric field causes the electrons to move to the positive electrode and the positive ions to move to the negative electrode. Thus, the current has two components and is considerably more complicated than for a metal.

Electrons and ions may be emitted from the electrodes (see Chapter 5) or formed by ionization of the gas molecules. Ionization of a gas molecule may occur as a result of a collision between the molecule and an electron, an ion, a photon, or another atom. All of these processes occur during electrical discharges

---

<sup>2</sup>In fact in atmospheric air at room temperature there may be  $10^6$  electrons/m<sup>3</sup>. While these relatively few electrons do not account for any measurable conductivity, they are crucial to the breakdown process. See section 3.3 for a description of how these electrons come about and section 6.1 for the current that results.

in gas. It is important they be understood so that breakdown can be avoided when it is not desired (for example, between phases of a transmission line) or enhanced when it is (for example, closing of a gas filled switch).

### 3.2 Collisions

In a gas, the electrons, ions, and molecules are in constant motion, and due to the large numbers involved, collisions between particles are inevitable. Collisions between molecules allow the gas volume to reach a steady state condition following a disturbance, while collisions between electrons and molecules are fundamental to the breakdown process in gases. Collisions between other combinations of particles also have roles to play in the various types of discharges. There is a great deal of literature, primarily in the physics journals, concerning collisions. Massey and Burhop (1969) published an extensive summary of the available data for all types of collisions. Electron-molecule collisions have been the subject of several review articles (Brode, 1933; Kieffer and Dunn, 1966; and Bederson and Kieffer, 1971). The brief summary below will help the reader understand why the breakdown voltage changes as system parameters (pressure, electrode separation, and electric field) are changed.

#### 3.2.1 Electron-Gas Molecule Collisions

The complexity of electrical discharges results not only from the large number of particles involved, but also from the variety of possible results of collisions. Collisions between



electrons and molecules may be categorized as elastic, inelastic, superelastic, or radiative (Massey and Burhop, 1969, p.3).

In an elastic collision, the energy exchanged between the electron and molecule is purely kinetic. In other words, there is no increase in the internal excitation of the molecule. The electron does lose some energy due to conservation of momentum, but this loss is of the order of the ratio of the electron mass to the molecular mass ( $<10^{-3}$ ). Thus, we will assume electrons lose no energy in elastic collisions with molecules.

In inelastic collisions, the electron loses kinetic energy, exciting internal motion in the molecule. Depending on circumstances, the inelastic collision may result in ionization of the gas molecule or just excitation to a higher energy state. Non-ionizing, inelastic collisions may be further classified by the state to which the molecule is excited.

Superelastic collisions are those in which an excited molecule collides with an electron, imparting some of its internal energy to the electron as kinetic energy. Radiative collisions are those in which the electron loses energy, at least some of which appears as radiation. In some cases, the electron may lose enough energy to be captured by the molecule, forming a negative ion. This is called electron attachment and is particularly important in certain types of corona (see section 8.2).

## 3.2.1.1 Collision Parameters

Before considering the individual types of collisions between electrons and molecules, we will consider several fundamental parameters which describe the collision process.

Assume a hypothetical gas, of density  $N$  molecules/m<sup>3</sup>, consists of solid, spherical molecules, each of radius  $R$  and cross sectional area  $Q = \pi R^2$ . If a parallel beam of uniform velocity electrons passes through the gas, some of them will be involved in collisions with the gas molecules. Neglecting the diameter of the electron and the speed of the molecule compared to that of the electron<sup>3</sup>, any molecule whose center is within distance  $R$  of an electron's path will collide with it (see figure 3-1). The probability of an electron being involved in a collision, after moving a small distance  $dx$ , will be the product of the particle density times the collision volume-- $NQdx$ . If the current at point  $x$  has a value  $I(x)$ , the current lost by collisions between  $x$  and  $dx$  will be:

$$dI = I(x)NQdx \quad (3.1)$$

Integrating equation 3.1 yields:

$$I(x) = I_0[\exp(-NQx)] \quad (3.2)$$

where  $I_0$  was the current entering the gas at  $x=0$ . Given a hypothetical gas containing solid molecules of unknown size, one could calculate  $Q$  by measuring the attenuation of the current  $I(x)/I_0$  as a function of  $N$  and  $x$ .

---

<sup>3</sup>This assumption is valid unless the temperature of the gas is very high

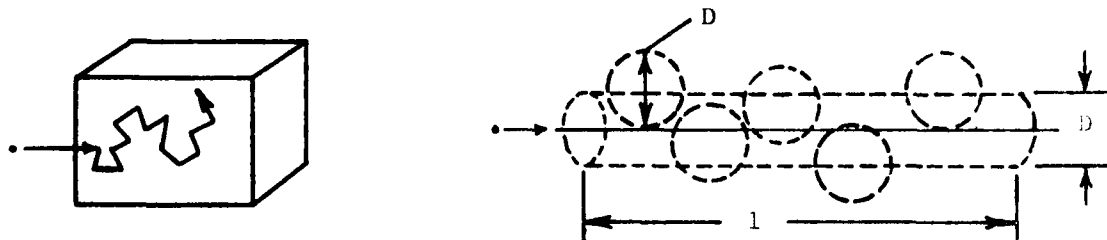


Figure 3-1: The collision volume of an electron moving through a gas.

Now, suppose the electron beam is fired into a real gas. As in the case of the hypothetical gas, some of the electrons will be involved in collisions and deflected out of the beam. If the attenuation is measured as a function of  $x$ , it will be found that:

$$I(x) = I_0[\exp(-\alpha x)] \quad (3.3)$$

where  $\alpha$  is an absorption coefficient of the gas for electrons of this energy. If  $\alpha$  is known, we can put equation 3.3 into the same form as equation 3.1 by letting:

$$\alpha = NQ \text{ or } Q = \alpha/N \quad (3.4)$$

where  $Q$  is defined as the total collision cross section of the gas, for electrons having a given velocity. It is called the total collision cross section, because all collisions, elastic or inelastic, are included. Elastic, inelastic, and ionizing cross sections may also be measured and it is found:

$$Q = Q_0 + \Sigma Q_n \quad (3.5)$$

where  $Q_0$  is the elastic collision cross section and  $Q_n$  is the collision cross section for excitation or ionization to a given state.

While the real gas seems to behave just as the hypothetical, hard sphere molecule gas, one must be careful to not overdo the analogy. In reality, the force between an electron and a molecule falls off continuously with distance rather than abruptly. As will be seen below, the total collision cross section is by no means the actual size of the molecule.

Early work in the measurement of total collision cross sections was done by Ramsauer and by Townsend, using different techniques (Bederson and Kieffer, 1971 review all of the experimental methods). Much work was done by Brode (1933), whose results have appeared in publications by many authors. Some of the early results were presented in terms of a so-called probability of collision,  $P_C$ . It is defined as the average number of collisions experienced by a projectile particle passing through one centimeter of gas at a pressure of 1 torr and temperature of 0°C:

$$P_C = N_0 Q = (3.536 \times 10^{16}) Q \quad (3.6)$$

where  $N_0$  is the gas molecular density (molecules/cm<sup>3</sup>) at 1 torr and 0°C. Clearly,  $P_C$  is not a probability, since it has units of collisions/cm and may be much larger than one. In fact,  $P_C$  is the absorption coefficient,  $\alpha$ , at 1 torr and 0°C.

Figure 3-2 shows some of Brode's results for several gases and for metal vapors. These figures all show the probability of collision as a function of the square root of the electron

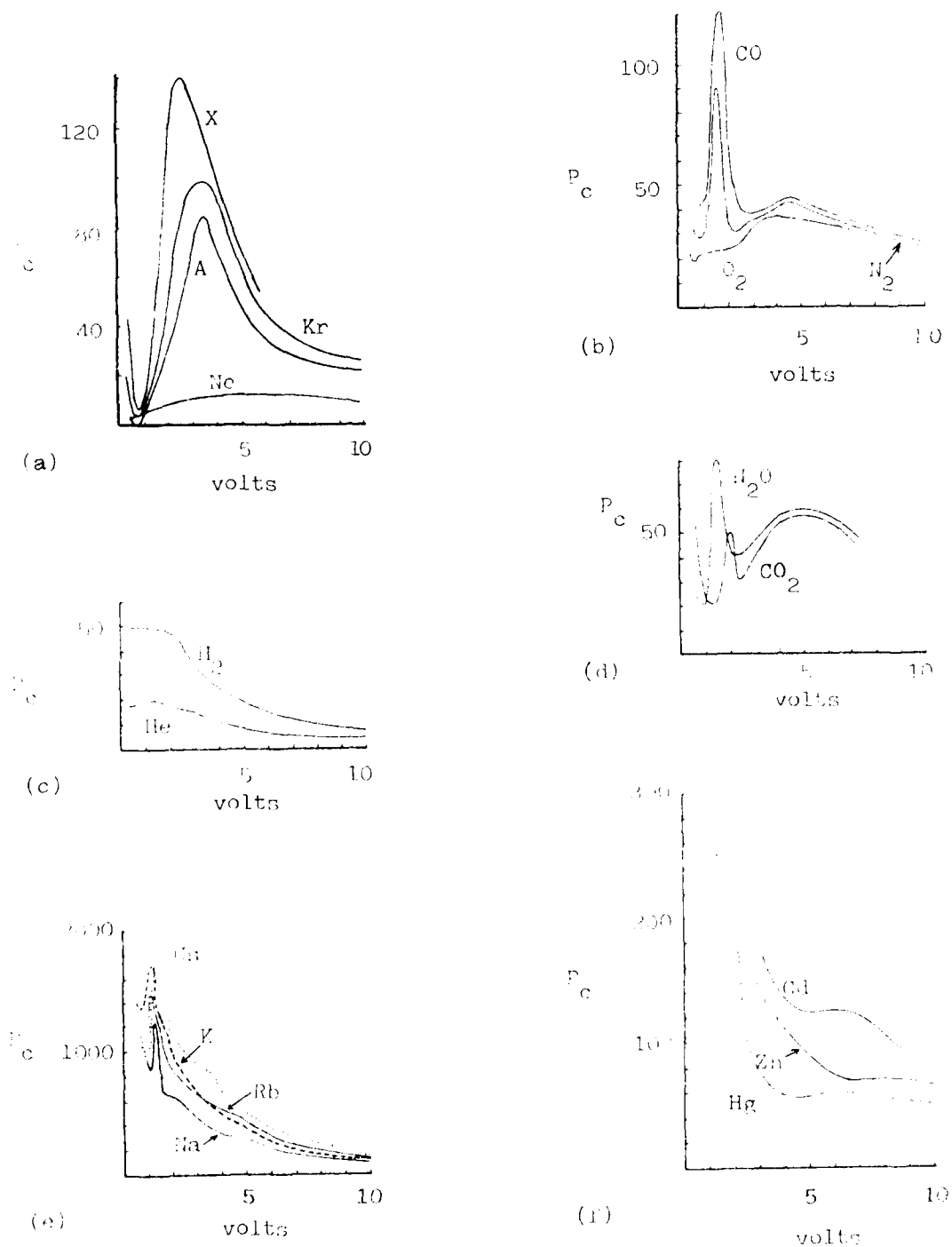


Figure 3-2: Probabilities of collision for several gases (after Brode, 1933).

energy (which is proportional to electron velocity). It is immediately apparent that real gases behave much differently than hard sphere molecules. Specifically,  $P_C$  (and hence  $Q$ ) is not constant, but is, instead, a function of the electron velocity. Figure 3-2a shows  $P_C$  for several of the noble gases. The pronounced minimum in the vicinity of 1 ev implies that the gas is virtually transparent to electrons of that energy. This effect, known as the Ramsauer effect, cannot be explained by classical mechanics, but can be by quantum mechanics (VonEngel, 1965, p.31). All of the curves for gases in Figure 3-2 are averages of several researchers and are considered to be within about 10% of the true value (Massey and Burhop, 1969, p. 25). The curves for metal vapor, however, were for many years the only reliable ones available, and Brode (1929) stated that there was some uncertainty as to the exact vapor pressure of the metal. More recent experimental and theoretical work indicates the values in figures 3-2 e & f may be high by about a factor of two and the pronounced peaks for the alkali metals may be exaggerated (Bederson and Kieffer, 1971, p. 633).

The total collision cross section can be found experimentally and can be used to calculate other parameters which are very useful in describing the breakdown process. Equation 3.2 tells us an electron beam current will be attenuated exponentially as it passes through the gas. If we were interested in a particular number of electrons entering the gas,  $N_{e0}$ , we would rewrite equation 3.2 as:

$$N_e(x) = N_{e0}[\exp(-NQx)] \quad (3.7)$$

or

$$f(x) = N_e(x)/N_{e0} = \exp(-NQx) \quad (3.8)$$

where  $N_e(x)$  is the number of electrons remaining at distance  $x$  into the gas and  $N$  is the molecular density.

Figure 3.3 shows a plot of  $f(x)$ , the percentage of electrons remaining, as a function of the distance travelled into the gas. This figure gives an indication of how far an electron might be expected to travel. This distance is given the name free path, and figure 3.3 shows the distribution of free paths. In particular, for any particular distance  $x_1$ , the percentage of electrons having a free path greater than  $x_1$  is  $f(x_1)$ . Note, the term  $(1/NQ)$  is a distance constant much like the familiar  $L/R$  and  $RC$  time constants of circuit analysis. The exponential decay means that only 37% of electrons have a free path greater than  $1/NQ$ .

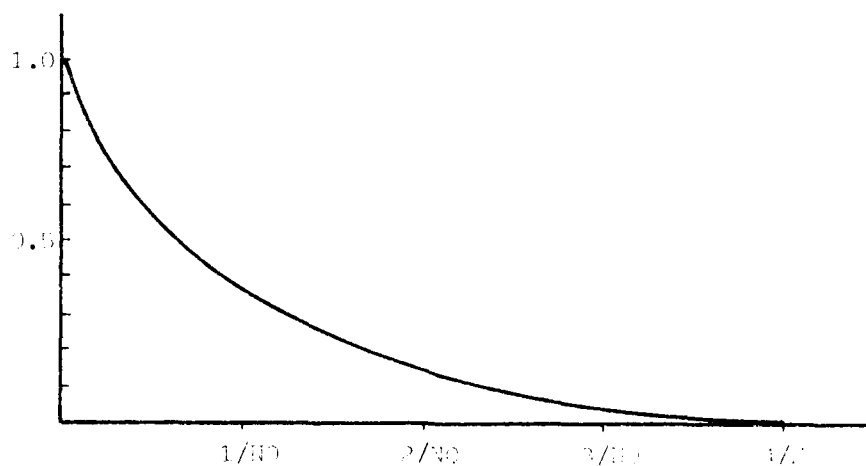


Figure 3-3: Distribution of electron free paths.

It can be shown (Cobine, 1957, p.24) that  $1/NQ$  is actually the mean free path (mfp); that is, the average distance travelled by an electron of a particular velocity between collisions. The mean free path, denoted by  $\lambda$  is a very important quantity in determining the mechanisms involved in the breakdown process. For example, if two electrodes are many mean free paths apart, then electron collisions will be very important. On the other hand, if the electrodes are closer than the mean free path, then collisions will not be as significant. This does not mean that there would be no collisions; after all, 63% of the free paths will be less than the mean free path.

We can relate the mean free path to the probability of collision as follows. The ideal gas law states:

$$N \propto p/T \quad (3.9)$$

thus,

$$N_0 \propto 1 \text{ torr}/273^\circ\text{K} \quad (3.10)$$

Dividing equation 3.9 by 3.10 yields:

$$\frac{N}{N_0} = \frac{p}{1 \text{ torr}} \times \frac{273^\circ\text{K}}{T} \quad (3.11)$$

where  $p$  is the pressure in torr, and  $T$  is the temperature in  $^\circ\text{K}$ . This ratio of gas densities is given the name reduced pressure,  $p_0$ , although it is a dimensionless quantity. From equations 3.6 and 3.11:

$$\lambda = 1/NQ = 1/p_0 P_c \quad (3.12)$$

Using values of  $P_c$  from figure 3.1, one observes that the electron's mean free path will be very short at atmospheric pressure.



Example 3-1: What is the mean free path for a 9.0 ev electron beam shot into argon at room temperature (23°C) and atmospheric pressure (760 torr)?

Solution: For an electron having an energy of 9.0 ev, the square root of the energy is 3.0, and from figure 3-2a, for Argon,  $P_C = 70$  coll/cm. For the given conditions:

$$p_0 = (760 \text{ torr}/1 \text{ torr})(273^\circ\text{K}/296^\circ\text{K}) = 701$$

Thus:  $\lambda = 1/p_0 P_C = 1/701(70) = 2.038 \times 10^{-5}$  cm or only 0.204 microns

Once the mean free path is known, the collision frequency,  $f_C$ , or its inverse, the collision period, can be calculated:

$$f_C = 1/\tau = \langle v \rangle / \lambda \quad (3.13)$$

where  $\langle v \rangle$  is the electron velocity. The collision period is the time between collisions, and gives an indication of how long transient disturbances will take to die out.

#### 3.3.1 Excitation and Ionization of Gas Molecules

The collision parameters described in the previous section include all types of collisions, and the total collision cross sections, shown in figure 3-2, give no indication of what types of collision are occurring. However, it is possible to make some generalizations:

- a. Low energy electrons do not have enough energy to excite or ionize the gas molecules. Virtually all of the collisions are elastic, and the electrons are scattered in various directions.

b. Electrons with more energy than the excitation energy of a particular state for the gas molecule may cause excitation to that state. Conservation of angular momentum prevents an electron whose energy is exactly equal to the excitation energy from exciting the molecule (VonEngel, 1965, p.42). Experiments have shown the probability of excitation,  $P_e$ , is zero when the electron has exactly the excitation energy, and  $P_e$  increases with electron energy, until it reaches a maximum. Figure 3-4 shows the excitation cross section for helium as a function of electron energy. Note, this curve includes transitions to several different states.

c. If the energy of the electron is less than the ionization energy of the gas, the probability of ionization (# of ion pairs/(cm)(torr) at 0°K and 1 torr) must be zero. As the electron energy increases,  $P_i$  increases to a maximum, and then drops off. Figure 3-5 shows  $P_i$  for several gases. It is also possible for multiple ionization to occur, and figure 3-6 shows  $P_i$  for several different ionization levels of mercury. The front (rising) portions of the curves in figure 3-5 are fairly linear, and may be described by

$$P_i = a(V - V_i) \quad (3.14)$$

where  $V_i$  is the ionization potential, and  $V$  is the electron potential. Table 3-1 (Cobine, 1941, p.80) shows values for "a" and the range for which equation 3.14 is valid. Very high energy electrons are relatively poor ionizers because they are not in the molecule's sphere of influence long enough to cause the polarization of charge which results in ionization.

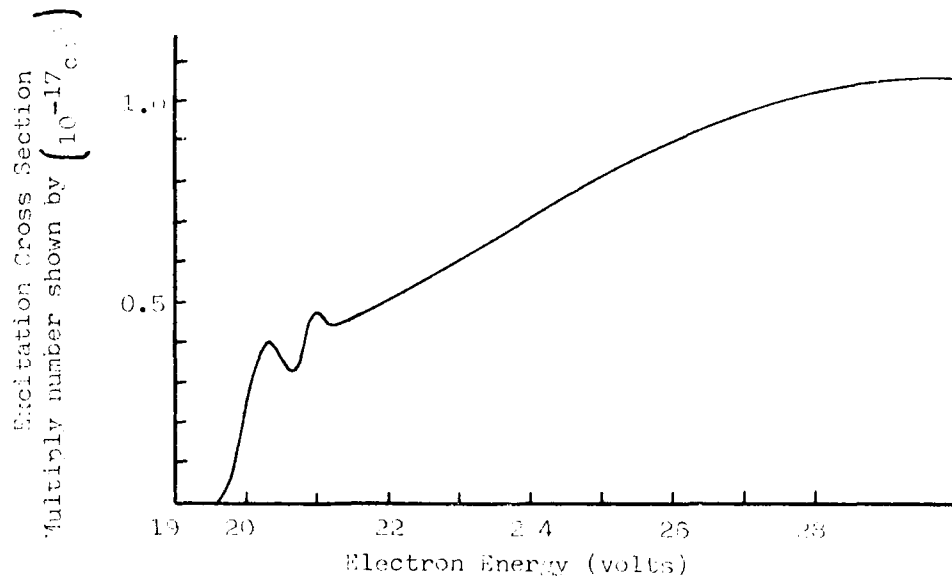


Figure 3-4: Cross section for excitation of helium as a function of electron energy (after VonEngel, 1965, p.47).

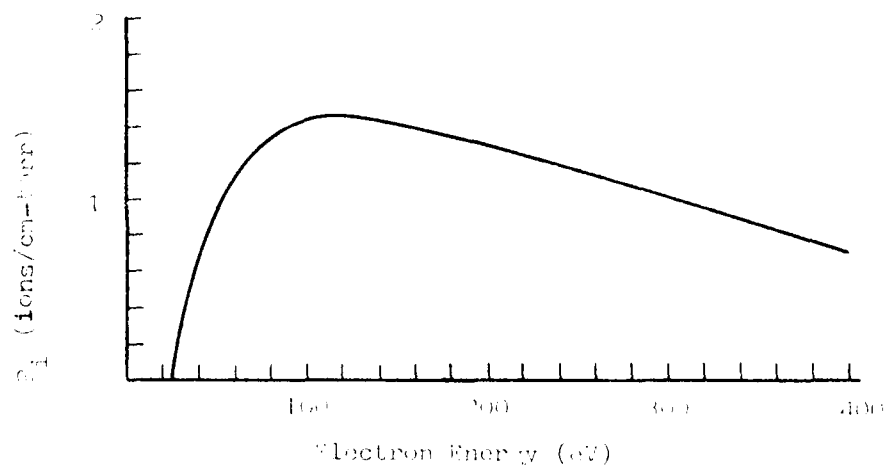


Figure 3-5: Probability of ionization for helium (after VonEngel, 1965, p.63)

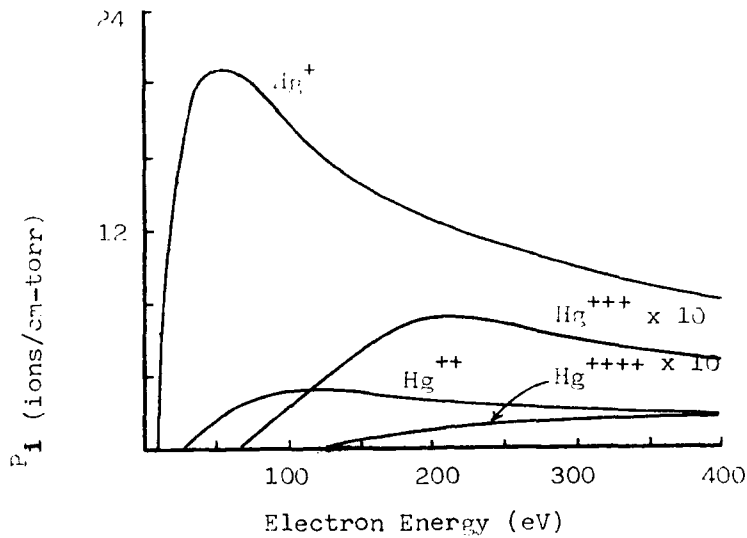


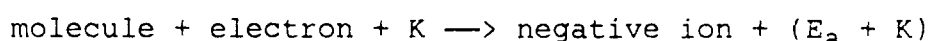
Figure 3-6: Probabilities of single and multiple ionization for mercury (after Bleakney, 1930, p.139)

Table 3-1: Differential Ionization Constant for Electrons (Cobine, 1957, p. 80)

Gas	Ion Formed	a	Voltage Range
Air	-	0.26	16 - 30
A	$A^+$	0.71	15 - 25
	$A^{++}$	0.031	45 - 80
He	$He^+$	0.046	24 - 35
$H_2$	$H_2^+, H^+$	0.21	16 - 35
Hg	$Hg^+$	0.82	10 - 16
	$Hg^{++}$	0.06	29 - 50
	$Hg^{+++}$	0.006	71 - 150
	$Hg^{++++}$	0.001	143 - 200
$O_2$	$O_2^+, O^+$	0.24	13 - 40
$N_2$	$N_2^+, N^+$	0.30	16 - 30

### 3.2.1.3 Electron Attachment

During a collision between an electron and a molecule, the electron may become attached to the molecule, resulting in the formation of a negative ion (VonEngel, 1965, p.86). The probability of electron attachment depends on the energy of the electron and the nature of the gas, especially the presence of impurities. The process may be represented as:



where  $K$  is the initial kinetic energy, and  $E_a$  is the electron affinity. The energy  $E_a + K$  is given off as radiation, and the larger  $E_a$  is, the more firmly bound is the electron.

In order to be attached, the electron must have enough kinetic energy to avoid being repelled by the atomic field, but not so much that it passes by without being captured. Typically, the average number of collisions an electron makes before becoming attached is quite high, from a few thousand to  $10^8$ , depending on the gas. However, due to the frequency of collisions, the time for an electron to become attached is only from a few nanoseconds to a millisecond (Cobine, 1957, p.97).

The halogens (F, Cl, Br, I), oxygen, water vapor, and monatomic hydrogen, among others, are capable of electron attachment. In addition, there is a group, known as electronegative gases, which includes:  $\text{SF}_6$  (sulfur hexafluoride),  $\text{CCl}_4$  (carbon tetrachloride),  $\text{CCl}_2\text{F}_2$  (freon 12), and  $\text{C}_3\text{F}_8$  (perfluoromethane). The electronegative gases are very good at attaching free electrons, due to their large cross sections and unfilled outer electron

rings.  $\text{SF}_6$ , in particular, is frequently used in high voltage equipment to increase the breakdown strength. On the other hand, the noble gases,  $\text{H}_2$ , and  $\text{N}_2$  will not form negative ions by attachment (if they are pure).

Once an electron has become attached, the ability of the electric charge to move about is much more restricted (see section 4.2). Because the negative ion is much more massive than the electron, an electric field will not accelerate the ion to as high a speed as it would the electron. This can have a significant influence on the formation of an electric discharge.

### 3.2.2 Collisions Between Gas Molecules

In the last section, we considered collisions between electrons and gas molecules. To simplify matters, we assumed the molecules were stationary with respect to the electrons. This assumption was justified due to the relative difference in speeds; however, the molecules are in constant motion. Since they are moving, they will collide with each other. These collisions are the primary mechanism for maintaining the Maxwell-Boltzmann velocity distribution and eliminating the effects of any transient disturbance to the system. In addition, molecular collisions may result in ionization (see section 3.3 below). We can calculate the mean free path for a molecule in a manner very similar to that which we used for the electron.

Consider a group of molecules of diameter  $D$ , and assume all are stationary except one which has a velocity,  $v$ . In this case, the projectile has a finite size, so any molecule whose center

is within a distance  $D$  of the projectile's center will collide with the projectile. Thus, the collision cross section is  $\pi D^2$ . Since the projectile has a velocity,  $v$ , the collision volume per second will be  $v\pi D^2$ , and the number of collisions per second will be  $Nv\pi D^2$ . The mean free path is then given by

$$\lambda = \frac{\text{velocity}}{\# \text{ collisions/sec}} = \frac{v}{vN\pi D^2} = \frac{1}{N\pi D^2} \quad (3.15)$$

In reality, all the molecules are moving, and the calculation of the mean free path is involved (Cobine, 1957, p.21). The result, however, is very similar

$$\lambda = \frac{1}{\sqrt{2}N\pi D^2} = \frac{kT}{\sqrt{2}p\pi D^2} \quad (3.16)$$

Table 3-2 gives some typical molecular diameters (McDaniel, 1964, p.35) and values of  $\lambda$  calculated using equation 3.16 with a pressure of 760 torr and a temperature of 273°K. In fact, the value for  $D$  will tend to decrease with temperature, but this is a second order effect (Cobine, 1957, p. 22).

Table 3-2: Typical Molecular Diameters and Mean Free Paths

Molecule	Diameter (in $10^{-10}$ m)	MFP (in $\mu\text{m}$ )
H <sub>2</sub>	2.74	0.112
He	2.18	0.176
Ne	2.59	0.125
N <sub>2</sub>	3.75	0.0596
O <sub>2</sub>	3.61	0.0643
A	3.64	0.0632
Xe	4.85	0.0356

### 3.3 Thermal Ionization

When two high energy molecules collide, one may ionize the other. Given the Maxwell-Boltzmann speed distribution, there is a finite probability of two molecules with very high velocity colliding, but at room temperature the probability is small. As the temperature of the gas increases, there are more high energy molecules available, and the probability of ionizing collisions increases. Thus, at higher temperatures, the ionization level of the gas increases. In a high temperature flame, such as an arc, many molecules have sufficient energy to ionize one another. In fact, thermal ionization is the principle source of ions in the high pressure arc.

The most successful analysis of this complex phenomenon was by M.N. Saha. Using thermodynamic reasoning, he concluded

$$\frac{x^2}{1-x^2}p = (2.4 \times 10^{-4})(T^{2.5})\exp(-q_e V_i/kT) \quad (3.17)$$

In equation 3.17,  $x$  is the ionization fraction, which is the density of ions,  $N^+$ , or electrons,  $N^-$ , divided by the original molecular density,  $N$  ( $x = N^+/N = N^-/N$ ). Also,  $p$  is in torr,  $T$  is in  $^{\circ}\text{K}$ , and  $V_i$  is the ionization potential in eV.

Three things should be noted about equation 3.17. First, if  $N^- \neq N^+$  (perhaps due to an electric field), then other forms of the equation must be used. Second, the gas is assumed to be homogeneous. Arcs usually burn in mixtures with varying ionization potentials, in which case the gas with the lowest ionization potential will be the most highly ionized. Also, container



walls and turbulence may affect the homogeneity. Finally, at high temperatures, polyatomic molecules become dissociated and other compounds, such as NO in air, may be formed. The ionization potentials of the resulting products should be used. (VonEngel, 1965, p. 82).

Figure 3-7 shows curves of  $x$  vs  $T$  for several values of  $p$  and  $V_i$ . Note, very high temperatures are required to ionize a large percentage of the gas molecules. Typically, a gas is considered weakly ionized when  $x < 10^{-4}$  and strongly ionized when  $x > 10^{-4}$ . In section 9.3, we will see the importance of thermal ionization to the arc discharge.

### 3.4 Photoionization

The final type of ionization to be considered is photoionization. Photoionization is extremely important because it provides the electrons which start the electric discharge. A photon may excite or ionize a molecule, if the energy of the photon is greater than the excitation or ionization energy of the molecule. The energy of the photon is  $h\nu$  where  $h$  is Planck's constant and  $\nu$  is the frequency. To ionize, we must have

$$h\nu \geq q_e V_i \quad (3.18)$$

Clearly, the probability of ionization will be zero if equation 3.18 is not satisfied. However, unlike ionization by collision, the probability of ionization by a photon reaches a maximum at 0.1 to 1.0 eV above  $q_e V_i$  and rapidly decreases as  $h\nu$  is increased further (VonEngel, 1965, p.74). The difference of the photon and the ionization energies ( $h\nu - q_e V_i$ ) will appear as kinetic

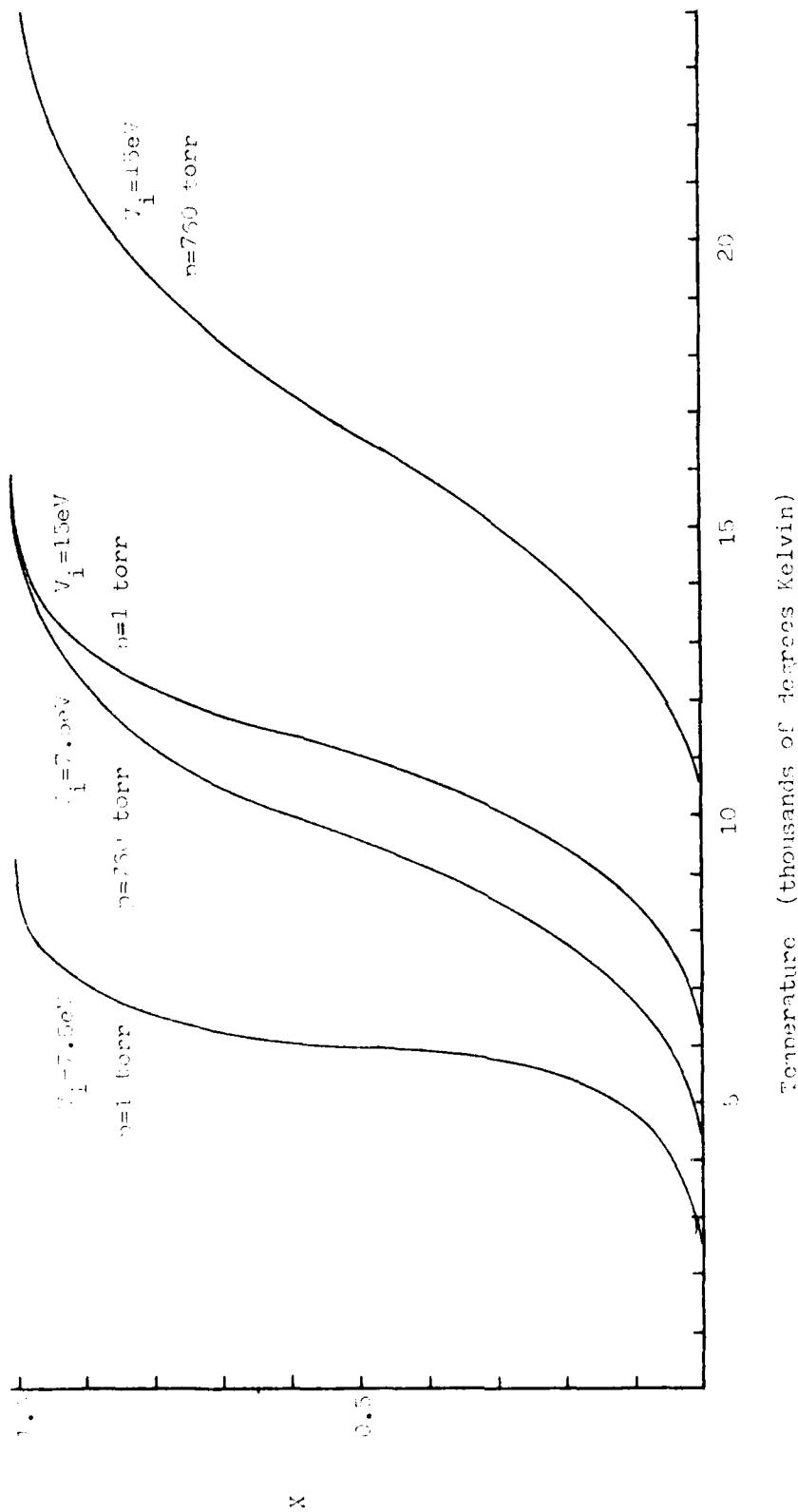


Figure 3-7: Curves showing the ionization of a gas, as predicted by Saha's equation for various values of pressure and ionization potential

energy of the released electron and/or as a photon of longer wavelength.

As a beam of radiation passes through a gas, some of the photons are absorbed and reradiated in random directions. The attenuation is similar in form to that of an electron beam

$$I(x) = I_0 \exp(-\mu x) \quad (3.19)$$

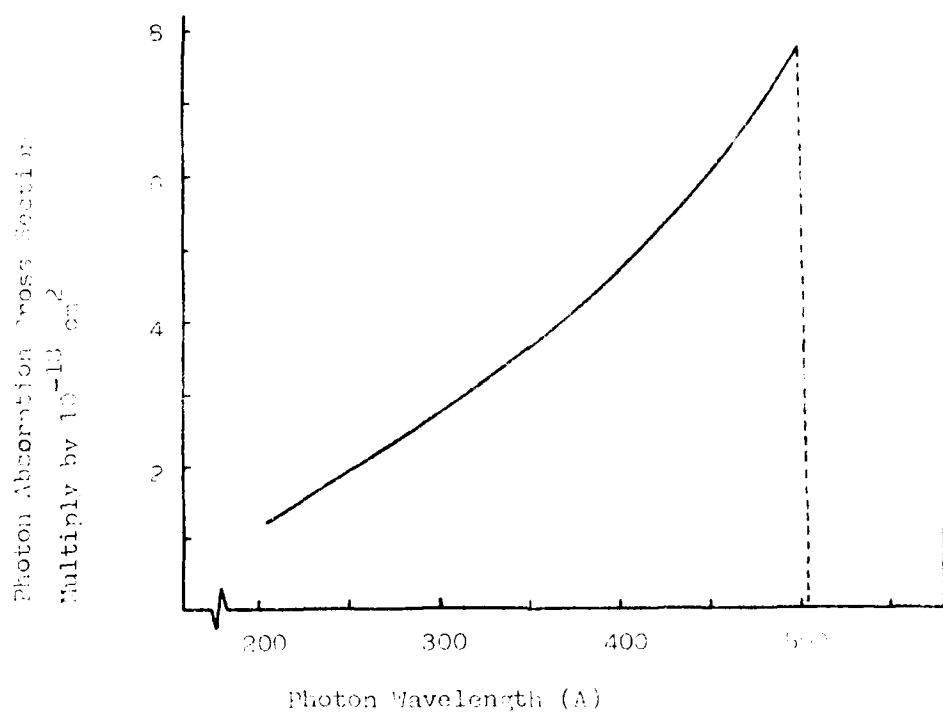
where  $I_0$  is the photon intensity entering the gas at  $x=0$ ,  $I(x)$  is the photon intensity at  $x$ , and  $\mu$  is the absorption coefficient. Values for  $\mu$  are usually measured at 1 atm (760 torr) and  $0^\circ\text{C}$  ( $273^\circ\text{K}$ ) (Lee and Weissler, 1955, p.540). A photoabsorption cross section can be defined as

$$q_p = \mu/N \quad (3.20)$$

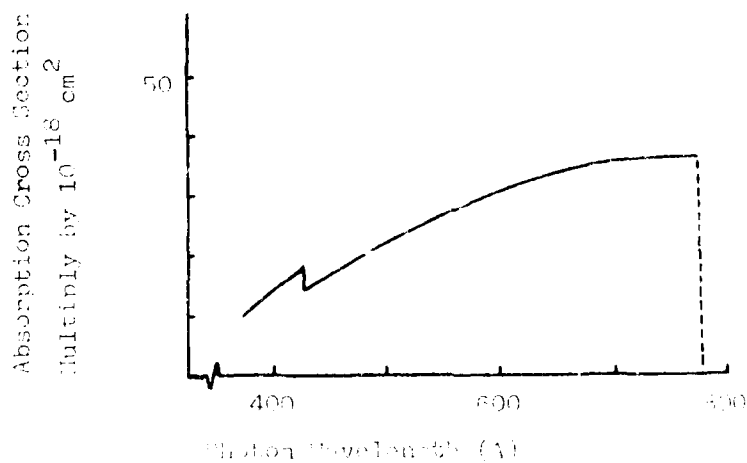
where  $N$  is the density at 760 torr and  $273^\circ\text{K}$  (Loschmidt's number).

Figure 3-8a shows  $q_p$  for helium, which is transparent to wavelengths longer than 504.8 Angstroms (A) except for resonance line absorption. An example of resonance line absorption is shown at 584.3 A. Light of this frequency is absorbed, resulting in photoexcitation. The continuous absorption for wavelengths below 504 A is due to photoionization. For helium,  $q_p$  decreases as the wavelength is decreased; however, things are slightly different for more complex atoms.

Figure 3-8b shows  $q_p$  for argon. Argon has a lower ionization potential than helium, so longer wavelengths are absorbed. Again, we see  $q_p$  decreasing with the wavelength, but there is a "spike" around 420 A. For wavelengths between 780 and 420 A, the ejected electron comes from the outer shell of the atom.



(a)



(b)

Figure 3-8: Photoabsorption cross sections for (a) helium and (b) argon

At 420 Å, however, the photon has enough energy to knock an electron out of the inner shell, which results in a higher cross section (VonEngel, 1965, p.78).

Further information may be found in Lee and Weissler (1955); Wainfan, Walker, and Weissler (1955); Weissler (1956); Axelrod and Givens (1959); and Baker, Bedo, and Tomboulion (1961).

### 3.5 Deionization

Deionization of an ionized gas takes place by two principal means. The first method is called volume recombination. In this case, an electron becomes attached to a neutral molecule, forming a negative ion. The negative ion then collides with a positive ion, and two neutral molecules are formed. In the second method, the electrons and positive ions diffuse to the walls of the container where they recombine.

Two points are worth noting. First, deionization takes place at the same time as ionization. Thus, the relative rates determine whether the system will become more, or less, ionized. Second, once the sources of ionization are removed, a finite amount of time is required for recombination to take place. This time depends on whether the gas must cool down, and is typically short (in the used to msec range). Although the recombination time is short, it may significantly affect the capability of a pulsed power system. An example could be the rate of a switch due to recombination delay.

### 3.6 Summary

In order to conduct electricity through a gas, it is essential that some of the molecules become ionized. In this chapter, we have briefly reviewed the major methods of ionization. Each of them is important, and each plays a unique role in the breakdown and conducting process. Ionization by electron collision usually causes the breakdown of a gas, but the initial source of electrons typically is photoionization by stray radiation. Finally, thermal ionization may be very important in maintaining a discharge, once it has started.

### REFERENCES :

- Axelrod, N.N. and Givens, M.P. (1959). Physical Review. Vol. 115, p. 97.
- Baker, D.J., Bedo, D.E., and Tomboulion, D.H. (1961). Physical Review. Vol. 124, p. 1471.
- Bederson, B. and Kieffer, L.J. (1971). Reviews of Modern Physics. Vol. 43, p. 601.
- Bleakney, W. (1930). Physical Review. Vol. 36, p. 1303.
- Brode, R.B. (1933). Reviews of Modern Physics. Vol. 5, p. 257.
- Brode, R.B. (1929). Physical Review. Vol. 34, p. 673.
- Cobine, J.D. (1957). Gaseous Discharges. Dover Publications, New York.
- Kieffer, L.J. and Dunn, J.H. (1966). Reviews of Modern Physics. Vol. 38, p. 1.
- Lee, P. and Weissler, G.L. (1963). Physical Review. Vol. 99, p. 540.
- Massey, H.S.W. and Burhop, E.H.S. (1969). Electronic and Ionic Impact Phenomena (vol. 1). Clarendon Press, Oxford.

## AN INTRODUCTION TO ELECTRICAL BREAKDOWN

1. Townsend, E.W. (1964). Collision Phenomena in Ionized Gases. Wiley, New York.
2. Phelps, A. (1965). Ionized Gases. Clarendon Press, Oxford.
3. Hays, N., Walker, W.C., and Weissler, G.L. (1955). Physical Review. Vol. 99, p. 542.
4. Hays, G.L. (1956). Encyclopedia of Physics. Vol. 21, Springer-Verlag, Berlin.

## CHAPTER 4

### MOTION OF PARTICLES

#### 4.1 Introduction

In the last chapter, we considered collisions between electrons and molecules. The electrons were assumed to be part of a beam of uniform energy. Although some switches are triggered with an electron beam, we generally have only the electrons from the system (electrodes and gas) to work with. In this chapter, we will consider the motion of charged particles (electrons and ions) through a gas. In particular, we are interested in how the motion is affected by the presence of an electric field and by concentration effects. Motion of a charged particle due to an electric field is called mobility, while motion due to concentration effects is called diffusion.

#### 4.2 Mobility

If an electric field,  $E$ , is applied to a region containing a free electron, the electron will experience a force and acceleration in the negative  $E$  direction. The force and acceleration are  $q_e E$  and  $q_e E / m_e$ , where  $q_e$  and  $m_e$  are the charge (coulombs) and mass (kg) of the electron. Figure 4-1 shows an electron between two electrodes in a tube. If there were a perfect vacuum in the tube, the electron would be accelerated by the field until it



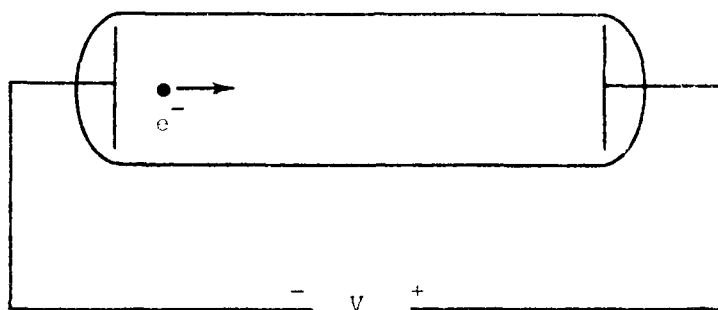


Figure 4-1: An electron subjected to an electric field.

hit the anode. At this time, however, we are interested in what happens if there is gas in the tube.

From Chapters 2 and 3, we know the electron and the gas molecules are in continual random motion and frequent collisions occur. Thus, when the electric field is applied, we would not expect the electron to be accelerated all the way to the anode. Rather, we would expect it to be accelerated toward the anode until it collides with a molecule. This process would then repeat until the electron eventually reached the anode. Between collisions, the electron gains an amount of kinetic energy determined by the strength of the electric field and the length of time between collisions. During the collision, a small fraction of the electron's kinetic energy is lost. Eventually, after a number of collisions, the energy lost during the collision equals the energy gained between collisions. At this point, the average kinetic energy of the electron is constant. Also constant is

the average velocity of the electron toward the anode, which is called the drift velocity (Howatson, 1976, p.35). It is sometimes easier to think of the drift velocity in terms of the motion of a group of electrons.

Figure 4-2 shows the same electrode system with a large number of electrons (called a swarm) concentrated in one region. The individual electrons have random velocities which will cause the swarm to expand (see diffusion below), but when the field is applied, the entire swarm will begin to move toward the anode. The velocity of the center of mass of the swarm is the drift velocity, and experiments to measure drift velocity utilize such a swarm (Meek and Craggs, 1978, p.89).

The same conclusion could be drawn for ions (positive or negative), but due to their much larger mass, the acceleration and final drift velocity will be much smaller than for electrons. Clearly, however, positive ions will drift in the positive E direction, toward the cathode.

Since the acceleration of a charged particle is proportional to E, the drift velocity should also be a function of E. Likewise, from equations 3.12 and 3.13, the collision frequency is proportional to pressure. More frequent collisions mean less time between collisions for acceleration; hence, the drift velocity should have an inverse relationship to pressure. If the drift velocity,  $u$ , is much less than the thermal velocity, then

$$u = \mu E \quad (4.1)$$

where  $\mu$  is the mobility (note,  $K$  is also frequently used for

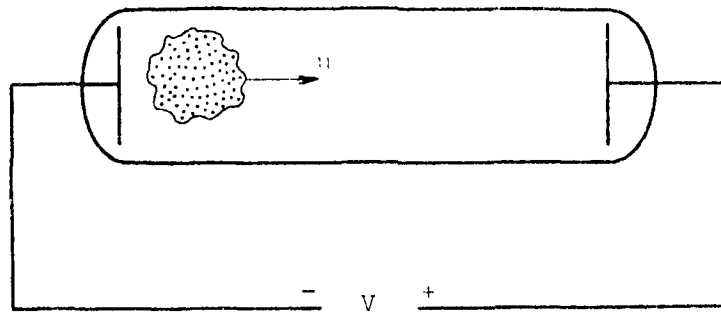


Figure 4-2: A swarm of electrons between two electrodes.

mobility). Clearly, based on the discussion above,  $\mu$  cannot be a constant.

A simple formula for  $\mu$  can be found by assuming that, at every collision, the charged particle loses all its momentum parallel to the field (Howatson, 1976, p.36). The average momentum of the charged particle in the  $E$  direction is  $um$ , and the rate of loss of momentum is thus  $f_c um$ . Newton's second law tells us the rate of change of momentum of a body is equal to the force exerted on it,  $qE$  in this case. Thus

$$qE = f_c um$$

or

$$\mu = u/E = q/mf_c = q^2/m\langle v \rangle \quad (4.2)$$

In fact, the charged particle may have some residual motion in the field direction, and equation 4.2 must be modified (Kuffel and Abdallah, 1971, p.14). Typically, the proportionality between

$E/p$  and  $u$  holds up to about 10 v/(cm)(torr) for ions and substantially less for electrons.

The ratio  $E/p$  is an important scaling parameter which we will see again in Chapter 6 when we consider the breakdown process. It is important because the energy gained along one mean free path is essentially constant for a given  $E/p$  ratio. The drift velocity is frequently plotted as a function of  $E/p$ ; however, during the last ten years or so, the ratio of electric field to gas density,  $E/N$ , has also been used. Figure 4-3 shows curves of  $u$  versus  $E/N$  for a family of gas mixtures which were investigated for use in repetitive opening switches (Christophorou and Hunter, 1983, p.33).

The mobility of charged particles, particularly electrons, is extremely important to the electrical breakdown process. It can also be used to find the conductivity of the gas. The current density,  $J$ , is the sum of a component due to the electrons,  $J_e$ , and a component due to ions,  $J_i$ . The electron and ion current densities are in turn  $N_e q_e u$  and  $N_i q_i u_i$  where  $N_e$  and  $N_i$  are the densities of electrons and ions. If the ions are singly charged,

$$J = J_e + J_i = q_e(N_e u_e + N_i u_i)$$

or

$$J = q_e E (N_e \mu_e + N_i \mu_i)$$

The conductivity is then found to be

$$\sigma = J/E = q_e (N_e \mu_e + N_i \mu_i) \quad (4.3)$$

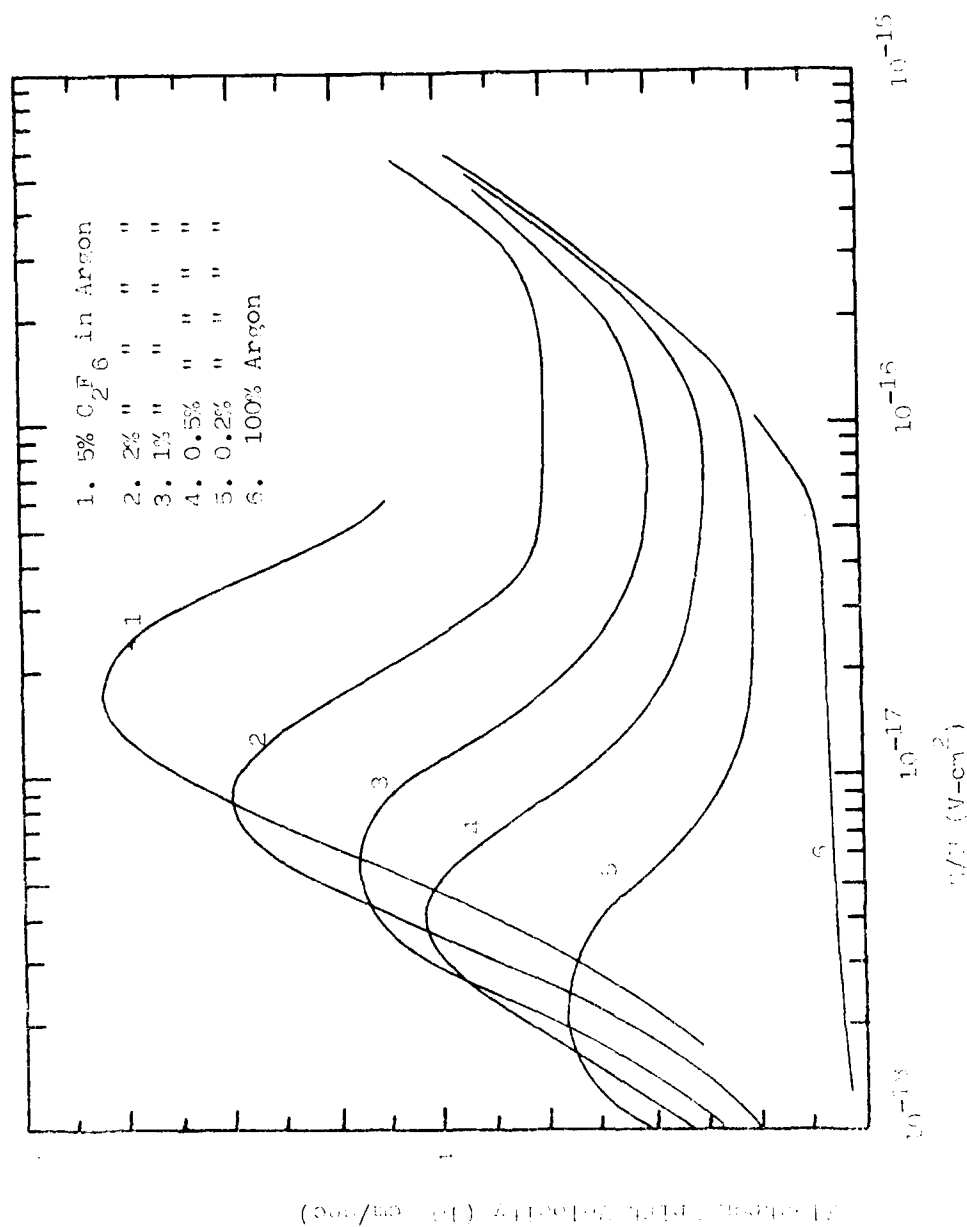


Figure 4-3 Electron drift velocities for several gases (after Christophorou and Hunter, 1983).

Typically,  $\mu_e \gg \mu_i$ , so most of the conductivity results from the electrons; however, if a space charge causes  $N_i \gg N_e$ , both current components may be significant (Howatson, 1976, p.36).

#### 4.3 Diffusion

If a gas has a non-uniform concentration, it will eventually reach a uniform concentration in its container through the random collision process described earlier. Likewise, if a barrier is removed from between two separate gases, they will become uniformly mixed. The process by which a state of equilibrium is reached is called diffusion. Diffusion occurs whenever there is a non-uniform concentration, and involves the migration of particles (molecules, ions, or electrons) from regions of higher concentration to regions of lower concentration. During an electrical discharge, diffusion causes deionization of higher ionized regions and ionization of lower ionized regions. As ions and electrons diffuse to the container walls they recombine (see section 3.5)

Diffusion occurs in all directions, but for simplicity, we will consider a hypothetical system in which there is a concentration gradient,  $\delta N/\delta x$ , only in the x direction. The flux of particles,  $\Gamma$ , across a unit area is given by

$$\Gamma = -D \frac{\delta N}{\delta x} \quad (4.4)$$

where D is called the diffusion coefficient. The flow of particles along a concentration gradient is similar to the flow of charged particles along an electric field line and can be described by a drift velocity.

The diffusion drift velocity for ions is given by

$$u_i = \frac{\Gamma_i}{N_i} = - \frac{D_i}{N_i} \frac{\delta N_i}{\delta x} = - \frac{D_i}{p_i} \frac{\delta p_i}{\delta x} \quad (4.5)$$

where  $N_i$  is the ion density and  $p_i$  is the partial pressure of ions. Now, suppose an electric field is applied which would cause a drift velocity,  $-\mu_i E$ , equal and opposite to that caused by the concentration gradient. Equating the two drift velocities yields

$$-\mu_i E = - \frac{D_i}{p_i} \frac{\delta p_i}{\delta x} = - \frac{D_i}{N_i kT} \frac{\delta p_i}{\delta x} \quad (4.6)$$

For the drift velocities to be equal, the diffusion force must be equal to the electric field force, or

$$\frac{1}{N_i} \frac{\delta p_i}{\delta x} = q_e E \quad (4.7)$$

Substituting 4.7 into 4.6 and rearranging yields

$$\frac{D_i}{\mu_i} = \frac{kT}{q_e} \quad (4.8)$$

Equation 4.8 is known as the Einstein relation and relates diffusion to mobility (Howatson, 1976, p.41). Substituting for  $\mu_i$

$$D_i = kT/mf_c \quad (4.9)$$

In general, negative ions have a higher mobility than positive ions; therefore, they diffuse at a faster rate (Kuffel and Abdullhan, 1971, p.17). Similarly, electrons diffuse much faster than ions. Diffusion of electrons and positive ions at different rates results in an important phenomena known as ambipolar diffusion.

#### 4.4 Ambipolar Diffusion

Consider a region, such as an arc channel, containing an equal number of positive ions and electrons. As the electrons "outrace" the ions, an electric field is established due to the separation of charges. This field will act to slow down the electrons and to speed up the positive ions. Eventually, a state of equilibrium is reached in which the electrons and ions diffuse at the same rate. This condition is called ambipolar diffusion.

Considering, again, a single direction system, the flux of electrons will be the difference between the diffusion effect and the electric field effect

$$\Gamma_e = -D_e \frac{\delta N_e}{\delta x} - N_e \mu_e E \quad (4.10)$$

The flux of positive ions will result from the two forces acting together

$$\Gamma_i = -D_i \frac{\delta N_i}{\delta x} + N_i \mu_i E \quad (4.11)$$

If we assume the charge separation is small compared to the charge density, then  $N_e = N_i = N$  and  $\delta N_e / \delta x = \delta N_i / \delta x = \delta N / \delta x$ . The ambipolar diffusion is defined as

$$\Gamma = \Gamma_e = \Gamma_i = -D_a (\delta N / \delta x) \quad (4.12)$$

where  $D_a$  is the ambipolar diffusion constant. Eliminating  $E$  from equations 4.10 and 4.11 and substituting 4.12 yields

$$D_a = \frac{D_e \mu_i + D_i \mu_e}{\mu_e + \mu_i} \approx \frac{D_e \mu_i + D_i \mu_e}{\mu_e} \quad (4.13)$$



The approximation is made since  $\mu_e \gg \mu_i$ . Applying the Einstein relation to 4.13, we obtain

$$D_a \approx D_i(1 + T_e/T_i) \quad (4.14)$$

or, if  $T_e = T_i$

$$D_a \approx 2D_i \quad (4.15)$$

Equations 4.14 and 4.15 are only approximate because the Einstein relation is not exact for electrons; however, they illustrate a couple important points. First, from 4.14, the ambipolar diffusion rate increases with electron temperature. Second, if  $T_e$  is the same as the gas temperature, then the ambipolar diffusion rate is of the same order as positive ion diffusion. This means the electrons slow down much more than the positive ions speed up (Kuffel and Abdullah, 1971, p.18). We will see later that  $T_e$  may be substantially different than  $T_i$  for certain types of discharges.

#### 4.5 Summary

In this chapter, we have looked briefly at the motion of charged particles through a gas, resulting either from an applied electric field or from a concentration difference. Motion due to an electric field is called mobility, while motion due to concentration effects is called diffusion. In both cases, the particle assumes a drift velocity. The drift velocity is much higher for electrons than for ions because the electron is so much lighter. Diffusion and mobility are related by Einstein's relation; although, the relation is only approximate for electrons. Finally, the concept of ambipolar diffusion is extremely

important in the analysis of gas discharges. Ambipolar diffusion occurs when the separation of electrons and positive ions causes an electric field which slows down the diffusion of electrons while speeding up that of the ions.

#### REFERENCES :

- Christophorou, L.G. and Hunter, S.R. (1983). Basic Studies of Gases for Fast Switches. Oak Ridge National Laboratory, Oak Ridge, Tennessee 37830. DTIC AD# A126343.
- Howatson, A.M. (1976). An Introduction to Gas Discharges (2nd edition). Pergamon Press, Oxford.
- Kuffel, E. and Abdullah, M. (1971). High Voltage Engineering. Pergamon Press, Oxford.
- Meek, J.M. and Craggs, J.D. (ed) (1978). Electrical Breakdown of Gases. John Wiley & Sons, Chichester.

THIS PAGE INTENTIONALLY BLANK

## CHAPTER 5

### ELECTRON EMISSION FROM METALS

#### 5.1 Introduction

The last three chapters have shown electrons and ions can form in a gas, and they conduct current by drifting along electric field lines. For a current to flow through a circuit consisting of electrodes separated by gas (recall Figure 4-1), there must be some process for the electrons to leave the metal electrode (called the cathode) and enter the gas volume. This process is known as electron emission.

Under normal circumstances, an electron is unable to leave the electrode because it is held in by electrostatic forces. However, if the electron is able to gain sufficient energy, it may be able to escape. There are five important ways that electron emission can take place:

a. If the metal is heated to a high temperature, electrons may gain enough energy to escape. This is thermionic emission.

b. An electric field, normal to the metal surface, may lower the energy required for an electron to escape so that less heating is required. This is called field enhanced thermionic or Schottky emission.

c. Very high electric fields may pull electrons out of cold metal through a "tunneling" effect called field or cold emission.

d. Photons striking the metal surface may excite an electron enough to allow its escape by photoelectric emission.

e. Finally, electron or ion bombardment of the metal surface may result in secondary emission.

This chapter will discuss each type of emission, but first it will be necessary to consider the physical description of metals.

### 5.2 The Theory of Electrons in Metals

The beginning of chapter 3 stated a metal could be visualized as a lattice-like array of positive ions surrounded by a sea of electrons which are relatively free to move about. The sea of electrons includes only the outer, or valence, electrons, since the inner electrons are tightly bound to the nuclei. However, there is still a very large number of electrons available. For example, copper has one free electron per atom, which means there are some  $8.4 \times 10^{22}$  free electrons per cubic centimeter (Rector, 1948, p.7). Drude developed the free electron theory of metals in 1900, and Lorentz extended it by applying Maxwell-Boltzmann statistics to the electrons. Unfortunately, the Maxwell-Boltzmann distribution does not apply to electrons in a metal, due to their light mass and high density. Thus, the classical free electron theory was unable to correctly predict some basic properties of metals (Azaroff and Brophy, 1963, p.146).

In 1928, Sommerfeld applied Fermi-Dirac statistics to Drude's theory, giving us the quantum free electron theory. This theory predicts most metallic properties and provides most of the

background for studying electron emission. However, this theory has limitations--it cannot explain why some crystals have metallic properties and others do not. The more general band theory is required to provide the full picture (Kittel, 1956, p.270).

In this section, we will look briefly at Fermi-Dirac statistics and the band theory. Then, we will look at a one dimensional model of a boundary between a metal and a vacuum. This model will provide the foundation for understanding the different types of electron emission.

#### 5.2.1 Fermi-Dirac Statistics

Quantum theory describes the energy of a free electron in terms of three quantum numbers and a spin number. Each energy state is unique or quantized; however, the separation between states may be less than  $10^{-18}$  eV. Thus, the energy states appear to be continuous. The occupation of energy states is governed by the Pauli exclusion and the Heisenberg uncertainty principles.

The Pauli exclusion principle states no two electrons can have the same quantum numbers and spin; that is, only one electron can occupy each energy state. The Heisenberg uncertainty principle states it is meaningless to prescribe a specific distribution of electron energies at any given time. Rather, one must consider the occupation probabilities, which are specified by the Fermi-Dirac distribution function.

If  $E_i$  is the energy level of the  $i$  th state, then the probability of the state being occupied is given by

$$f(E_i) = \frac{1}{\exp[(E_i - E_f)/kT] + 1} \quad (5.1)$$

where  $E_f$  is a constant of the metal, called the Fermi energy. The significance of the Fermi energy is best understood by plotting the distribution function.

Figure 5-1 shows plots of the Fermi-Dirac distribution at  $T = 0^\circ\text{K}$  (absolute zero) and at  $T = 300^\circ\text{K}$  (room temperature). Consider, first, the curve for absolute zero. As  $T$  goes to zero, the argument of the exponential in equation 5.1 goes to  $\pm \infty$ . Specifically, for  $E_i < E_f$ , the argument goes to  $-\infty$ , the exponential goes to zero, and  $f(E_i)$  goes to one. However, for  $E_i > E_f$ , the argument goes to  $+\infty$ , the exponential blows up, and  $f(E_i)$  goes to zero. Thus, every energy state below  $E_f$  is occupied, and every state above  $E_f$  is empty. The Fermi level can be defined as the highest occupied energy state at absolute zero. Note, this is fundamentally different than a gas where it is assumed the molecules all have zero energy at absolute zero. The difference results from the application of the exclusion principle which makes it impossible for all the electrons to have zero energy.

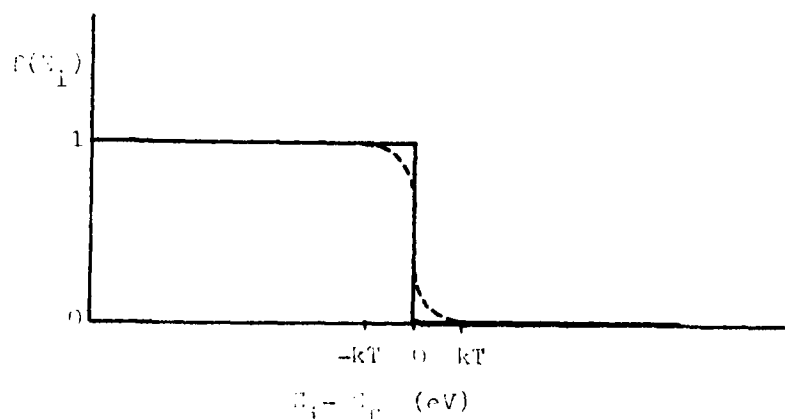


Figure 5-1: The Fermi-Dirac distribution for  $T=0^\circ\text{K}$  and  $T=300^\circ\text{K}$ .

Next, consider the curve at room temperature. At any temperature greater than zero, it is possible for some electrons to have energies greater than the Fermi energy. However, for  $(E_i - E_f) \ll -kT$ , the exponential will be much less than one, and  $f(E_i)$  will still be one. Similarly, for  $(E_i - E_f) \gg kT$ , the exponential will grow very large, and  $f(E_i)$  will quickly tend toward zero. For  $|E_i - E_f| < kT$ , the value for  $f(E_i)$  will lie between zero and one, as shown by the rounded portions of the room temperature curve. An electron can expect to gain an amount of energy equal to about  $kT$  by heating. At room temperature,  $kT$  is approximately 0.0259 eV. Physically, this means only electrons having energies near the Fermi energy are likely to be excited by heating. The lower energy electrons are "locked in" by the exclusion principle, since all the states immediately above are already filled. Table 2-1 shows values for several important emission constants of several materials. The first column shows the Fermi energy; the remaining columns will be discussed in the following sections.

### 5.2.2 Electron Band Theory

Since no two electrons can have the same energy level, the question that might arise is, "What happens to electrons from individual atoms, which had the same energy level, when the atoms are brought together to form a molecule or crystal?" The band theory solves this by proposing that the levels in the atoms split whenever the orbitals belonging to that level overlap. Figure 5-2 shows two examples. In both, we see the levels expanding as the



Table 5-1: Emission Constants of Materials

Material	$E_f$ Fermi Energy (eV)	$\Phi_t$ Thermionic Work Function (eV)	$\Phi_p$ Photoelectric Work Function (eV)	A Thermionic Constant (A/cm <sup>2</sup> °K <sup>2</sup> )
Ag	5.51 <sup>4</sup>	4.08 <sup>1</sup> , 4.8 <sup>4</sup>	4.74 <sup>5</sup>	60.2 <sup>2</sup>
Al		(2.5-3.6) <sup>5</sup>	3.57 <sup>2</sup>	
Au	5.51 <sup>4</sup>	(4.42-4.92) <sup>5</sup>	4.73 <sup>2</sup> , 4.9 <sup>1</sup>	60.2 <sup>2</sup>
BaO		0.95 <sup>3</sup> , 1.7 <sup>6</sup>		0.1 <sup>3</sup> , 2.5 <sup>2</sup>
Ca		(2.24-3.2) <sup>5</sup>		60 <sup>5</sup>
C		3.93 <sup>2</sup> , 4.5 <sup>6</sup>	4.82 <sup>2</sup>	5.93 <sup>2</sup> , 48 <sup>6</sup>
Cu	7.04 <sup>4</sup>	4.5 <sup>6</sup>	(4.1-4.5) <sup>2</sup>	65 <sup>2</sup>
Cs	1.53 <sup>1</sup>	1.81 <sup>1</sup> , 1.94 <sup>6</sup>	1.90 <sup>1</sup>	160 <sup>4</sup>
Fe		4.5 <sup>6</sup> , 4.72 <sup>1</sup>	4.48 <sup>1</sup> , 4.77 <sup>5</sup>	26 <sup>1</sup>
Hg		4.52 <sup>5</sup>	4.53 <sup>2</sup>	
K	2.14 <sup>1</sup>	(1.76-2.25) <sup>5</sup>	2.24 <sup>5</sup>	
Li	4.72 <sup>1</sup>	(2.1-2.9) <sup>5</sup>	2.28 <sup>5</sup>	
Mg		2.42 <sup>5</sup> , 3.6 <sup>6</sup>		
Mo		4.15 <sup>5</sup> , 4.3 <sup>1</sup>	4.15 <sup>5</sup>	55 <sup>1</sup> , 60 <sup>5</sup>
Ni		4.61 <sup>1</sup> , 4.9 <sup>6</sup>	4.01 <sup>1</sup> , 5.01 <sup>2</sup>	30 <sup>1</sup> , 27 <sup>2</sup>
Pt		5.3 <sup>4</sup> , 6.27 <sup>2</sup>	6.3 <sup>1</sup>	32 <sup>1</sup>
W		4.5 <sup>3</sup>	4.49 <sup>4</sup> , 4.58 <sup>1</sup>	60 <sup>3</sup> , 75 <sup>4</sup>
W/Ba		1.56 <sup>4</sup>		1.5 <sup>4</sup>
W/Cs		1.36 <sup>5</sup>		3.2 <sup>5</sup>
W/Th		2.63 <sup>5</sup>		3 <sup>5</sup>

## References:

1. Azaroff and Brophy (1963)
2. Cobine (1957)
3. Fink and Christiansen (1982)
4. Kittel (1956)
5. Rector (1948)
6. VonEngel (1965)

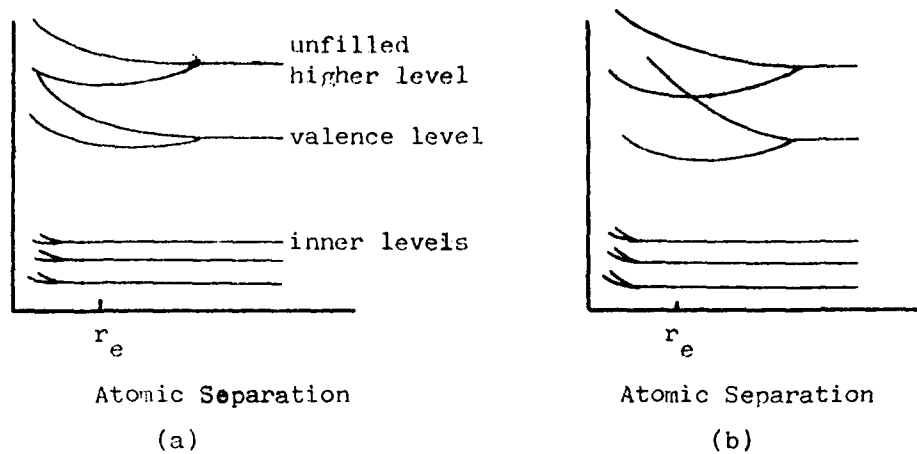


Figure 5-2: Sketch showing how energy levels split as the inter-atomic separation decreases: (a) an insulator and (b) a metal (after Azaroff and Brophy, 1963, p.180)

atoms are brought closer together in a crystal. Figure 5-2a shows a case where the energy bands do not overlap at the equilibrium separation,  $r_e$ . The gap between the filled valence band and the empty upper level (conduction band) is called a forbidden band--no electron can occupy any energy level within it. Under normal conditions, the valence electrons cannot move up to the conduction band, and this material would be an insulator.

In figure 5-2b, however, the valence band and upper band overlap. This material will conduct since electrons can move up to the conduction band with only a slight increase in energy. In all metal crystals, the valence band has been found to overlap the conduction band (Azaroff and Brophy, 1963, p.184). With these basics in hand, we can now consider what is required for a material to emit electrons.

### 5.2.3 A Metal-Vacuum Boundary

The valence electrons of a metal can be considered to be imprisoned in a potential well of depth  $E_0$ . Figure 5-3 shows a one dimensional model first used by Schottky (Meek and Craggs, 1978, p.131). While it appears very busy, it is not as bad as it looks. The model shows a metal-vacuum interface and a superimposed potential energy diagram. To the left of the y-axis is the metal emitter, and to the right is the vacuum. The y-axis is used for energy and the x-axis is used for distance from the emitter surface.

At 0°K, the electrons lie at the bottom of the potential well, possessing energies between  $E_0$  and  $\Phi$ . The difference between  $E_0$  and  $\Phi$  is the Fermi energy,  $E_f$ , as shown. If an electron is removed from the metal, it will leave behind an image charge which results in a potential,  $-q_e^2/4\pi\epsilon_0 x$ .<sup>1</sup> This potential is shown as curve 1 in figure 5-3. An electron which is an infinite distance away from the emitter surface would have zero potential energy. Thus an electron in the Fermi level would require the addition of  $\Phi$  eV to its energy to escape.

The amount of energy,  $\Phi$ , required to escape from the Fermi level is known as the work function. It varies for each material, and its value may be influenced by the presence of surface contaminants and irregularities. The energy for an electron may

---

<sup>1</sup>There is a discontinuity at the metal-vacuum boundary which we will neglect here, because many other factors contribute more significant errors (Meek and Craggs, 1978, p.132).

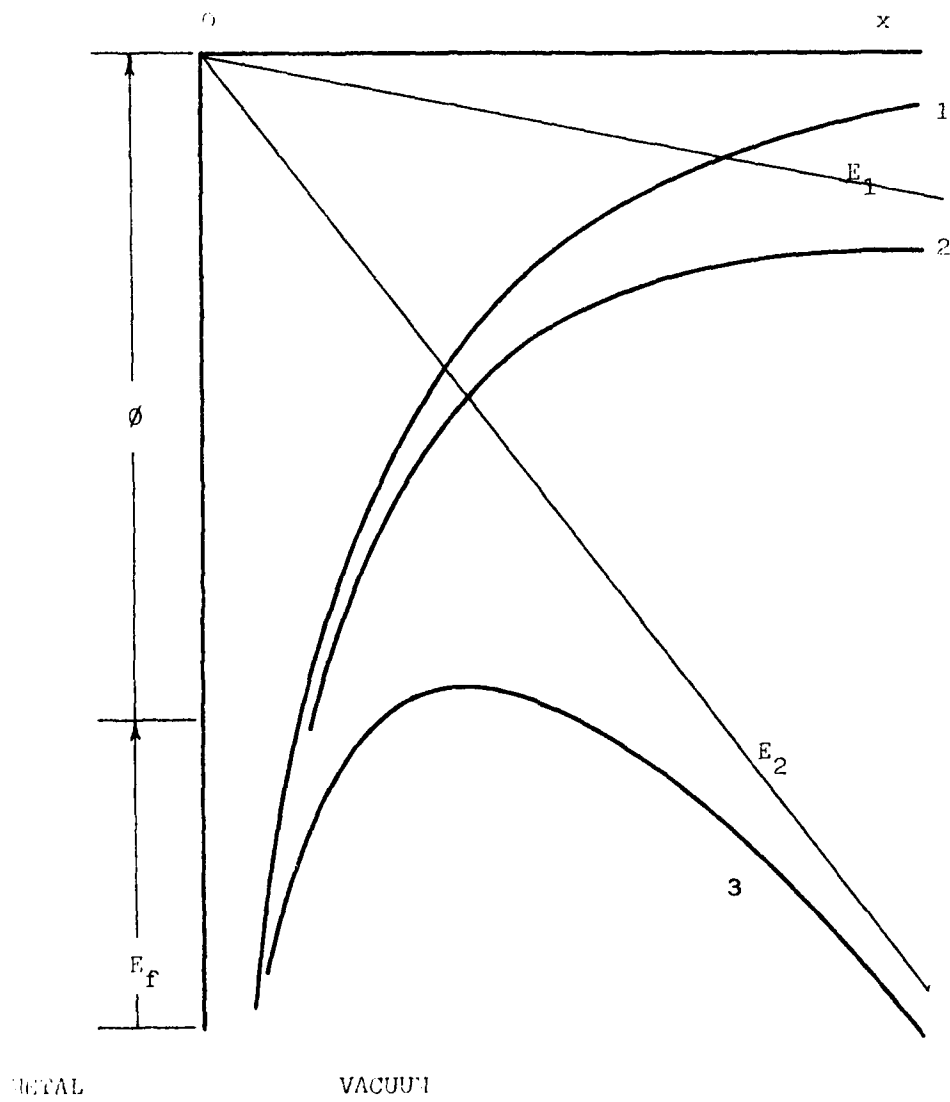


Figure 5-3: Potential energy diagram at a metal-vacuum interface for several conditions

be provided by heating or by photon absorption; however,  $\Phi$  may be slightly different for the two cases. Table 2-1 shows  $\Phi_t$  and  $\Phi_p$ , the work functions for thermionic and photoelectric emission, respectively. Note the low values for barium and caesium on tungsten. Such materials are very useful for cathode filaments in thyratrons and vacuum tubes.

Next, consider the addition of an external electric field normal to the emitter surface. The potential distribution will be increasingly negative in the x-direction, and will help pull electrons away from the emitter. Curves  $E_1$  and  $E_2$  in figure 5-3 show the potential due to a weak and a strong electric field, respectively. The potential due to the electric field combines with the image charge potential, resulting in a lowering of the potential barrier seen by an electron inside the metal. The reduced potential barriers are shown in curves 2 and 3 of figure 5-3. Thus, an electron requires an amount of energy less than  $\Phi$  to escape. When the energy is provided by heating, a lower temperature is required. This is known as Schottky emission.

Finally, note the potential barrier becomes narrower for strong external fields (curve 3). Quantum theory predicts, and experiments show, that electrons may be pulled out of the metal at very high field intensities. This is a tunneling phenomenon and is called field or cold emission.

Figure 5-3 provides the basis for understanding all the types of electron emission from metals. Next, we will consider the formulas and some specifics for each type of emission.

### 5.3 Thermionic Emission

In section 5.2.1, we saw that electrons are able to occupy energy states above the Fermi level as the temperature of the metal increases. When the temperature is increased to very high levels (several thousand degrees for most materials), some electrons gain enough energy to escape from the metal. This process is known as thermionic emission and was first observed by Thomas Edison (Nottingham, 1956, p.7). The thermionic emitter is the most frequently used type of cathode. Examples include the filament in the picture tube of a television set, thyratrons, and vacuum tubes.

Richardson derived two equations for thermionic emission, the second of which is

$$J_{th} = AT^2 \exp(-q_e \Phi / kT) \quad (5.2)$$

where  $J$  is the current density in  $A/cm^2$ ,  $A$  is a constant (discussed below),  $\Phi$  is the work function in volts,  $T$  is the temperature in  $^{\circ}K$ ,  $k$  is Boltzmann's constant, and  $q_e$  is the charge of an electron in coulombs. His first equation was similar in form, but the exponent of  $T$  was 0.5 instead of 2.0. Both equations predicted values within experimental error of the day, but Dushman provided a more rigorous derivation which showed this version to be correct. Thus, equation 5.2 is commonly referred to as the Richardson-Dushman equation. A quick calculation will show that thermionic emission is negligible at moderate temperatures. For example, at  $T = 273^{\circ}K$  and  $\Phi = 3eV$ , the current density is only  $\approx 10^{-43} A/cm^2$ .

The form of the curve represented by equation 5.2 is shown in figure 5-4a. This curve represents a so-called saturation current--it is assumed there is an electric field which is high enough to carry every emitted electron to the anode. If, in fact, the electric field is fixed, then temperature saturation occurs, and the current levels off, even if the temperature is increased further. This effect is shown for two electric fields ( $E_2 > E_1$ ) in figure 5-4b.

The constant  $A$ , in equation 5.2, is called the thermionic emission constant. Theoretically, it is a universal constant for all metals, having a value

$$A = 4\pi m_e q_e k^2 / h^2 = 120.4 \text{ A/(cm}^2)(^\circ\text{K}^2) \quad (5.3)$$

Experimentally,  $A$  has a value of about 60 for most metals, with some extreme variations. The last column of table 2-1 shows values of  $A$  for several materials. The discrepancy between theory and experiment has been attributed to several possibilities including: approximations in the derivation of equation 5.2, reflection of electrons at the surface of the metal, and neglect of the temperature variation of  $\phi$  (Rector, 1948, p.13).

#### 5.4 Schottky Emission

As the field normal to the emitting surface increases, the potential barrier is lowered. At a given temperature, therefore, more electrons will be able to escape. Schottky's equation describes this phenomenon

$$J = J_{th} \exp(43.89\sqrt{E}/T) \quad (5.4)$$

where  $E$  is the electric field in volts/meter.

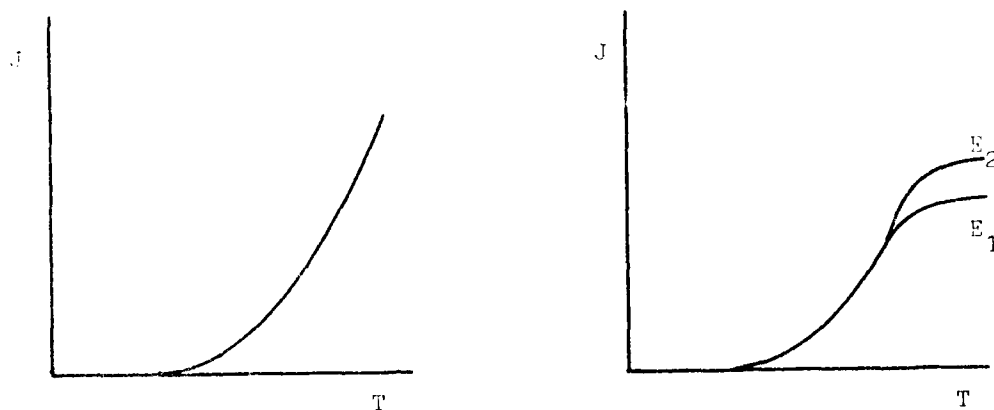


Figure 5-4: Curves showing the form of the Richardson-Dushman equation. (a) saturation current (b) temperature saturation

The form of the equation is illustrated by figure 5-5, which shows  $J$  vs  $E$  at a constant temperature. With purely thermionic emission, we would expect the current to increase with the field until all the thermionically emitted electrons are collected. At that point, field saturation (shown by the dotted line) should occur. However, the effect of field enhancement is to allow the current to continue to build up, as shown by the solid line. The effect is negligible at low values of  $E$ , and the equation does not apply to composite surfaces (Cobine, 1957, p.118).



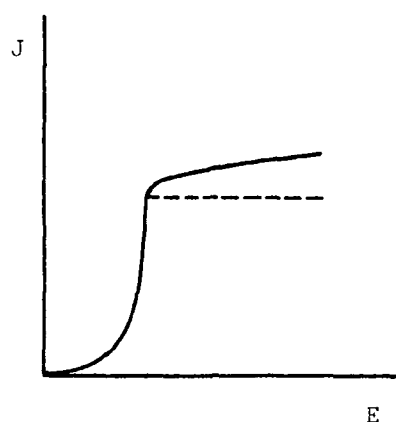


Figure 5-5: Curve showing thermionic current as a function of the electric field for fixed temperature. Dotted line shows field saturation. Solid line shows enhancement due to Schottky effect.

### 5.5 Field Emission

The thermionic and Schottky emission currents are completely negligible at room temperature. However, if a very strong field (typically  $>10^7$  v/cm) is applied to the cathode surface, a measurable current ( $\approx \mu\text{Amps}$ ) results (Alston, 1968, p.99). This is known as field or cold emission, and is capable of producing current densities of the order of thousands of amperes per  $\text{cm}^2$ .

A history of the analysis of field emission is provided by Good and Muller (1956, p.176). Fowler and Nordheim used the wave equation to derive the following expression for the emitted current at absolute zero

$$J = \frac{1.541 \times 10^{-6} E^2}{\Phi t^2(y)} \exp \left[ \frac{-6.831 \times 10^7 \Phi^{1.5}}{E} v(y) \right] \quad (5.5)$$

where  $J$  is in  $\text{A/cm}^2$  and  $V$  is in  $\text{V/cm}$ . The values  $v(y)$  and  $t(y)$  are functions, involving elliptic integrals, of the variable

$$y = 3.795 \times 10^{-4} \sqrt{E/\Phi}$$

The variable  $y$  is constrained to values from zero to one, and Miller (1966) provided tables of  $v(y)$  and  $t(y)$  for the entire range at intervals of 0.01. Similarly, Dolan (1953) calculated tables of the common log of  $J$  for various values of  $\Phi$  and  $E$ . Table 5-2 shows selected values. Values between those shown can be found by interpolation.

In calculating the tables, Dolan assumed  $t(y)=1.0$ . In fact, as  $y$  goes from zero to one,  $1/t^2(y)$  goes from 1.0 to 0.81. Thus the currents obtained from the tables are high by from zero to 25%. This accuracy is acceptable for two reasons. First, the field emission tends to increase somewhat with temperature (Meek and Craggs, 1978, p.134 provide a temperature corrected equation). Second, and more importantly, the value used for  $E$  is the peak local field intensity which is calculated on the basis of approximate field intensification factors.

Field emission is typically the least important source of electrons in gas discharges, but it can be significant in vacuum devices and between the grid and anode in thyratrons. It is also the subject of a lot of research because of the potential it has for achieving very high current densities.

#### 5.6 Photoelectric Emission

In 1887, Heinrich Hertz observed that electrons could be emitted from a metal surface as a result of light falling on it. In 1899, researchers made two important observations. First, increasing the intensity of the light increased the number of electrons, but did not affect their kinetic energy. Second, the

Table 5-2: Common Logarithms of Field Emission Current Density  
(Dolan, 1953)

E ( $10^7$ V/cm)	$\Phi$ (ev)							
	2.0	2.5	3.0	3.5	4.0	4.5	5.0	6.3
1.0	3.04							
2.0	7.48	5.59	3.56	1.39				
3.0		7.71	6.30	4.82	3.25	1.61		
4.0		8.80	6.30	6.57	5.37	4.11	2.80	
5.0			8.59	7.65	6.66	5.64	4.58	1.62
6.0			9.18	8.38	7.55	6.68	5.78	3.28
7.0				8.92	8.19	7.43	6.65	4.48
8.0				9.33	8.68	8.01	7.31	5.40
9.0					9.07	8.46	7.84	6.12
10.0					9.39	8.83	8.26	6.69
12.0						9.40	8.91	7.58
14.0						9.83	9.39	8.23
16.0							9.76	8.72
18.0								9.12
20.0								9.44

energy of the emitted electrons increased with the frequency,  $\nu$ , of the illumination. Finally, in 1905, Einstein proposed that light consisted of quanta, each having energy  $h\nu$ .

Consider a photon, of energy  $h\nu$ , impinging on a metal surface. If the photon is absorbed by an electron and  $h\nu > \phi_p$ , the electron may be emitted. The probability, however, is very low due to reflection and reabsorption effects. Since the photon energy must be greater than the work function, we can define a threshold frequency,  $\nu_0$ , at which photoelectric emission can begin

$$h\nu_0 = q_e\phi_p \quad (5.6)$$

The difference between the photon energy and the work function represents the energy which may be converted to kinetic energy of the electron. Einstein's photoelectric equation states

$$m_e v_{\max}^2 / 2 = h\nu - q_e\phi_p \quad (5.7)$$

where  $v_{\max}$  is the maximum velocity of the emitted electron. The velocities of the emitted electrons are distributed between zero and  $v_{\max}$ , with a peak at about  $0.4v_{\max}$ .

Figure 5-6 shows a schematic illustration of the photoelectric yield,  $\gamma_p$ , as a function of wavelength. As the wavelength is reduced from the critical value, the yield increases to a maximum, which varies from 0.1 to 1.0 electrons/photon, depending on the material and surface condition. As the x-ray region is encountered, the photons have enough energy to knock inner shell electrons out of the metal. This effect is similar to that observed for photo-ionization. When an inner shell electron is knocked out,  $\phi_p$  must be replaced by the internal energy in

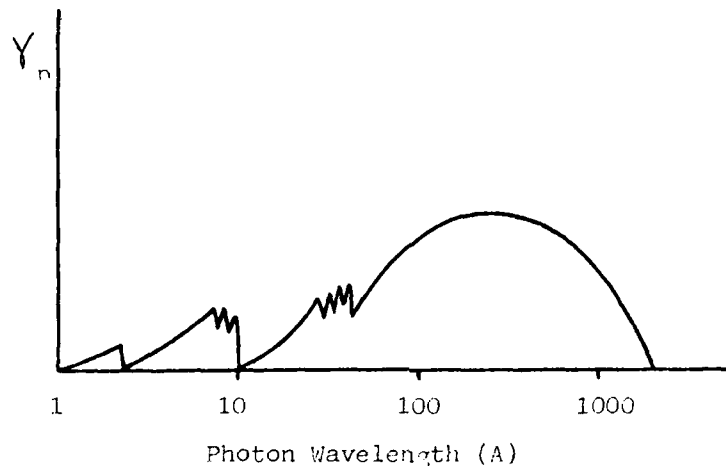


Figure 5-6: Typical photoelectric yield as a function of wavelength.

equation 5.7. Except for the alkali metals, most materials respond only the ultraviolet and below (VonEngel, 1965, p.101).

The electric breakdown of a gas usually requires a few electrons to start the process. These are often supplied by photoelectric emission and photo-ionization. In addition, the discharge produces photons which may cause secondary emission (see section 6.3). Thus, photoelectric emission is a very important process.

#### 5.7 Emission by Particle Bombardment

When an electron or ion collides with the cathode surface, it is possible for an electron to be emitted. These processes are referred to as secondary emission.

### 5.7.1 Emission by Electron Bombardment

If an electron strikes a surface, an electron may be emitted. The mechanism is not as well understood as others, but it cannot occur directly as the result of a collision, since that would violate the conservation of momentum (Rector, 1948, p.27). The secondary emission properties of a material are described by the yield,  $\delta$ , which is the number of secondary electrons emitted per primary electron.

The yield is found by launching a collimated electron beam at the material and measuring the rate and velocity distribution of all electrons leaving. Figure 5-7 shows the characteristic curve of the yield as a function of electron energy. Low energy electrons are unlikely to cause the release of an electron, while high energy electrons may penetrate too deeply to allow the secondary electron to reach the surface. Thus, the curve reaches a maximum value, as shown. Typically, for metals,  $\delta_{\max}$  is between 1.0 and 1.5; however, surface impurities may cause up to a four-fold increase in secondary emission (Cobine, 1957, p.113). The primary electron energy at  $\delta_{\max}$  is usually some several hundred electron volts. Calculating the yield is complicated because it is impossible to distinguish between primary and secondary electrons, except by their velocity.

Figure 5-8 shows a schematic diagram of the velocity or energy distribution of electrons leaving the target of an electron beam. The curve has three distinct regions as shown. Region I consists of primary electrons which were elastically scattered

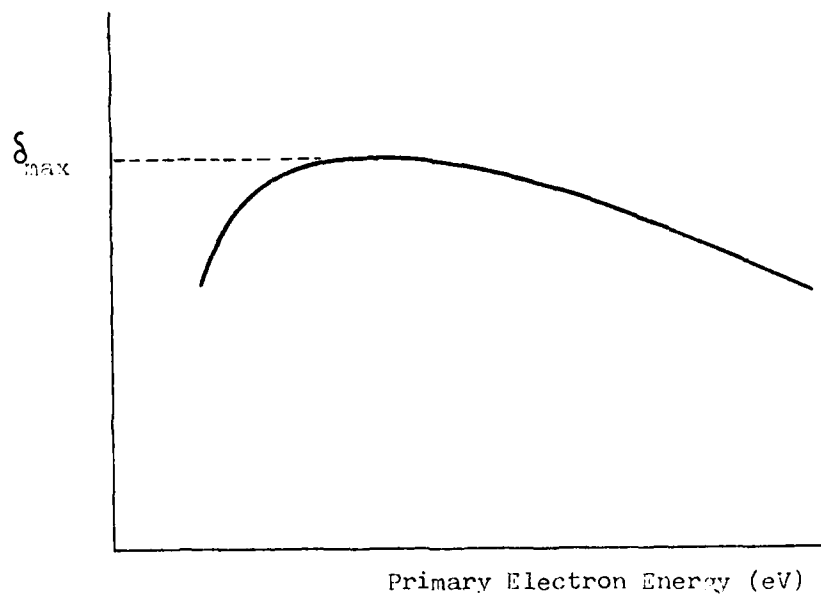


Figure 5-7: Secondary electron yield as a function of primary electron energy.

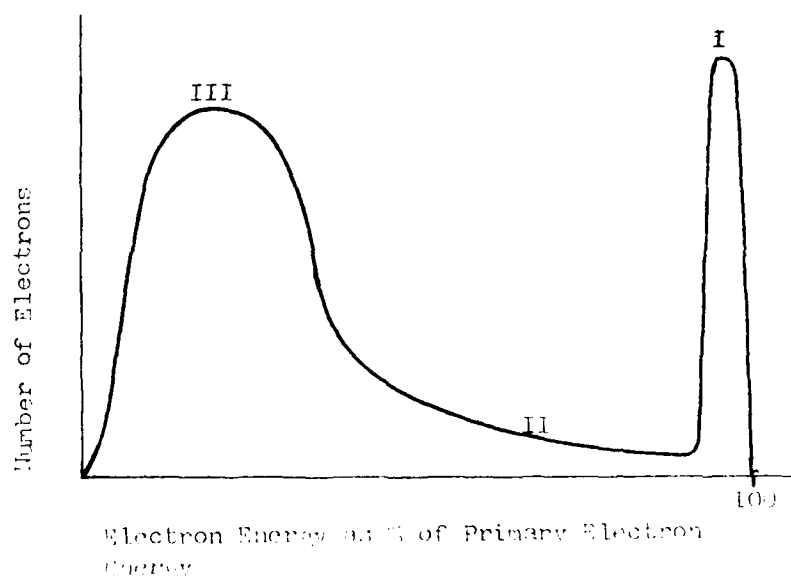


Figure 5-8: Distribution of secondary electron energies.

and have essentially 100% of their initial energy. Region II contains primarily inelastically scattered primary electrons, and region III contains mostly true secondary electrons, having energies of 0 to 30 eV (Brown, 1966, p.112).

In an electric discharge, the electric field draws the electrons away from the cathode. Thus, secondary emission by electron impact is not as important as secondary emission by positive ion impact.

#### 5.7.2 Emission by Positive Ion Bombardment

Positive ion bombardment of the cathode may result in secondary electron emission. The ion must actually release two electrons, one of which is necessary to neutralize the ion. Therefore, the minimum ion energy (kinetic plus ionization) for electron emission is twice the work function. If the ionization energy ( $q_e V_i$ ) of the ion is greater than  $2\Phi$ , there is a finite probability of electron emission occurring from an ion with zero velocity. The yield of electrons per incoming ion depends on the nature and energy of the ion, the emitter material, and the surface condition. At very low kinetic energies, as few as two or three electrons per 100 ions may be released. The yield rises with ion energy, reaching a peak of 3 to 10 electrons per ion at ion energies of  $10^5$  eV (VonEngel, 1965, p. 95). Most of the emitted electrons have energies of only 1 or 2 eV (Cobine, 1957, p.115).

When a metal is subjected to ion bombardment, some of the metal may be ejected. This process is called sputtering, and



results in a gradual deterioration of the metal surface. The rate of metal loss depends on the metal, the gas, the ion energy, the current density of incoming ions, the pressure, and the temperature. Aluminum, manganese, and zinc form a surface oxide which inhibits sputtering, while cadmium, silver, and lead sputter the most (Cobine, 1957, p.115).

Secondary emission by positive ion bombardment is one of the key factors in determining whether a discharge will become self-sustaining. This will be examined further in chapter 6.

#### 5.8 Summary

The emission of electrons from an electrode is an essential requirement for the formation and maintenance of any electrical discharge. In this chapter, we first considered some of the basic physics underlying the emission process. We then looked briefly at each type of emission, including thermionic, Schottky, field, photoelectric, and particle impact. All five types of emission are important and contribute to current flow.

This completes the first portion of this text which described some of the important physical phenomena occurring in gas discharges. In chapter 6, we will look at the electrical breakdown process in a gas. Chapters 7 to 9 will then describe the major types of gas discharges.

## REFERENCES :

- Alston, L.L. (ed.) (1968). High-Voltage Technology. Oxford University Press, London.
- Azaroff, L.V. and Brophy, J.J. (1963). Electronic Processes in Materials. McGraw-Hill, New York.
- Brown, S.C. (1966). Introduction to Electrical Discharges in Gases. John Wiley & Sons, New York.
- Cobine, J.D. (1957). Gaseous Conductors. Dover Publications, New York.
- Fink, D.G. and Christiansen, D. (ed.) (1982). Electronic Engineers' Handbook. McGraw-Hill, New York.
- Dolan, W.W. (1953). Physical Review. Vol. 91, p. 510.
- Good, R.H. and Muller, E.W. (1956). Encyclopedia of Physics. Vol. 21, p. 176. Springer-Verlag, Berlin.
- Kittel, C. (1956). Introduction to Solid State Physics. John Wiley & Sons, New York.
- Meek, J.M. and Craggs, J.D. (ed) (1978). Electrical Breakdown of Gases. John Wiley & Sons, Chichester.
- Miller, H.C. (1966). Journal of the Franklin Institute. Vol. 282, p. 383.
- Nottingham, W.B. (1956). Encyclopedia of Physics. Vol. 21, p. 1. Springer-Verlag, Berlin.
- Rector, B.E. (ed) (1948). Industrial Electronics Reference Book. John Wiley & Sons, New York.
- VonEngel, A. (1965). Ionized Gases. Clarendon Press, Oxford.

THIS PAGE INTENTIONALLY BLANK

## CHAPTER 6

### BREAKDOWN IN GASES

#### 6.1 INTRODUCTION

Electrical discharges in gas are customarily divided into two major types: self-sustained and non-self-sustained. To understand the distinction, consider again a simple two electrode system as shown in figure 6-1. The system is essentially the same as the one considered in chapter 4; however, the field is assumed to be uniform and an external source of photons is included. This external source could be stray radiation, or it could be deliberately applied. In either event, some free electrons are available as a result of photoionization or photoelectric emission. If no voltage is applied, the rate of formation of electron-ion pairs balances the recombination rate, and the number of charged particles is essentially constant. When a voltage is applied, the electrons will drift to the anode, and the current can be measured.

Figure 6-2 shows the current voltage characteristic for the two electrode system. At very low voltage (region I of the curve), the current increases with voltage. In this region, the electrons achieve a drift velocity which is proportional to the voltage. Thus, as the voltage increases, the electrons are collected at a faster rate. Eventually, however, the electrons are collected as fast as they form, and the current reaches a

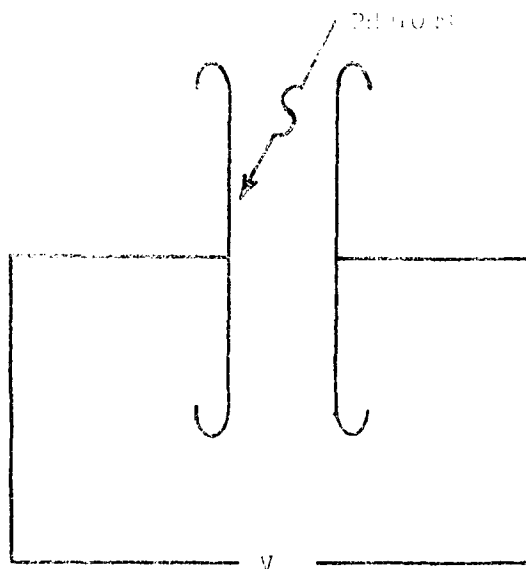


Figure 6-1: A uniform field, two electrode system.

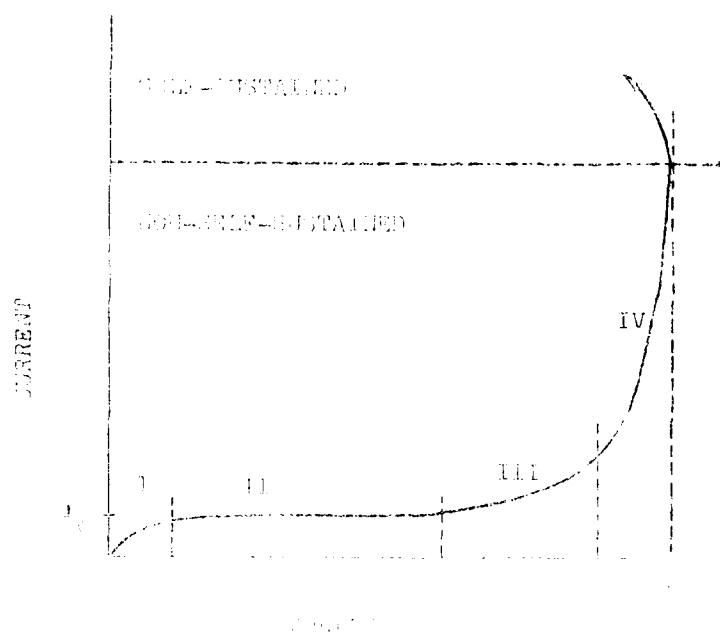


Figure 6-2: Current-voltage characteristics for the system of figure 6-1.

saturation level,  $I_0$  (region II of the curve). The saturation current is dependent on the level of illumination, but it is typically in the pA to  $\mu$ A range. Unless additional electrons can be produced, there will be no further increase in the current.

In fact, there is a considerable range of voltage for which the current is constant, as shown in the figure. However, J.S. Townsend determined that eventually the current begins to increase again with voltage--first slowly (region III) and then rapidly (region IV). These two regions are called Townsend discharges, and regions I to IV are collectively referred to as the dark discharges.

The dark discharges are so named because the density of excited molecules which emit visible light is exceedingly small. These discharges are non-self-sustaining. They require an external source to produce electrons through ionization or emission. The photons are the cause of the free electrons in this case, but the result would be the same for a thermionically emitting cathode.

Eventually, a voltage (shown as  $V_S$ ) is reached at which the current is growing extremely rapidly. The voltage,  $V_S$ , is called the sparking or breakdown voltage. At this point, the current typically has a value of some 10s of  $\mu$ As, and a sudden transition occurs. This transition, called a spark, may occur with explosive suddenness and marks the change to a self-sustained discharge. A self-sustained discharge is one in which each electron leaving the cathode establishes secondary processes that replace it with

another electron leaving the cathode. The type of discharge and the current are determined by a number of variables, including the gas, pressure, circuit impedance, and electrode material.

In chapters 7 through 9, we will examine the characteristics of the glow, corona, and arc discharges. In the remainder of this chapter, we will concern ourselves with the Townsend discharges and the breakdown process. First, we will examine the two regions of the Townsend discharges, and develop Townsend's criteria for gas breakdown. Then, we will consider the sparking voltage for uniform fields, time lags and theories of breakdown, non-uniform field breakdown, and surface flashover.

## 6.2 Townsend's First Ionization Coefficient

In chapter 3, we learned an electron can ionize a gas molecule by colliding with it. Similarly, in chapter 4, we learned an electron is accelerated by an electric field until it reaches an average drift velocity. Once it achieves its drift velocity, the electron effectively loses as much energy during a collision as it gains during acceleration. If the electric field is strong enough, an electron may gain enough energy to ionize a molecule. The original electron, and the new one, would then be accelerated, and further ionizing collisions might take place. The result would be a multiplication of charges or electron avalanche, as shown in figure 6-3<sup>1</sup>. Thus, instead of one electron arriving

---

<sup>1</sup>Figure 6-3 is for illustrative purposes only. It should not be interpreted to mean every collision is an ionizing one or that the electrons travel the same distance between every collision.

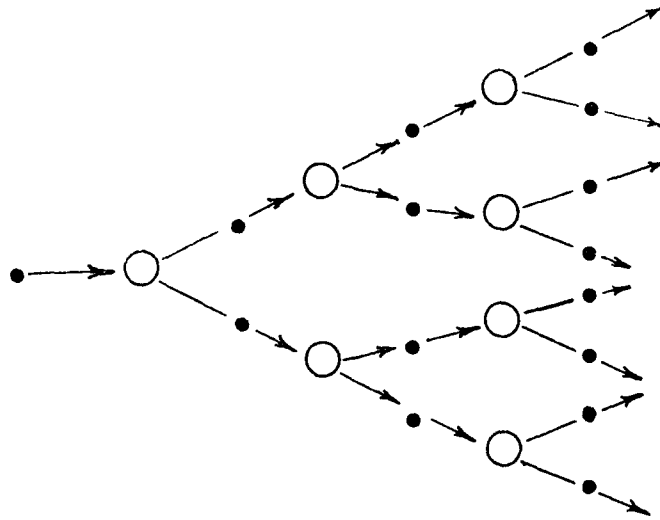


Figure 6-3: Generation of an electron avalanche.

at the anode, there would be an exponential buildup of current. The exact amount will be a function of  $E$  and  $\lambda$ . This process is known as field intensified ionization.

Townsend proposed that the buildup of current in region III of figure 6-2 was due to field intensified ionization. To explain it, he defined an ionization parameter,  $\alpha$ , as the number of electrons produced by an electron in one centimeter of travel in the direction of the field. This parameter is usually called Townsend's first ionization coefficient (VonEngel, 1965, p.172)



Now, assume a number of electrons,  $N_e$ , drift past a point between the electrodes. The number of new electrons created by them in travelling a small distance will be

$$dN_e = N_e \alpha dx \quad (6.1)$$

Integrating from the cathode ( $x=0$ ) to the anode ( $x=d$ ) yields

$$\int_{N_{e0}}^{N_e} \frac{dN_e}{N_e} = \int_0^d \alpha dx$$

or

$$N_e = N_{e0} e^{\alpha d} \quad (6.2)$$

where  $N_{e0}$  is the number of electrons leaving the cathode. Thus, for every electron leaving the cathode,  $e^{\alpha d}$  electrons arrive at the anode. Equation 6.2 can be rewritten in terms of current

$$I(d) = I_0 e^{\alpha d} \quad (6.3)$$

Equations 6.2 and 6.3 describe phenomena which are steady state but not self-sustaining. If the source of radiation is removed, the current will die out. In the steady state, the anode current must be equal to the cathode current, but the number of electrons arriving at the anode is  $e^{\alpha d}$  times the number leaving the cathode. For the currents to be equal, each electron leaving the cathode must be accompanied by  $(e^{\alpha d} - 1)$  positive ions arriving. Since the mobility of ions is much less than that of electrons, the ion concentration in the gap must be higher than the electron concentration. Figure 6-4 shows the steady state distribution of charges in a gap. These equations hold only for small values of current, since large space charges would distort the electric field (Cobine, 1957, p.145).

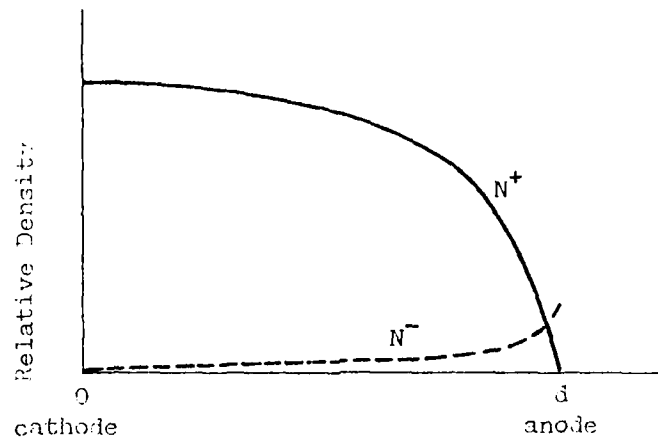


Figure 6-4: Relative densities of electrons and positive ions in a gap (after VonEngel, 1965, p.173).

Equation 6.3 can be rewritten as

$$\ln[I(d)/I_0] = \alpha d \quad (6.4)$$

This representation implies the relation between  $\ln[I(d)/I_0]$  and  $d$  will be linear, and the slope of the line will be  $\alpha$ . Remember, however,  $\alpha$  is a function of  $E$  and  $\lambda$  or  $E/p$ . Therefore, measurements made at varying electrode distances should be at the same value of  $E/p$ . Figures 6-5 and 6-6 show curves of  $\log(I/I_0)$  vs  $d$  for air and nitrogen, respectively. The numbers, adjacent to the curves, show the value of  $E/p$  in V/cm-torr. The curves are seen to be linear for a while, but they asymptotically approach a maximum separation. This maximum separation represents breakdown and will be discussed in the next section. First, we will consider the relation between  $\alpha$ ,  $E$ , and  $p$ .

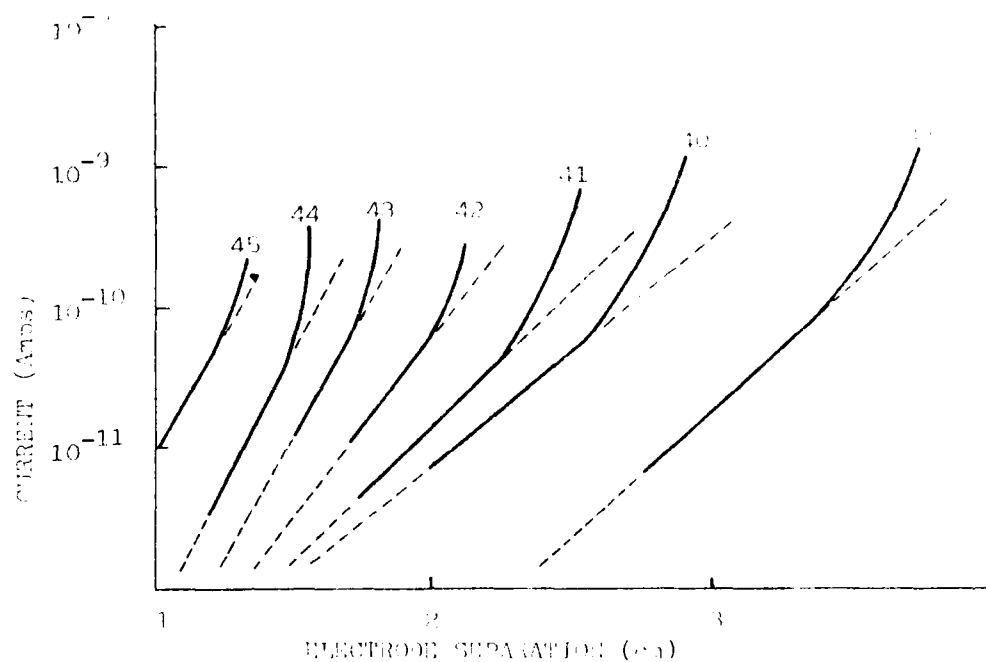


Figure 6-5: Curves of  $\ln[I(d)/I_0]$  vs  $d$  for air for various values of  $E/p$  (after Llewellyn-Jones and Parker, 1952).

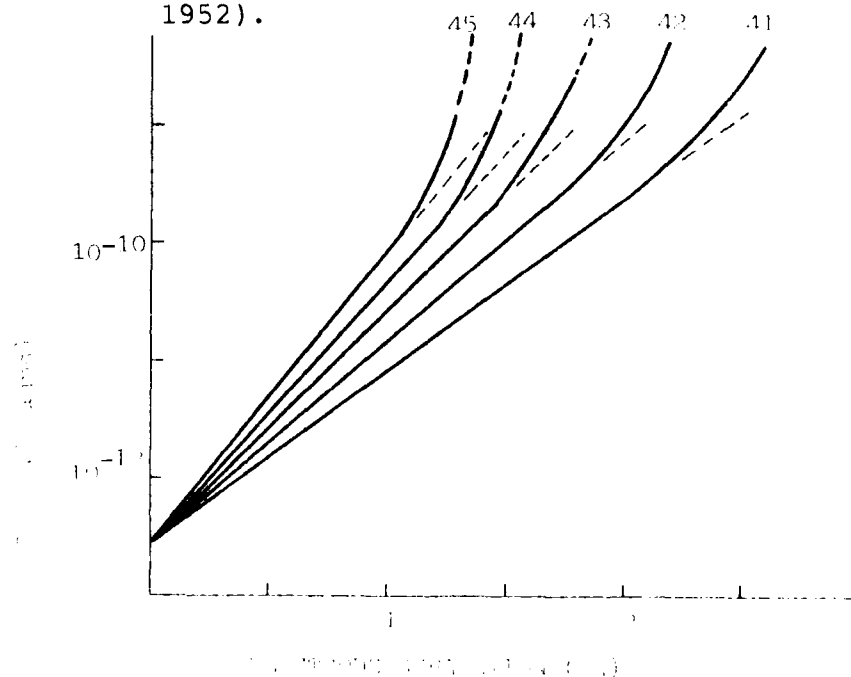


Figure 6-6: Curves of  $\ln[I(d)/I_0]$  vs  $d$  for nitrogen for various values of  $E/p$  (after Dutton, et al, 1952).

Since  $\alpha$  is the number of electrons produced in one cm,  $\alpha\lambda$  is the number produced in one mean free path. This number should be a function of  $E/p$ , so we postulate

$$\alpha\lambda = F(E/p) \quad (6.5)$$

where  $F$  is some function. The mean free path is inversely proportional to pressure, so equation 6.5 can be rewritten

$$\alpha/p = f(E/p) \quad (6.6)$$

Experimentally, Townsend found the relationship between  $\alpha/p$  and  $E/p$  to be a smooth curve, indicating that equation 6.6 accounts for the appropriate factors. He derived an approximate form for  $f(E/p)$  as follows (Cobine, 1957, p.148).

Since  $\lambda$  is inversely proportional to pressure, we can write

$$1/\lambda = Ap \quad (6.7)$$

where  $A$  is a constant. Equation 6.7 gives the average number of free paths per cm. Now, define an ionizing free path as

$$\lambda_i = V_i/E \quad (6.8)$$

In figure 3-3, we saw the distribution of free paths is exponential. Therefore, the number of free paths greater than  $\lambda_i$  is given by

$$n = n_0 \exp(-\lambda_i/\lambda) = n_0 \exp(-V_i/\lambda E) \quad (6.9)$$

where  $n_0$  is the total number of free paths. Thus, the probability of a free path being greater than  $\lambda_i$  is  $\exp(-V_i/\lambda E)$ . If the average number of free paths per cm (eq. 6.7) is multiplied by the probability of a free path being of ionizing length, we should get the probable number of ionizing collisions per cm. Thus

$$\alpha = Ap \exp(-V_i/\lambda E) = Ap \exp(-V_i Ap/E)$$

or

$$\frac{\alpha}{p} = A \exp\left[\frac{-V_i}{E/p}\right] = A \exp\left[\frac{-B}{E/p}\right] \quad (6.10)$$

Inherent in the above derivation are several significant assumptions. First, it was assumed electrons do not gain energy from collisions. Second, the field was assumed so strong that electrons only move in its direction. Finally, the probability of ionization was assumed to be zero if the electron's energy was less than  $V_i$  and one if the energy was greater than  $V_i$ . From the discussion of collisions in chapter 3, it should be apparent these assumptions are not true. Nevertheless, the principles used in deriving the equation, and its final form, are useful.

An indication of the accuracy of the derivation can be obtained by comparing the theoretical values of A and B with values found experimentally. From equation 6.7, A is the inverse of the mean free path at a pressure of one torr, and from equation 6.10, B is  $AV_i$ . Table 6-1 shows experimental values of A and B, and the range of validity, for several gases. As an example, the mean free path for nitrogen, at one torr, is about 0.03 cm which would make  $A \approx 33$ . The ionization potential for nitrogen is 14.5 eV (from table 2-1), so B should be  $\approx 480$ . From the table, we find  $A=12$  and  $B=342$ , a fairly large discrepancy. The primary use for equation 6.10 is as a form for fitting a curve to experimental data. It will also be useful in calculating the breakdown voltage in section 6.5. Finally, as  $E/p$  gets larger,

Table 6-1: Values of the Coefficients A AND B for Various Gases  
(VonEngel, 1965, p. 181)

GAS	A (1/cm-torr)	B (V/cm-torr)	RANGE OF VALIDITY E/p
N <sub>2</sub>	12	342	100- 600
H <sub>2</sub>	5.4	139	20-1000
air	15	365	100- 800
CO <sub>2</sub>	20	466	500-1000
H <sub>2</sub> O	13	290	150-1000
A	12	180	100- 600
He	3	34	20- 150
Hg	20	370	200- 600

equation 6.10 predicts  $\alpha/p$  will also get larger. In fact,  $\alpha/p$  has a maximum value, very much like the maximum for the probability of ionization (VonEngel, 1965, p.181).

### 6.3 Townsend's Second Ionization Coefficient

In the previous section, we attributed the increase in current with voltage to field enhanced ionization. Ions were regarded only as carriers of current. This theory cannot explain, however, the rapid increase in current shown in region IV of figure 6-2 or in the non-linear portions of figures 6-5 and 6-6. Townsend first tried to explain the faster current increase by assuming the positive ions were being accelerated enough to ionize gas molecules by collision. In fact, ions must possess energy

levels of the order of thousands of eVs before they become effective ionizers. Thus, his first explanation was not satisfactory.

Later, cathode secondary emission by ion collision was proposed as the source of the additional current. Changing the cathode material and surface condition changed the current characteristics, confirming the new theory. The number of electrons emitted by ion bombardment should be proportional to the number of ions generated by electron collisions in the gas volume. To account for this, Townsend's second ionization coefficient,  $\gamma$ , was defined as the number of secondary electrons emitted per ionizing collision in the gas volume (Cobine, 1957, p.156).

Although ion bombardment of the cathode was originally considered to be the cause of the secondary emission, it is now recognized there are other causes. These include photons from within the gas volume and collision of metastable and neutral particles with the cathode. While ion bombardment is the principle cause of secondary emission, all these processes may be present, and the  $\gamma$  coefficient may be thought of as the total result of the different secondary processes (VonEngel, 1965, p.175).

From section 6.2, we know each electron which leaves the cathode results in  $e^{ad}$  electrons arriving at the anode. Thus, there are  $(e^{ad}-1)$  electron-ion pairs formed by collisions. For a discharge to become self-sustaining, each electron which leaves the cathode must be replaced by another through secondary processes. The number of secondary electrons is the product of  $\gamma$  and the number of ionizing collisions. When this product is equal

to one, the original electron is replaced, resulting in Townsend's breakdown criterion

$$\gamma(\epsilon^{\text{ad}} - 1) = 1 \quad (6.11)$$

Generally,  $\epsilon^{\text{ad}} \gg 1$  and the above can be simplified to

$$\gamma \epsilon^{\text{ad}} = 1 \quad (6.12)$$

Clearly,  $\gamma$  will be a very small number.

This process can be continued through several cycles, as shown in figure 6-7. In the figure,  $N_0$  electrons formed by photo-electric emission start the process. They form an avalanche, and as a result of secondary processes, more electrons are emitted from the cathode. The secondary electrons form avalanches, and the process continues. The first three iterations are shown, and it may be noted that the total number of electrons arriving at the anode is (Krebs and Reed, 1959, p.41)

$$N = \sum_{n=0}^{\infty} [N_0 \gamma^n (\epsilon^{\text{ad}} - 1)^n] \quad (6.13)$$

letting  $y = \gamma(\epsilon^{\text{ad}} - 1)$  yields

$$N = N_0 \epsilon^{\text{ad}} \sum_{n=0}^{\infty} y^n = N_0 \epsilon^{\text{ad}} / (1 - y) \quad (6.14)$$

where the second equality results from the application of a series expansion. Replacing  $y$  and putting equation 6.14 in terms of current yields

$$I = \frac{I_0 \epsilon^{\text{ad}}}{1 - \gamma(\epsilon^{\text{ad}} - 1)} \quad (6.15)$$

where  $I_0$  is the saturation current from figure 6-2.





Equation 6.15 describes the current in the non-linear portions of figures 6-5 and 6-6, until breakdown occurs. When Townsend's breakdown criterion is satisfied, however, equation 6.15 blows up. In fact, equation 6.15 describes a steady state condition, and breakdown is a transient event. Thus, the breakdown criterion should be considered as a physical interpretation of conditions in the gap rather than as a mathematical criterion (Kunhardt, 1980, p.132). Using equation 6.12, Loeb (1948) gave the following explanation:

a. For  $\epsilon^{ad} < 1$ , the current is given by equation 6.15 and is not self-sustained. If the saturation current,  $I_0$ , is removed, the current stops.

b. For  $\epsilon^{ad} = 1$ , each avalanche of  $\epsilon^{ad}$  electrons produces one new secondary electron. This is the sparking threshold for a self-sustained discharge.

c. For  $\epsilon^{ad} > 1$ , more electrons are created than start, as the ionization of successive avalanches is cumulative. Due to their lower mobility, positive ions accumulate in the gap near the cathode, producing a very efficient secondary mechanism. This allows the discharge to continue as a glow or arc.

As might be expected,  $\gamma$  is greatly affected by the nature of the cathode and the gas. Generally, a lower work function yields a high  $\gamma$ , and  $\gamma$  increases with  $E/p$  since the ions gain more energy. Contamination of the cathode surface, especially by mercury vapor, may have a marked effect on the value of  $\gamma$ .

#### 6.4 Sparking Voltage--Paschen's Law

The current curves of figures 6-5 and 6-6 were found by increasing the electrode separation until breakdown occurred. More often, we are interested in the value of voltage,  $V_S$ , required to breakdown a fixed gap. We will again assume the electric field is uniform, so that  $\alpha$  is constant. Then

$$E_S = V_S/d \quad (6.16)$$

where  $E_S$  is the electric field at breakdown. Taking the logarithm of equation 6.12 yields

$$\ln(1/\gamma) = \alpha d \quad (6.17)$$

Substituting equation 6.10 for  $\alpha$  and equation 6.16 for  $E$

$$\ln(1/\gamma) = A p d \exp(-B p d / V_S) \quad (6.18)$$

Solving for  $V_S$ , we obtain

$$V = \frac{B p d}{\ln\left[\frac{A p d}{\ln(1/\gamma)}\right]} \quad (6.19)$$

Equation 6.19 is known as Paschen's Law, because he discovered, in 1899, that the breakdown voltage was a function only of the product of the gas pressure and electrode spacing.

Figure 6-8 shows the sparking voltage for several gases as a function of the pressure distance product. While the curves are different for each gas, the shape of each curve is generally the same. Note, there is a distinct minimum value of sparking voltage which occurs at a specific value of  $pd$ . For air, the product  $pd$  has a value of only  $\approx 0.6$  cm-torr at the minimum

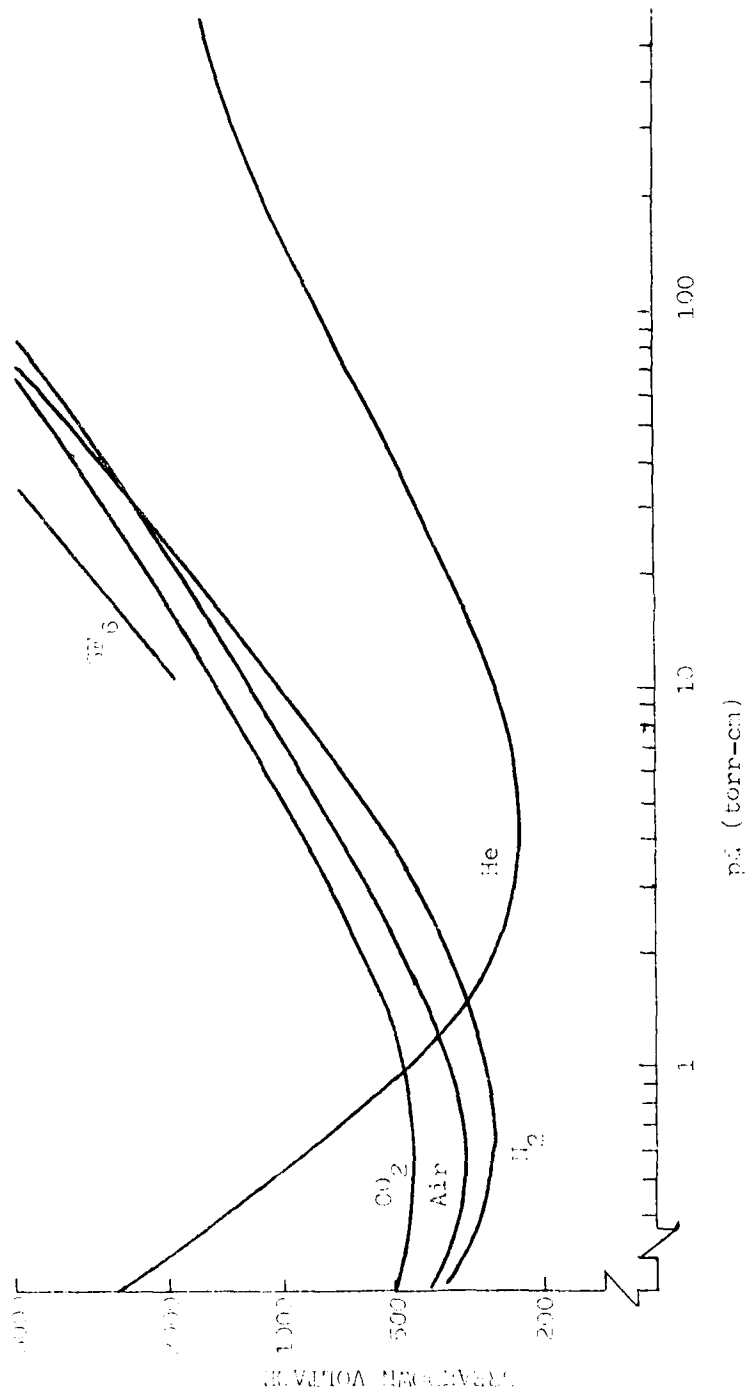


Figure 6-8: Breakdown voltage between parallel plates for several gases (after Dunbar, 1966, p.40).

sparking voltage of about 330 volts. Table 6-2 shows minimum sparking voltages and the corresponding pd product for several gases.

The low values of  $V_s$  obtained at low pd are extremely important for spacecraft systems, where a number of Paschen minimums may be passed through during ascent. To avoid breakdown, most spacecraft systems operate at voltages below 200 V. Where high voltages are required, encapsulation of the circuitry may be necessary. However, any voids in the solid encapsulant may breakdown, so special techniques are required. Sutton and Stern (1975), Dunbar (1966), Henning (1966), and Krebs and Reed (1959) all consider the problems encountered when working with spacecraft or high altitude aircraft.

The shape of the Paschen curve is also important for understanding high voltage switches which are often said to operate on the right or left hand side of the Paschen curve. The left side is particularly interesting. Note, if the electrode separation is reduced at constant pressure, the breakdown voltage actually increases. The shape of the Paschen curve can be deduced with a little reasoning.

Consider the electrode separation to be fixed. As the pressure is increased, the mean free path,  $\lambda$ , is reduced and the collisional frequency is increased. Thus, more voltage is required to accelerate the electrons enough to cause ionization. Conversely, at very low pressure,  $\lambda$  begins to approach the electrode separation, and the number of collisions is greatly reduced. As

Table 6-2: Minimum Sparking Voltage Between Steel Parallel Plate Electrodes for Several Gases (Dunbar, 1966, pgs. 40-41)

Gas	Minimum $V_s$ Volts (DC)	pd at Minimum $V_s$ (cm)(torr)
Air	315	0.55
CO <sub>2</sub>	430	0.6
He	189	1.3
N <sub>2</sub>	265	0.66
A	280	
O <sub>2</sub>	440	
SF <sub>6</sub>	520	

$e^{ad}$  gets smaller, more voltage is required to increase  $\gamma$  to satisfy the breakdown criterion.

As shown in figure 6-8 and table 6-2, the sparking voltage depends on the gas. However, equation 6.19 is a function of  $\gamma$ , so we should expect the electrode material to influence the sparking voltage. Figure 6-9 shows the effect of the cathode in the vicinity of the Paschen minimum, as reported by Llewellyn-Jones and Henderson (1939). There, the minimum value of  $V_s$  is seen to range from about 255 volts to about 315 volts. The effect of the cathode material is much more significant near the Paschen minimum, than for higher or lower values of pd.

The condition of the electrodes may also affect the breakdown voltage. At high pressures (1 to 40 atmospheres), the sparking voltage has been found to drop substantially when the electrodes

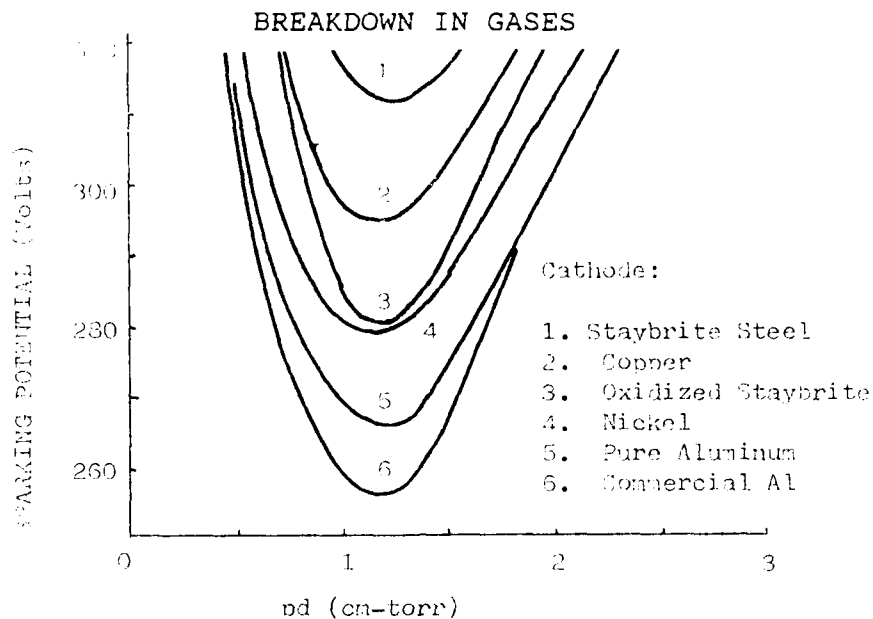


Figure 6-9: Sparking voltage for hydrogen in the vicinity of the Paschen minimum for various cathodes

are cleaned with sandpaper. After prolonged sparking, the breakdown voltage eventually recovers to its former value. This process of raising the breakdown voltage by repeated sparking is known as conditioning. Following a thorough cleaning, microscopic field enhancement increases the electron emission. The conditioning process tends to smooth out the surface. Typically, more conditioning is required at higher pressures (Kuffel and Abdullah, 1971, p.40).

The presence of gases having metastable states may also affect the breakdown voltage. A molecule of gas A may ionize a molecule of gas B by collision, if the energy of the metastable state of A is greater than the ionization energy of B. This effectively increases the first ionization coefficient,  $\alpha$ , and may result in a lower breakdown voltage than either gas would have by itself. Figure 6-10 shows Paschen curves for several

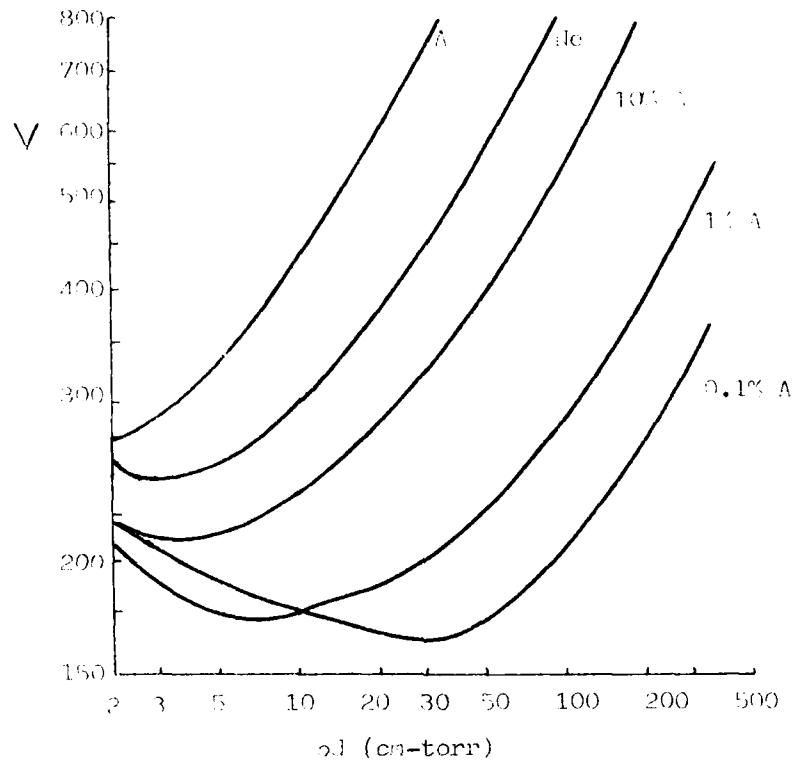


Figure 6-10: Paschen curves for neon-argon gas mixtures (after Penning, 1931).

mixtures of neon and argon. Note, there seems to be an optimum concentration of approximately 0.1% argon which produces the minimum breakdown voltage. The lowest excited state of neon is metastable, and has about 0.9 eV more than the ionization potential of argon (Kuffel and Abdullah, 1971, p. 39). Thus, the addition of small amounts of argon greatly increases the ionization level. This is known as the Penning effect after its discoverer. Other Penning combinations include helium and argon, helium and mercury, and argon and iodine. This effect is important, because commercially available gas usually contains traces of other gases.



### 6.5 Alternate Theories of Breakdown

The Townsend theory and Paschen's law agreed quite well with experimental results for values of  $pd < 200$  cm-torr. However, for  $pd > 200$  cm-torr, early researchers found several discrepancies. Meek (1940) compiled a list of them. Three of his more important objections were:

- a. The breakdown voltage appeared to be independent of the cathode material at high values of  $pd$ .
- b. When voltages greater than the breakdown voltage were suddenly applied to longer gaps, the time for the discharge to form was much faster than the time for positive ions to drift to the cathode.
- c. Photographs of sparks indicated that breakdown at higher pressure occurred along narrow channels or filaments with frequent branching.

As a result of these discrepancies, new theories were developed. Kunhardt (1980) provided a review of the development of the different breakdown theories. In this section, we will first consider the time lags involved in electrical breakdown. Then, we will look at the streamer theory of breakdown. Finally, the statistical nature of breakdown will be mentioned very briefly.

#### 6.5.1 Time Lags for Breakdown

Although the transition from a non-self-sustaining to a self-sustaining discharge is abrupt, a finite time is required for the discharge to develop. Similarly, if a voltage greater than the breakdown voltage is suddenly applied to a gap, there will

be a delay before a self-sustained discharge forms. The time lag for a discharge to develop is extremely important in pulsed power switches for two reasons. First, it may affect the risetime of the current or voltage pulse being applied to a load. Second, a considerable amount of energy may be dissipated in the switch during the breakdown, and may ultimately limit the rep-rate of the switch.

The time lag for breakdown is composed of two components. The first component is independent of the voltage applied, and is statistical in nature. This so-called statistical time lag,  $t_s$ , is the time required for a free electron to appear in the gap to start the breakdown process. These free electrons, as we have seen previously, may be created by photons (cosmic rays) or by molecular collisions. In either event, one must form to start the discharge. This can be very critical when dealing with fast voltage pulses, as the pulse could be over before an electron forms. In such cases, artificial illumination may be required to insure electrons are available. For laser or electron beam triggered switches, the statistical time lag is completely negligible (Kunhardt, 1980).

The second component is called the formative time lag,  $t_f$ . It is the time required for the self-sustaining discharge to form once an initial electron is available. This portion of the time lag is a function of which type of secondary process is dominant. For example, if ion bombardment is the dominant secondary process, then  $t_f$  should closely correspond to the time required for a

positive ion to drift across the gap. Although the formative time lag is very sensitive to a relatively small voltage change above the breakdown voltage (Meek and Craggs, 1953, p.111), it should be in the  $\mu\text{sec}$  range for a one cm gap at atmospheric pressure (Meek, 1940).

In fact, researchers found the formative time lag to be less than 100 nsec, which was far below the time required for ions to drift across the gap. That, coupled with the other discrepancies, led Meek, Loeb, and Raether to independently develop the streamer theory of the spark (Kunhardt, 1980).

#### 6.5.2 The Streamer Theory

The streamer theories differed in some of their details, but all assumed that photoionization became the dominant breakdown mechanism at some point in the development of an avalanche. Loeb and Meek assumed this occurred when the avalanche reached the anode, while Raether allowed that it could happen with the avalanche in the middle of the gap.

Loeb and Meek's assumption resulted in cathode directed streamers. Figure 6-11 illustrates the process. In figure 6-11a, we see a completed electron avalanche. The electrons, with their high mobility, have been swept away, leaving behind the positive ions. Due to the exponential buildup of the avalanche, the density of the positive ion space charge is greatest near the anode. In fact, 50% of the ions will be in the last  $1/\alpha$  cm. The positive space charge causes a radial electric field given by

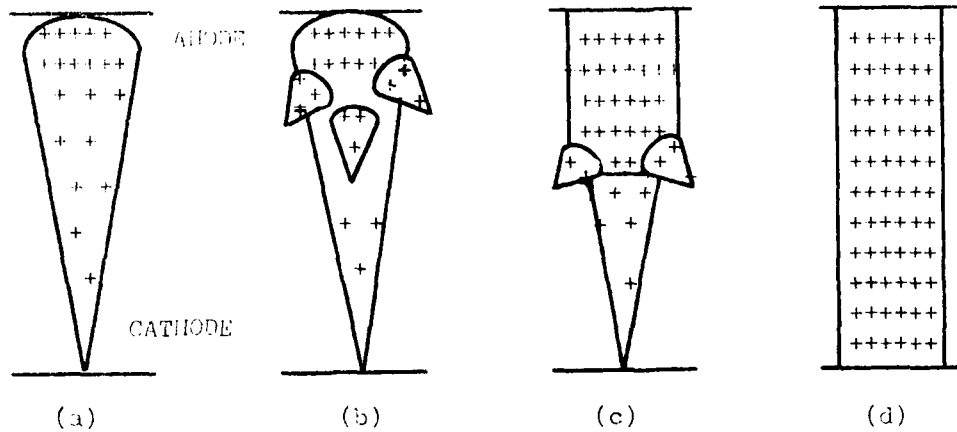


Figure 6-11: Development of a cathode directed streamer.

$$E_r = \frac{4\alpha q_e \epsilon^{ad}}{3\sqrt{(2D/\mu)(d/E)}} \quad (6.20)$$

or considering the ratio  $D/\mu$  for electrons

$$E_r = 5.27(10^{-7})\alpha\epsilon^{ad}/\sqrt{d/p} \quad (6.21)$$

where  $p$  is in torr,  $d$  is in cm, and  $E_r$  is in V/cm. When  $E_r$  is approximately equal to the externally applied field, free electrons, formed by photoionization, may be drawn to the space charge, creating mini-avalanches as shown in figure 6-11b. These mini-avalanches lengthen and intensify the space charge, as shown in figure 6-11c, until the streamer reaches the cathode, figure 6-11d. At that point, the gap is bridged by a high conductivity plasma and breakdown ensues (Meek and Craggs, 1953, p. 253-255).

Raether based his theory on experimental cloud chamber observations of electron avalanches. He proposed that the avalanche reached a critical dimension as it developed toward the anode. Figure 6-12a shows the avalanche in the middle of the gap. Once this critical dimension was reached, secondary ionization could occur from photons generated within the avalanche, as shown in figure 6-12b. Those secondary electrons located near the axis of the avalanche are in a high field region due to field enhancement by the space charge. Thus, they multiply very rapidly, creating a new space charge cloud, as shown in figure 6-12c. The process repeats itself until the space charge reaches the anode. Electrons are then drawn into the original avalanche, extending the streamer back to the cathode. As before, breakdown occurs when the gap is bridged by the streamer (Kunhardt, 1980).

Meek developed a modified form of Paschen's law, and Raether used his theory to predict the formative time lag. Both theories agreed with experimental observations; however, a debate continued over the years between the proponents of Townsend breakdown and streamer breakdown. Eventually, researchers found that cathode effects on  $V_g$  could be detected for  $pd$  values as high as 12,000 cm-torr, if ultra-stable voltage supplies were used, and long formative time lags could be observed for  $pd$  values of 1.00 cm-torr, if the voltage was just above  $V_g$ . Further, they found that  $t_f$  decreased with the percent overvoltage applied to the gap. These results indicated the two models were not

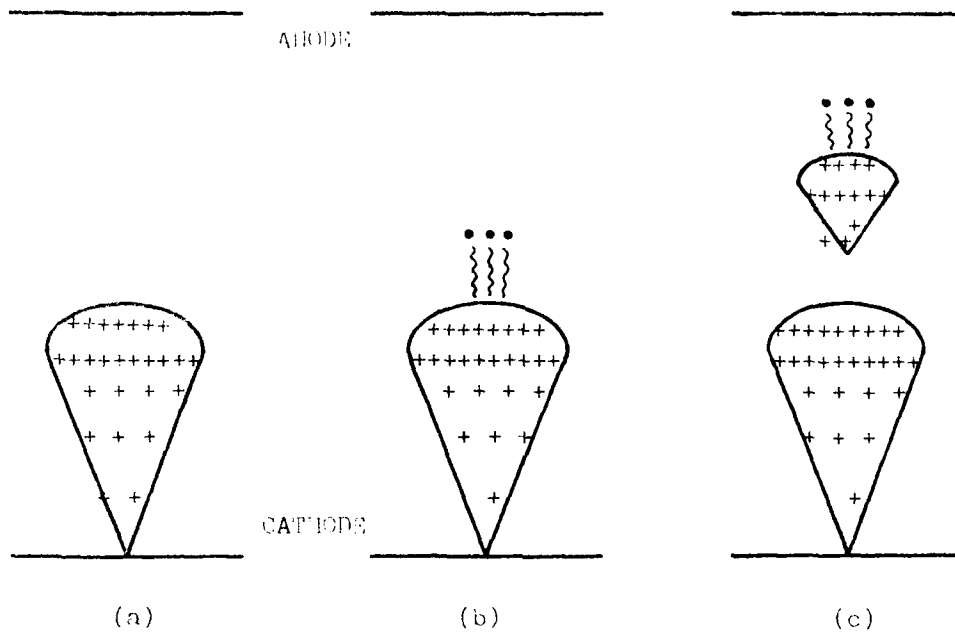


Figure 6-12: Development of an anode directed streamer.

separated by a particular value of  $pd$  product, but instead by the overvoltage of the gap (Kunhardt, 1980).

Today, the Townsend theory is considered valid for overvoltages less than 20%, while the streamer theory applies when the overvoltage is greater than 20%. In addition, other theories may apply as the overvoltage is further increased (Kunhardt, 1980).

### 6.5.3 Statistical Nature of Electrical Breakdown

In section 6.2 and figure 6-3, we considered an electron avalanche. According to the Townsend theory, an electron produces  $e^{ad}$  electrons as a result of the avalanche. However, there is no guarantee the electron will ionize a molecule each time it travels  $1/\alpha$ , although on the average it does. Thus, an individual avalanche will generate a number of electrons which may be above or below  $e^{ad}$ . The same argument holds for the secondary coefficient,  $\gamma$ , so the product  $\gamma e^{ad}$  may vary substantially (Loeb, 1948).

The Townsend breakdown criterion requires  $\gamma e^{ad}=1$ , but variations in the ionization coefficients may result in the breakdown condition being satisfied at voltages which are higher or lower than the predicted breakdown voltage. Loeb (1948) described the breakdown voltage as a Gaussian distribution (Bell curve) with a mean of  $V_S$  and a standard deviation of about two percent of  $V_S$ . This phenomenon is extremely important when working with spark gap switches.

Current research involves the development of stochastic computational models of gas breakdown. Some include the variations mentioned above as well as space charge effects on the electric field. Kunhardt and Luessen (1983), Kunhardt (1984), and Mack and Craggs (1978) provide details and additional references.

### 6.6 Non-uniform Field Breakdown

Until now, we have been considering breakdown under uniform field conditions. In real life, however, pulsed power and power system engineers are often faced with non-uniform fields. For example, the field between the conductors of a transmission line will be non-uniform, whether the transmission line is a three phase power line or a gas filled coaxial line in a laboratory. Thus, the effects of non-uniform fields should be considered.

If we consider the Townsend breakdown criterion,  $\gamma e^{\alpha d} = 1$ , and apply it to the non-uniform field, two things come to mind. First,  $\alpha$  will vary with the electric field. Thus, the product  $\alpha d$  should be replaced by  $\int_0^d \alpha dx$ . This makes computation of the breakdown voltage extremely tedious. Second,  $\gamma$  will depend on the cathode field, which means the breakdown voltage may depend on the polarity, if the electrodes are asymmetric. Specifically, the secondary emission will be larger when the cathode is in the high field region, which means  $V_S$  will be lower.

In general, at low values of  $pd$ ,  $V_S$  is lower when the high field region is at the cathode. For many gases, the preceding statement is also true at high values of  $pd$ . However, there are notable exceptions, including air and oxygen. At high values of  $pd$ , these breakdown at a lower voltage when the anode is in the high field region. Thus, there is a "cross-over" effect as



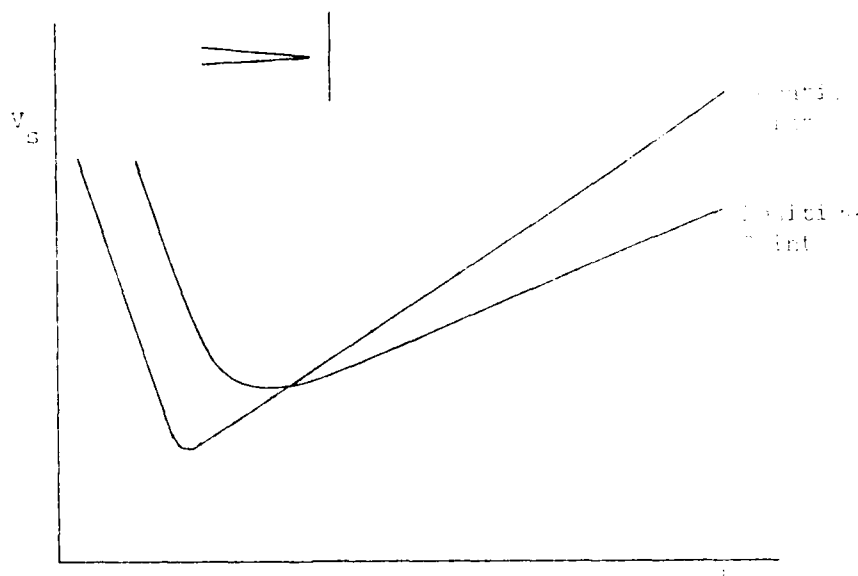


Figure 6-13: Schematic breakdown curves for a point to plane gap.

shown in figure 6-13. This effect is apparently due to electron attachment which occurs when the high field is at the cathode. Meek and Craggs (1953, pgs.101-106) show curves for a variety of gases.

Regardless of the polarity, breakdown in a non-uniform field gap may be expected at a lower voltage than for a uniform field gap of the same length. Figure 6-14 shows the breakdown voltages obtained between 5 cm diameter parallel plates, 0.64 cm round rods, and pointed electrodes. In each case, the gap was 1 cm and the pressure was varied. These curves were obtained using 400 hz alternating current supplies, but at low frequencies, the peak value for AC breakdown is approximately equal to the DC

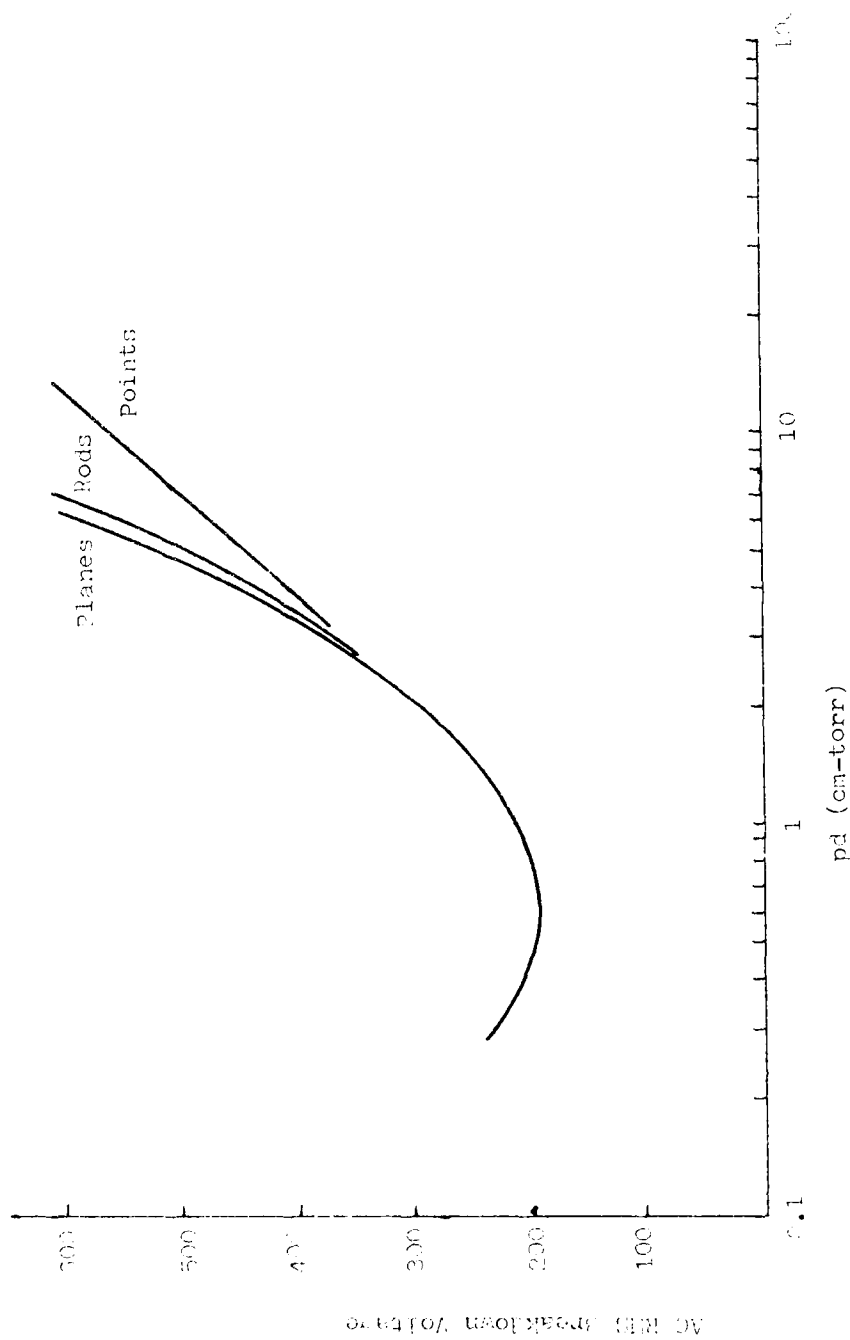


Figure 6-14: RMS breakdown voltage between planes, rods, and points in nitrogen (after Dunbar, 1966, p. 86).

breakdown voltage (allowing for any polarity effects). Note, the more non-uniform the field, the lower is the breakdown.

Finally, sphere gaps, point to plane gaps, and point to point gaps are often used in atmospheric air to measure voltages or to protect equipment against overvoltages. An example of the latter is the lightning arrestor which, in its simplest form, consists of a gap between the conductor and ground. The length of the gap is long enough to allow the system to operate under normal conditions, but short enough to flash over under the high voltage of a lightning strike. Standard breakdown tables are available in IEEE Standard 4-1978, "Standard Techniques for High Voltage Testing." The standard also includes instructions to adjust the breakdown voltage to account for changes in temperature, barometric pressure, and relative humidity.

Non-uniform breakdown often leads to corona, which will be discussed in chapter 8. Alternating current arcs will be discussed in chapter 9. The final topic to be considered in this chapter is surface flashover.

#### 6.7 Surface Flashover

The old saying that a system is only as strong as its weakest part is certainly true of any high voltage system. While we have been discussing breakdown through a gas, we must remember that high voltage conductors must be mechanically connected to something. A power transmission line must be connected to the towers by insulator strings, and high voltage connections must often pass through an equipment enclosure. The result of these connec-

tions is a boundary between two different types of material--gas and solid, vacuum and solid, solid and liquid, etc. These boundaries are often the weak link of the system.

Cobine (1957, p.166) has shown that placing a solid insulator between two parallel plates may reduce the maximum breakdown voltage by 30 to 50%, depending on the gap length. The situation may be even worse for vacuum-solid interfaces (Mitchell and Blaher, 1981, p.2). The reduction in breakdown strength may be due to surface space charge effects, surface contamination, or a combination thereof.

The primary way to decrease the probability of flashover is to lengthen the flashover path. For that reason, insulators are usually designed with corrugated surfaces. Figure 6-15 shows the precautions which are taken at the edge of a typical pulsed power transmission line.

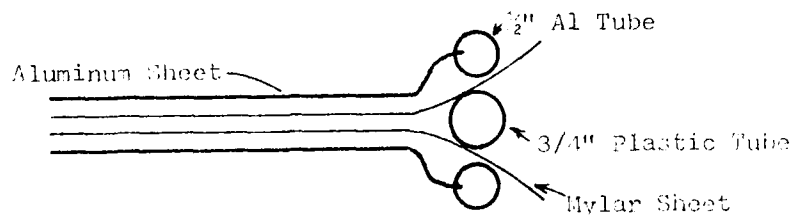


Figure 6-15: Edge treatment of a parallel plate transmission line to eliminate flashover.

### 6.8 Summary

In this chapter, we have looked at the breakdown process in gas. By breakdown, we mean the transition from a discharge which is sustained by an external ionizing source to a discharge which produces its own electrons. The non-self-sustained discharges were investigated extensively by Townsend, who used two ionization coefficients to describe the current. With these ionization coefficients, Townsend developed a criterion for breakdown which led to an equation for the breakdown voltage. The Townsend equation showed that breakdown was dependent only on the product of gas pressure and electrode separation, for a given gas and electrode. This had been found experimentally by Paschen. The so-called Paschen curves show there is a minimum breakdown voltage which occurs at a specific value of  $pd$ . Increasing or decreasing the pressure-distance product from that point will raise the breakdown voltage.

While Townsend's theory worked well at low values of  $pd$ , several difficulties arose at higher values. These prompted the development of the streamer theory, which provided a faster mechanism of breakdown. Today, the applicability of the two theories is determined by the amount of overvoltage applied to the gap.

Although the Paschen curve was derived for uniform electric fields, the general shape holds true for non-uniform fields. However, the breakdown voltage usually drops as the field becomes more non-uniform. Also, if the field is asymmetrical (such as a point to plane gap), there will be polarity differences in the

breakdown voltage. Finally, boundaries between different types of insulators often are the weakest point in the system, and special care is required to avoid flashover breakdown.

The next three chapters will look at the three primary types of gas discharges--glow, corona, and arc. These chapters will generally be more descriptive and less quantitative than chapters 2 through 6.

#### REFERENCES :

- Cobine, J.D. (1957). Gaseous Conductors. Dover Publications, New York.
- Dunbar, W.G. (1966). Corona Onset Voltage of Insulated and Bare Electrodes in Rarefied Air and Other Gases. US Air Force Aero-Propulsion Laboratory Technical Report 65-122, Wright-Patterson AFB, OH 45433. DTIC AD# 483820.
- Dutton, J., et al (1952). Proceedings of the Royal Society of London. Series A, V. 213, p. 203.
- Henning, R.C. (1966). Corona Prevention in the SST. Lockheed California Co. Report No. LR-19366. DTIC AD # 817832L.
- IEEE (1978). Standard Techniques for High Voltage Testing, IEEE Standard 4-1978. New York.
- Krebs, W.H. and Reed, A.C. (1959). Low Pressure Discharge Studies. Space Technology Laboratories, Inc. TR-59-0000-09931, Los Angeles. DTIC AD # 605984.
- Kuffel, E. and Abdullah, M. (1971). High Voltage Engineering. Pergamon Press, Oxford.
- Kunhardt, E.E. (1980). IEEE Trans. on Plasma Science. V. PS-8, p. 130.
- Kunhardt, E.E. (1984). Digest of Technical Papers, 4th IEEE Pulsed Power Conference, 1983. p. 206. Library of Congress Catalog No. 83-80951. IEEE Catalog No. 83CH1908-3.
- Kunhardt, E.E. and Luessen, L.H. (ed.) (1983). Electrical Breakdown and Discharge in Gases (2 vols.). Plenum Press, New York.

- Llewellyn-Jones, F. and Henderson, J.P. (1939). Philosophical Magazine. 7th Series, V. 28, p. 185.
- Llewellyn-Jones, F. and Parker, A.B. (1952). Proceedings of the Royal Society of London. Series A, V. 213, p. 184.
- Loeb, L.B. (1948). Proceedings of the Physical Society of London. V. 60, p. 561.
- Meek, J.M. (1940). Physical Review. V. 57, p. 722.
- Meek, J.M. and Craggs, J.D. (1953). Electrical Breakdown of Gases. Clarendon Press, Oxford.
- Meek, J.M. and Craggs, J.D. (ed) (1978). Electrical Breakdown of Gases. John Wiley & Sons, Chichester.
- Mitchell, O.J. and Blaher, R.J. (1981). "Soft Photon Effects on Vacuum Power Flow." Unpublished Master's Thesis, School of Engineering, Air Force Institute of Technology (AU), Wright-Patterson AFB, Ohio.
- Penning, F.M. (1931). Philosophical Magazine. 7th Series, V. 11, p. 961.
- Sutton, J.F. and Stern, J.E. (1975). Spacecraft High-Voltage Power Supply Construction. NASA TN D-7948. National Aeronautics and Space Administration, Washington, D.C.
- VonEngel, A. (1965). Ionized Gases. Clarendon Press, Oxford.

## CHAPTER 7

### THE GLOW DISCHARGE

#### 7.1 Introduction

In the last chapter, we looked at the Townsend discharges and the breakdown process. Now, we are interested in what happens after the spark. Specifically, what type of discharge develops and what are its characteristics? The type of discharge depends on a number of factors: the external circuit, gas type, pressure, electrode material and geometry, electrode separation, and the nature of the applied voltage. In this chapter, we will be looking at the glow discharge, but first we need to define the various types of discharges.

Figure 7-1 shows a simple uniform electrode gap filled with gas at low pressure and a plot of the gap voltage and current. The coordinate axes have been reversed from figure 6-2--the abscissa is current and the ordinate is voltage. The portion of the curve from the origin to point a represents the dark discharges. At point a, the gas breaks down. As a result of the decrease in resistivity of the gas, the current increases. The current increase causes a decrease in the voltage across the gap and an increase in the voltage across the external resistance. The region from a to b has been given a variety of names (Krebs and Reed, 1959, p.3), but we will consider it to be a transition region.



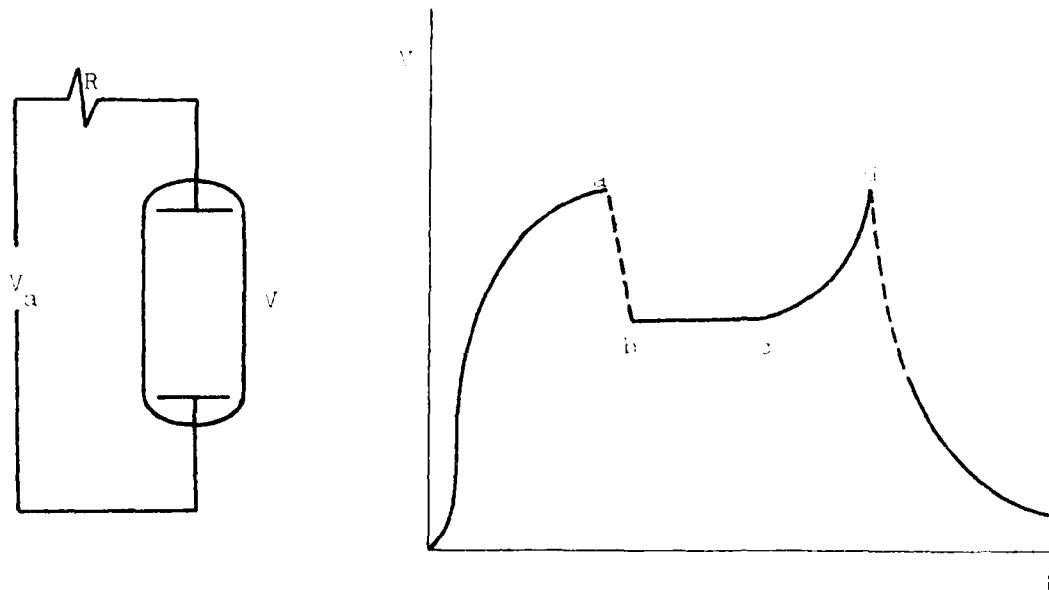


Figure 7-1: A discharge tube and the voltage as a function of current over several orders of magnitude of current.

At point  $b$ , the current is typically in the milli-ampere range, and the discharge voltage is relatively high. As the source voltage is increased, the current continues to grow, but the discharge voltage remains constant. The region between  $b$  and  $c$  is known as the normal glow discharge. Beyond point  $c$ , further increases in the source voltage cause the discharge voltage and current to increase. The region from  $c$  to  $d$  became known as the abnormal glow discharge; however, it is no more abnormal than any other discharge. At point  $d$ , a transition to a low voltage, high current discharge begins. The region from  $d$  to  $e$  is sometimes considered to be a glow discharge and sometimes is

called the glow to arc transition. The region beyond point e is the arc discharge, which will be discussed in chapter 9.

The glow discharge (region b to d) is primarily a low pressure discharge. At atmospheric pressure, the glow discharge appears as corona, in the vicinity of the breakdown voltage, but it rapidly transitions into an arc at higher voltages. Although corona is a form of glow, it will be treated in chapter 8.

The glow discharge has several important commercial uses. "Neon" signs are glow discharge tubes in which different colors are produced by different gases. Fluorescent lights are glow discharges in mercury vapor, but the photons given off are in the ultraviolet. Thus, phosphors coat the inside of the tube to absorb the discharge radiation and give off visible light. Finally, thyatron and ignitron switches are used extensively in pulsed power systems, and operate in the region d to e of figure 7-1. In the next section, we will examine the phenomena associated with the glow discharge.

## 7.2 Phenomena

The early researchers were attracted to the glow discharge because of its unique visual appearance, which consists of a number of alternating light and dark regions. The terms light and dark should be considered in the relative sense, as the dark regions are not completely dark. Figure 7-2a illustrates the regions which would be seen at a gas pressure of about 1 torr.

The figure shows eight individual regions in the discharge. Starting from the cathode, they are (Howatson, 1976, p.85):

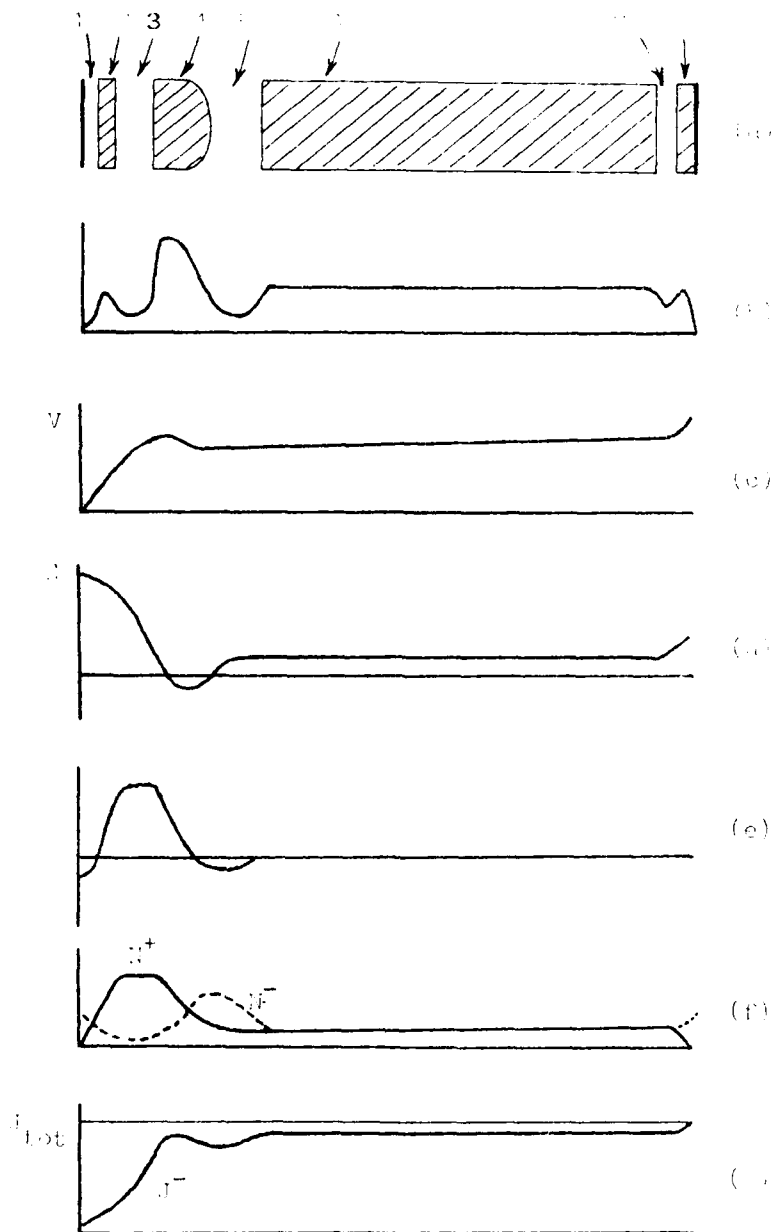


Figure 7-2: Characteristics of the glow discharge:  
 (a) visual appearance; (b) light intensity;  
 (c) voltage; (d) electric field; (e) net charge  
 density; (f) positive and negative charge densi-  
 ties; (g) electron and positive ion current  
 densities.

1. The Aston dark space
2. The cathode glow
3. The Crookes dark space (also called the cathode or Hit-torf dark space)
4. The negative glow
5. The Faraday dark space
6. The positive column
7. The anode dark space
8. The anode glow

Also shown in figure 7-2 are schematic representations of the light intensity, voltage, electric field, net charge density, positive and negative charge densities, and current densities. Each region will be considered in turn, and the reader should refer to figure 7-2 while following the discussion. Sources for the following discussion include Cobine (1957, ch.8), Howatson (1976, pgs.84-91), VonEngel (1965, ch.8), and Brown (1966, Ch.13).

#### 7.2.1 The Visual Phenomena

The Aston dark space is less than 1 mm in width at a few torr pressure, and is totally obscured by the cathode glow at higher pressures. Here, the electrons, emitted by positive ion bombardment of the cathode, accumulate and form a negative space charge. The majority of the current is due to positive ions arriving from the Crookes dark space, and the light intensity is very low.

The cathode glow is the first region with appreciable illumination, and its length depends on the gas and the pressure. It may take on one of three distinct characteristics. At low pressure and voltage, the light results from the loss of electron energy to gas excitation. This is called the "first cathode layer." At higher pressure and voltage, the cathode appears

covered by the "cathode glow" which results from recombination of positive ions with slow electrons. The third type is the "cathode light" which is observed when the cathode is covered by a thin metallic or oxide layer. Atoms from the layer may sputter off and become excited. This region has a slightly positive space charge.

The Crookes dark space contains a high positive ion density which causes a substantial voltage drop. In fact, nearly all of the discharge voltage drop is across the first three regions. This voltage is called the cathode fall, which may be as low as 64 V for potassium in argon and as high as 490 V for platinum in carbon monoxide. In this region, electrons are accelerated toward the negative glow region.

The negative glow is very intense at the cathode end, as the electrons which accelerated through the Crookes dark space suffer inelastic collisions. This is the brightest region, but the illumination intensity decreases toward the anode, because the electrons are not accelerated by the low electric field. The low electric field results from the essentially equal concentrations of ions and electrons. These concentrations are very high, as much as 10 to 100 times those of the positive column. The boundary between the negative glow and the Faraday dark space is ill-defined, as the light tapers off gradually. The electric field opposes the current flow there, so the current is due to diffusion, primarily of electrons.

In the Faraday dark space, the electric field again becomes positive which accelerates the electrons from the negative glow region. The current flow is primarily due to the electrons. Once they have gained enough energy to ionize, the positive column begins.

As will be seen, the positive column is a passive region which expands or contracts to connect the cathode region to the anode. The electric field is low ( $\approx 1$  V/cm) and constant, which makes the positive column drop much less than the cathode drop. Thus, the electron drift velocities are low, and ionization is due to electrons acquiring large thermal velocities by a large number of elastic collisions. The plasma of the positive column is an excellent conductor, so the effect of the positive column is to establish a virtual anode at the end of the Faraday dark space. At low pressure, the plasma fills the tube. At higher pressure, the plasma constricts, and ambipolar diffusion to the walls occurs. It is the positive column which provides the light in "neon" signs.

At the anode, electrons are attracted and positive ions are repelled. Thus, there is a negative space charge which causes an increase in the electric field and a voltage drop known as the anode fall. The anode fall is often accompanied by an anode dark space. Electrons which accelerate through the anode fall may be able to ionize molecules immediately in front of the anode, producing an anode glow.

The colors of the glow regions and the positive column are characteristic of each gas. Table 7-1 shows the characteristic colors for a number of gases. The size of each region is primarily a function of the pressure and the length of the tube.

#### 7.2.2 Variation of Pressure or Tube Length

The visual display, shown in figure 7-2, is typical of pressures of about 1 torr. The dimensions of the first five regions (Aston dark space to Faraday dark space) are very dependent on the pressure. As the pressure is increased, these regions tend to compress and the positive column expands to fill the space. By about 100 torr, the negative glow appears to be on the cathode--the Aston and Crookes dark spaces and the cathode glow cannot be seen. Also at this pressure, the positive column contracts away from the walls of the tube.

If the pressure is reduced from 1 torr, the effects are essentially the opposite. Regions 1 through 5, but especially the negative glow and Faraday dark space, expand at the expense of the positive column. Eventually, the positive column disappears. The discharge can operate without one, which indicates the cathode processes are essential for maintaining the discharge. Further pressure reduction causes the Faraday dark space to move into the anode, and the discharge extinguishes unless the voltage is increased. If the voltage is increased, the negative glow can be driven into the anode at about  $10^{-3}$  torr. At that point, the discharge bears more resemblance to an electron beam, however.

Table 7-1: Characteristic Glow Discharge Colors for a Number of Gases (Brown, 1966, p. 214)

Gas	First Cathode Layer	Negative Glow	Positive Column
Air	pink	blue	salmon pink
Hydrogen	brownish-red	pale blue	pink
Nitrogen	pink	blue	red
Oxygen	red	yellowish-white	pale yellow with pink center
Helium	red	green	red to violet
Argon	pink	dark blue	dark red
Neon	yellow	orange	brick red
Krypton		green	
Xenon		olive-green	
Bromine		yellowish-green	reddish
Chlorine		" "	whitish-green
Iodine		buff	reddish-blue
Lithium	red	light red	
Sodium	pink to orange	whitish	yellow
Potassium	green	pale blue	green
Mercury	green	green	greenish



At constant pressure and current, the length of the cathode region is constant. Thus, changing the length of the tube only changes the length of the positive column. If enough voltage is applied, the positive column can be made quite long, as in a neon sign. However, if the electrodes are pushed too close together, the positive column disappears, and the discharge eventually goes out.

### 7.2.3 Normal and Abnormal Glow

As shown in the introduction, the normal glow is characterized by a constant discharge voltage, even when the current increases. Experimentally, it was determined that the normal glow discharge does not cover all of the cathode. As the current increases, the amount of the cathode covered by the discharge increases. Thus, the current density remains constant and no additional cathode drop is required. Eventually, however, the entire cathode is covered by the discharge.

When the glow covers the entire cathode, the only way to get more current is to increase the current density. This requires an increase in the cathode fall to provide more energy to the bombarding ions. The increase in cathode fall is accompanied by a decrease in the thickness of the cathode region.

Insight into the adjustment of the cathode fall length and the current density at the cathode can be gained by considering, again, the system of figure 7-1. The system, of course, has a non-uniform field. However, we will assume the breakdown voltage

is still a function of  $pd$ , and that a Paschen shaped curve still applies.

Figure 7-3 shows a hypothetical breakdown curve. Assume, first, the pressure-distance product corresponds to point A on the curve. As voltage is applied, the dark current flows, leaving a positive space charge in the gap. As was shown in chapter 2, the space charge causes a virtual anode which effectively shortens the electrode separation. Since we are on the left side of the Paschen curve, more voltage will be required for breakdown. In fact, it may be very difficult to achieve breakdown, unless the electric field becomes large enough to cause field emission. Thus, if the pressure is too low, or the gap length too short, a discharge cannot be maintained.

Next, consider formation of a discharge at point B. Assume the current is limited by the external resistance, and the current density is uniform over the entire cathode, when the discharge begins (point a of figure 7-1). If, for any reason, part of the cathode were to contribute more than its share of the current, the area covered by the discharge would shrink. Experimentally, it has been found that an increase in current density is accompanied by a decrease in thickness of the cathode fall. But, that effectively reduces  $pd$  and the voltage required to maintain the discharge, say to point C. Since less voltage is required by the discharge, more must appear across the resistance. This requires more current, so the current density increases again, and we go further down the curve. Eventually, we wind up at point

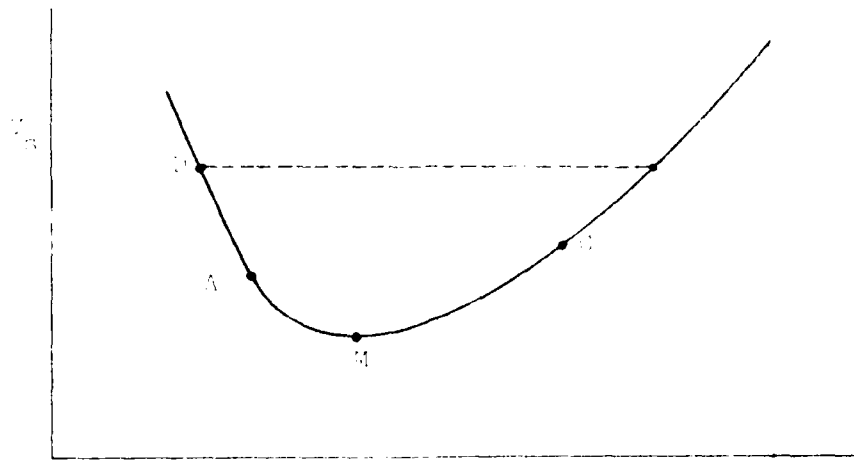


Figure 7-3: Paschen type breakdown curve for the system of figure 7-1.

M, where the length of the cathode fall is such as to produce the minimum discharge voltage. Any change of pressure will cause the cathode region length to change to maintain the operation of the discharge at point M. Thus, as soon as a spark occurs, the discharge area shrinks on the cathode and the cathode region contracts to the values required to operate at point M. The shrinking process takes place rapidly, and may be due to variations in the electric field at the cathode surface. In any event, it is accompanied by an increase in current to a level determined by the external resistance. This is the breakdown process shown between points a and b in figure 7-1.

Once the discharge is at point M, a further increase in the source voltage appears across the resistance, requiring a higher current. One of two things happens. If the discharge does not

cover the entire cathode, the discharge area can expand to provide the extra current at constant current density. In this case, the length of the cathode region and the discharge voltage are unchanged. Once the discharge completely covers the cathode, however, the current density must increase to provide the extra current. In this case, the cathode region will contract, moving the discharge toward point A and increasing the cathode fall. The first case corresponds to the normal glow, while the second case is the abnormal glow.

Finally, if the external resistance of the circuit is negligible, then all of the source voltage must appear across the discharge. In this case, the discharge will move from point B directly to the abnormal glow shown at point D. Normally, however, this current would be sufficient to heat the cathode enough to begin thermionic emission. This would be rapidly followed by transition to a potentially destructive arc.

### 7.3 Grid Control of the Glow Discharge

The difficulty of initiating a discharge on the left hand side of the Paschen curve can be used to our advantage. The thyatron and other tubes use a third electrode, called the grid, to control the start of a discharge (that is, closing of the switch).

Figure 7-4 shows a three electrode, gas filled tube. The grid electrode is physically constructed of a fine, screen-like material and completely shields the anode. The grid is placed very close to the anode, typically 1 or 2 mm. Thus, the pd product for the grid-anode gap is on the left hand side of the

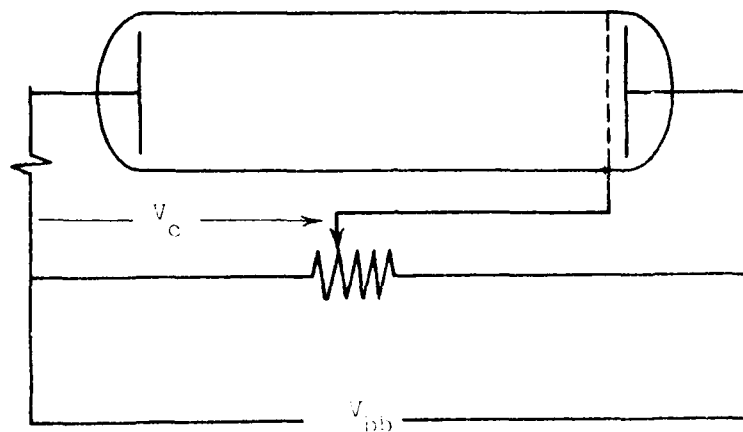


Figure 7-4: Three electrode, gas filled tube.

Paschen curve. The cathode-anode separation is chosen to be on the right hand side, such that

$$V_{sga} \gg V_{sgc}$$

where  $V_{sga}$  is the breakdown voltage between the grid and anode, and  $V_{sgc}$  is the breakdown voltage between the grid and cathode.

Voltages are applied to the device as shown. The voltage  $V_{bb}$ , applied to the cathode and anode, exceeds the normal breakdown potential, but if  $V_c=0$ , no discharge occurs between the cathode and grid. Thus, the entire voltage appears between the grid and anode. There will be no discharge here, either, because of the close spacing between the grid and the anode. Finally, due to the shielding of the grid, the cathode does not "see" the anode

potential, and there is no discharge between the anode and cathode.

Next, consider what happens as the voltage on the grid,  $V_g$ , is raised. Eventually, the voltage between the grid and cathode exceeds the breakdown strength, and breakdown occurs between the cathode and grid. If the anode is sufficiently positive with respect to the grid, the discharge transfers to the anode and the switch is closed.

After breakdown, the grid loses all control of the discharge. For example, consider making the grid negative in an attempt to stop the discharge. The negative voltage on the grid screen attracts positive ions and a positive sheath forms around it. To electrons, the combination of the negative grid and positive sheath appears neutral, and they continue on to the anode. If the grid is made positive, an electron sheath forms, and the discharge is unaffected. Note, the charges in the sheath are continually replenished, and a grid current flows. The only effect of varying the grid potential is to change the grid current.

#### 7.4 Summary

In this chapter, we have been interested in the glow discharge. It is characterized by a relatively high discharge voltage and a low current. Because of its interesting physical appearance at low pressure, the glow discharge was investigated extensively by early researchers. Today, the glow discharge has practical applications in the areas of lighting and certain types of pulsed power switches.

## REFERENCES :

Brown, S.C. (1966). Introduction to Electrical Discharges in Gases. John Wiley & Sons, New York.

Cobine, J.D. (1957). Gaseous Conductors. Dover Publications, New York.

Howatson, A.M. (1976). An Introduction to Gas Discharges (2nd edition). Pergamon Press, Oxford.

Krebs, W.H. and Reed, A.C. (1959). Low Pressure Discharge Studies. Space Technology Laboratories, Inc. TR-59-0000-09931, Los Angeles. DTIC AD # 605984.

VonEngel, A. (1965). Ionized Gases. Clarendon Press, Oxford.

## CHAPTER 8

### CORONA

#### 8.1 INTRODUCTION

Corona is a self-sustained discharge which occurs in highly non-uniform electric fields, usually slightly below the breakdown voltage. The corona discharge is characterized by a visible glow around small wires and sharp points, an audible crackling sound, and radio noise. A form of the glow discharge, corona is often associated with air at sea level pressure, but it can also be observed at very low pressures.

The name corona is derived from the French word "couronne," which literally means crown. The name comes from the visual display of the discharge. Near the threshold voltage, the light display takes on various characteristic shapes, including glows, multiple spots, haloes, coronas (concentric circles), brushes, and streamers. Corona occurs in a region of high electrical stress, and most experiments are done with a point to plane gap (Loeb, 1965, pgs.2-5).

The corona is called positive or negative, depending on whether the pointed electrode is the anode or the cathode. As can be seen, the two coronas are very different in appearance and their general nature. Negative corona tends to produce a reddish purple glow, while positive corona produces an intense



electric blue light. The color differences result from the different excitation states in nitrogen. With a pointed anode, electrons gain more energy than with a pointed cathode, and are able to excite the nitrogen to a higher state (Loeb, 1965, p.7).

The voltage at which corona begins is called the corona onset voltage, and it is usually lower for negative corona than for positive corona. Once corona has begun, the voltage must be reduced to the corona offset voltage to extinguish the discharge. Because of heating during the discharge, the offset voltage is subject to variation, and is not as reliable as the onset voltage (Dunbar, 1966, p.4).

Corona is always a problem for high voltage engineers. On transmission lines, corona represents a costly power loss. It may lead to deterioration of insulators through ion bombardment or chemical action.<sup>1</sup> On the positive side, the corona discharge is used in the operation of electrostatic precipitators, geiger counters, and several other processes in the chemical industries.

The study of corona was an area in which little progress was made, until the development of high speed test equipment. Much of our understanding of corona phenomena is due to the work carried out by Loeb and his graduate students beginning in 1937. As late as 1960, researchers were still postulating new theories about the nature of some types of corona. Loeb (1965) compiled a 700 page book which includes virtually all of the corona

---

<sup>1</sup>ozone and various oxides of nitrogen are formed by corona in air. The nitrogen oxides form nitric acid when water vapor is present.

research up to that time. A volume edited by Kunhardt and Luessen (1983) contains a chapter devoted to corona which includes work up to 1981.

This chapter will describe the phenomena and explain the theories of the negative and positive point coronas in atmospheric air. Then, some techniques to detect and control corona will be considered. The chapter will conclude with a discussion of partial discharge, which is the term applied to a corona-like discharge in solids and liquids.

## 8.2 Negative Point Corona

The first extensive study of negative point corona began in 1937 by G.W. Trichel, one of Loeb's students. The study showed the corona current flowed in the form of very regular pulses. The existence of these pulses was actually disclosed to Loeb by a colleague earlier in 1937, but Trichel (1938) provided the first study and theoretical explanation of them. Thus, Loeb named them Trichel pulses.

Figure 8-1 shows the characteristic shape of the Trichel pulses. The frequency of the pulses increases with voltage, but the amplitude remains constant. Variation of the electrode separation from 0.75 to 6.0 cm had little effect on the frequency of the pulses, but changing the sharpness of the point or the gas pressure had a strong effect on the pulse frequency. The dependence of the pressure on point size and pressure is illustrated in figures 8-2 and 8-3, respectively (Trichel, 1938). At higher

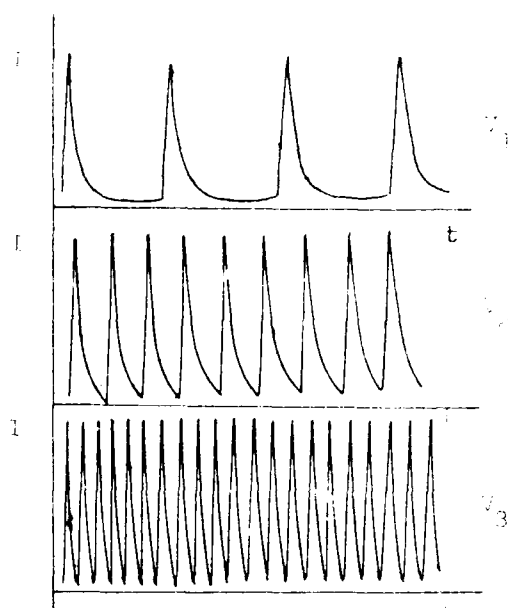


Figure 8-1: Characteristic shape of Trichel pulse and variation of frequency with voltage (after Trichel, 1938).

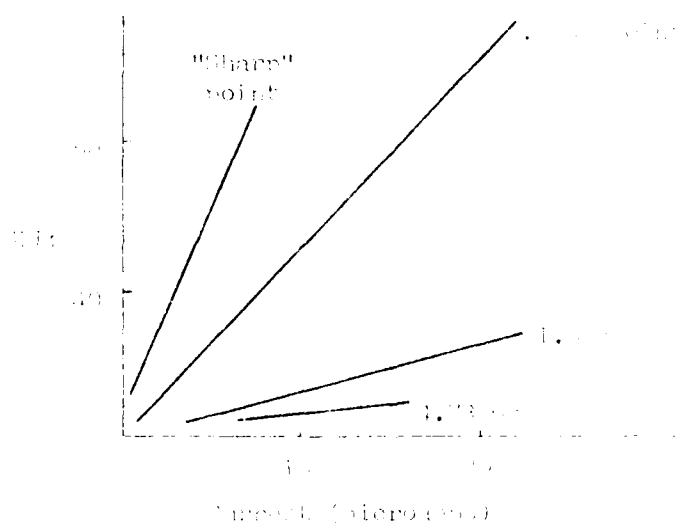


Figure 8-2: Variation of pulse frequency with point diameter (after Trichel, 1938).

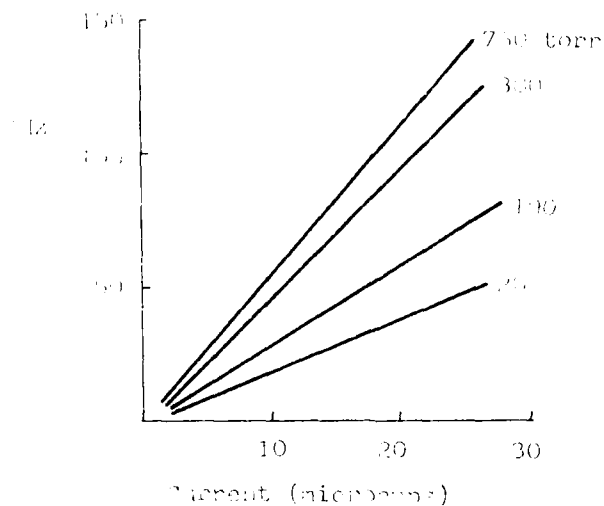


Figure 8-3: Variation of pulse frequency with gas pressure (after Trichel, 1938).

voltages, the pulses give way to a steady corona, and eventually to complete breakdown. Figure 8-4 shows the different regions which occur as a function of voltage and pressure-distance product (Loeb, 1965, p.393).

The lack of change in pulse frequency over a wide range of electrode separation, coupled with the strong dependence on point sharpness, caused Trichel to conclude the pulsing nature was caused by conditions very near to the point.

#### 8.2.1 Theory of the Trichel Pulse

Trichel assumed a randomly created positive ion could be drawn into the cathode, creating a secondary electron. The high cathode field would then cause the electron to form an avalanche. As the field weakened with distance from the point, the avalanche

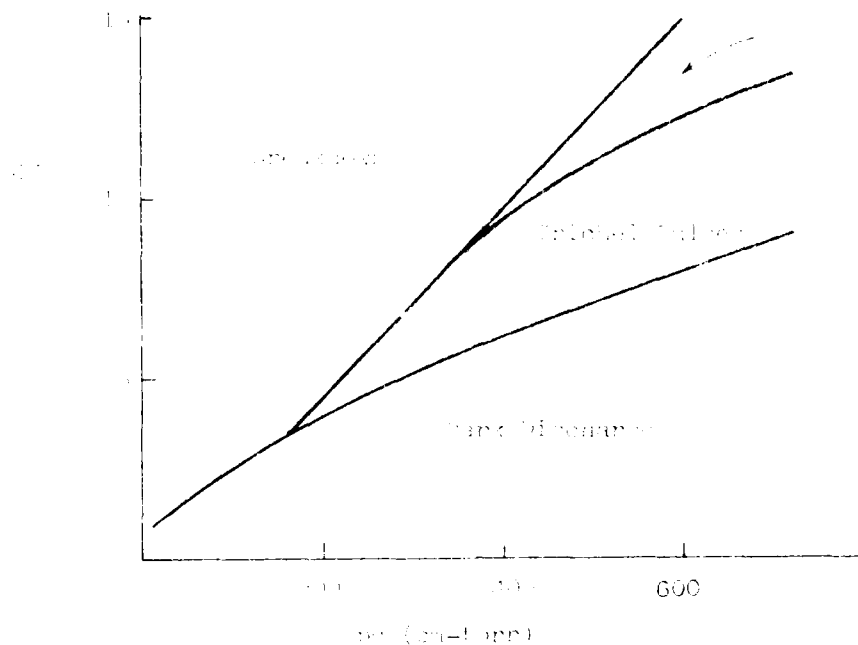


Figure 8-4: Negative point corona modes as a function of voltage and pressure-distance product (after Loeb, 1965, p. 393).

would eventually die out. Photons from the ionizing zone cause the release of additional electrons, and more avalanches. This process repeats for several generations, resulting in a very fast increase in current. The electrons, having high mobility, move out into the low field region where they can attach to  $O_2$  molecules. Meanwhile, the positive space charge intensifies the field at the cathode, increasing the amount of ionization. Figure 8-5a shows the distribution of space charge, at this stage, and the effect it has on the potential distribution.

Eventually, the positive ions drift to the cathode, and the negative ions drift further out. The field between the space charges is opposite to the applied field, resulting in a region with a low net field. Triebel believed the distance between the

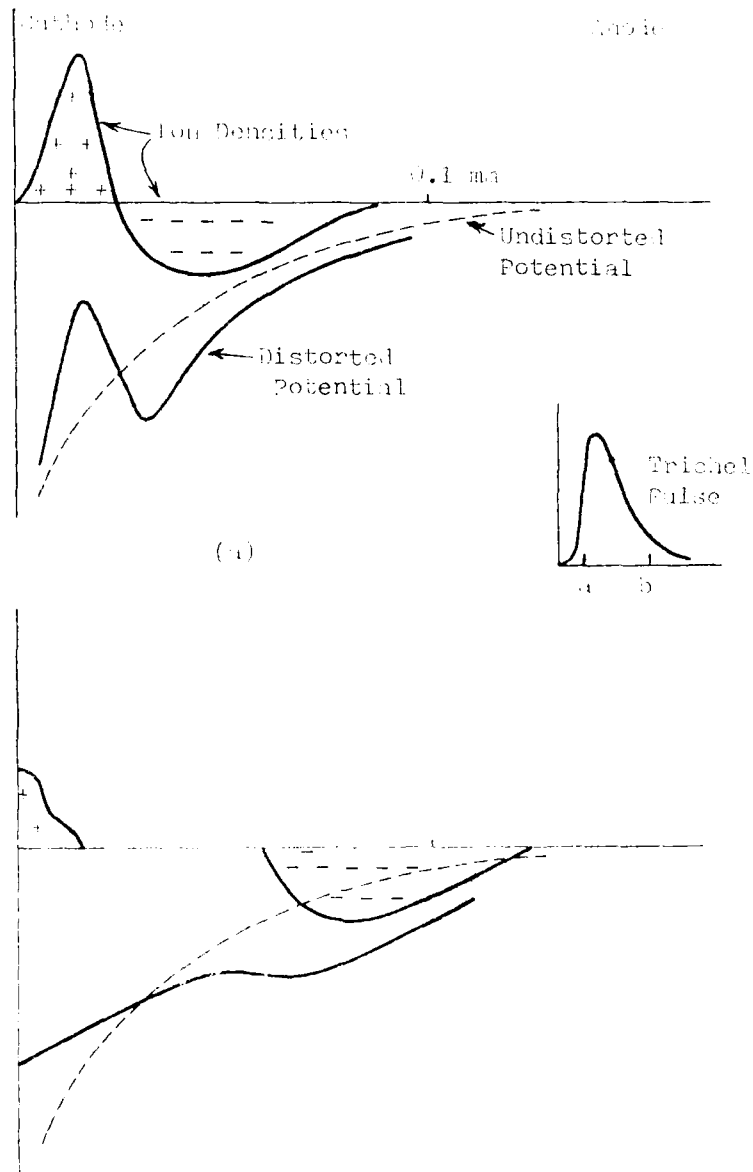


Figure 8-5: Schematic illustration of the movement of space charges in negative point corona: (a) early in the Trichel pulse; (b) late in the pulse (after Trichel, 1938).

positive space charge and the cathode would grow too short for newly emitted electrons to cause ionization. Since the field beyond the positive space charge is low, no ionization takes place there, either. Thus, the discharge is choked off. As the positive ions are neutralized at the cathode, the current decreases. Figure 8-5b shows the space charge distribution late in the pulse. Finally, after almost all of the positive ions become neutralized, the cathode field is restored, and one of the last ions causes a secondary electron which starts the process over again.

At the time of Trichel's work, the speed of oscilloscopes was not fast enough to accurately measure the rise time and duration of the pulses. Later observations required some modifications to the theory.

Two observations, in particular, required changes in the beginning and end of Trichel's explanation. The first observation was the absence of Trichel pulses in clean, dry air as well as when extremely sharp points were used. Examination of conditioned electrodes in atmospheric air showed the points always had dust specks on them. Further, dusting the points in clean air with  $0.01$  mm diameter particles restored the pulses. Thus, it is now believed the insulating dust particles acquire a positive charge and cause localized field emission from the point. This theory was also confirmed by the lack of influence of cathode material on the discharge formation (Loeb, et al, 1941).

The second observation was the absence of pulses in pure  $H_2$ ,  $N_2$ , or A, all non-attaching gases. This pointed out the importance of negative ions to the pulse formation process. Since the positive ions are neutralized at the cathode, the negative space charge grows at a faster rate than the positive space charge. The negative space charge weakens the field at the cathode, reducing ionization and preventing further current. As the negative space charge drifts toward the anode, the cathode field grows in strength, and eventually the pulse process starts over again. The negative space charge may only have to move one or two millimeters for this to occur. (Loeb, et al, 1941)

#### 8.2.2 Physical Appearance of Negative Corona

The negative corona was found to be similar to the cathode region of the glow discharge. At atmospheric pressure, the regions within the discharge were too small to measure; however, by reducing the pressure, they could be made larger. The size of the atmospheric discharge was then deduced by assuming  $pd$  is constant.

Figure 8-6 shows a sketch of the discharge at atmospheric pressure. The negative glow appears as a bright, bluish purple button, approximately 0.01 cm in diameter and half as thick. The glow is separated from the cathode by a Crookes dark space, some  $2 \times 10^{-4}$  cm in length. The negative glow is followed by a Faraday dark space and a positive column. The positive column is shaped like a shaving brush, giving off a violet glow.



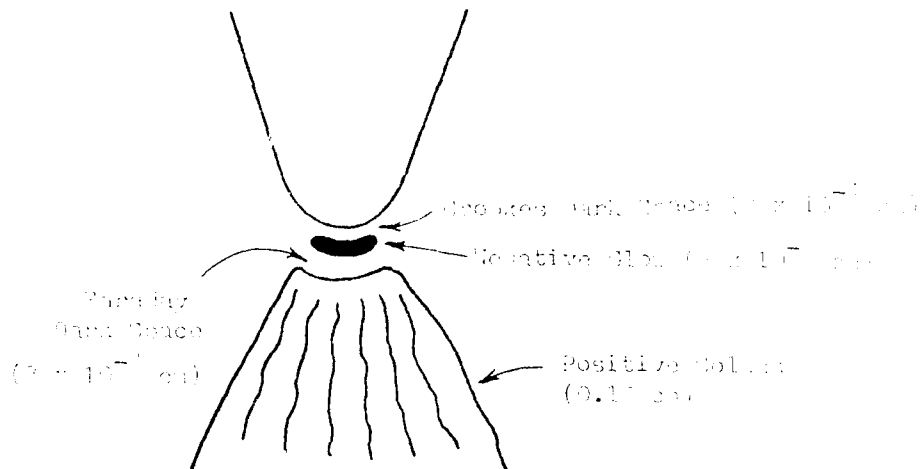


Figure 8-6: Physical appearance of negative point corona (after Loeb, 1948).

### 8.3 Positive Point Corona

The application of high speed oscilloscopes to positive point corona also began in Loeb's laboratory. Loeb and Trichel did some early work, but Kip, another graduate student, carried out the first comprehensive analysis. Kip studied points from 0.5 mm to 4.7 mm diameter and gaps from 1 to 8 cm in length.

He found the corona current increased steadily with voltage until breakdown occurred, and the corona manifested itself in several different forms. Figure 8-7 shows a typical voltage-current characteristic for positive point corona. The curve on the left shows the initial current on an expanded scale. In region A, free electrons avalanche toward the point, creating a current. Essentially, this is the field intensified ionization current.

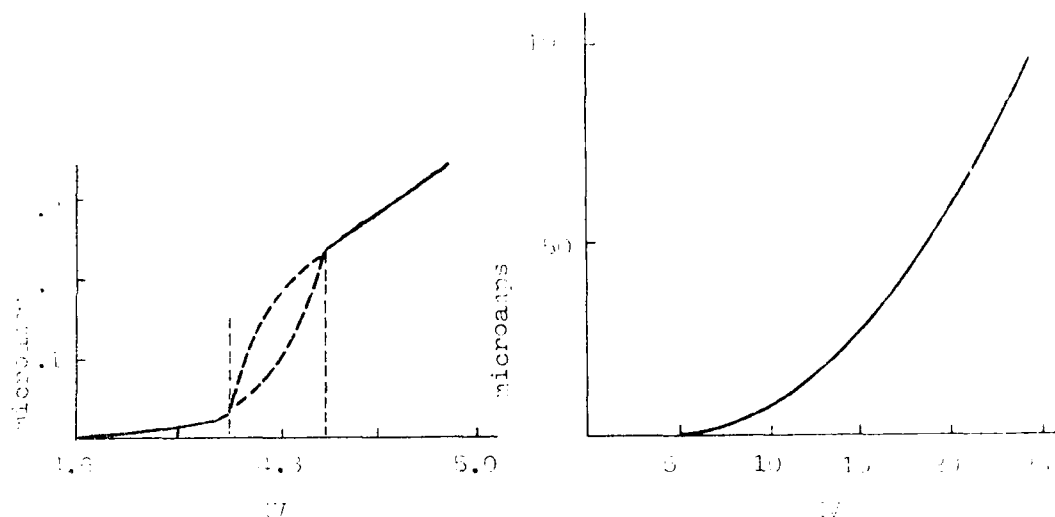


Figure 8-7: Voltage-current characteristic for positive point corona (after Kip, 1938).

Region B is called the geiger counter region and lies just below the onset of self-sustained corona. Corona occurs in region B if there is an auxiliary source of ionization. Kip used radioactive material, and the total current depended on the amount used. Region C begins at  $V_0$ , the corona onset voltage, and the current increases linearly with voltage. Finally, in region D (shown in the right hand curve), the current increases faster than the voltage until complete breakdown occurs at  $V_S$ . (Loeb, 1965, pgs. 75-77)

In the geiger counter region, the current consists of bursts, each burst being caused by an electron avalanching into the anode. Kip found it difficult to detect the corona onset voltage, unless the radioactive source was used. Without it, there was

a time delay before the discharge began, and the delay became longer as the applied voltage approached  $V_0$  from above. Once the discharge formed, however, the voltage could be slowly reduced and the discharge ceased when  $V_0$  was reached. Thus, the easiest way to find the onset voltage was to find the offset voltage.

At the onset of corona, Kip observed two types of pulses which increased in frequency as the voltage increased. Figure 8-8 shows the characteristic shapes of the pulses. The right pulse shows two so-called burst pulses, the middle trace shows a streamer followed by a short burst, and the right trace shows a streamer followed by a long burst. (Kip, 1939)

The discharge was often observed to begin with a single visible streamer propagating from the point. If the gap was too short, breakdown followed with no corona. However, if the streamer did not propagate to the cathode, its space charge inhibited further streamers. As a result, shorter burst pulses followed. While a streamer could trigger burst pulses, the bursts could also start by themselves. In either case, as long as the bursts continued, no streamers could propagate. As the voltage was raised further (region D of figure 8-7), a steady burst corona was observed. Finally, streamers could reappear, just below the breakdown voltage. (Loeb, 1965, pgs. 75-85)

Figure 8-9 shows the breakdown regions, for a one cm diameter spherical anode and a plane cathode, as a function of the gap distance. The bottom region represents a non-self-sustained discharge, while the top region represents complete breakdown. Thus,

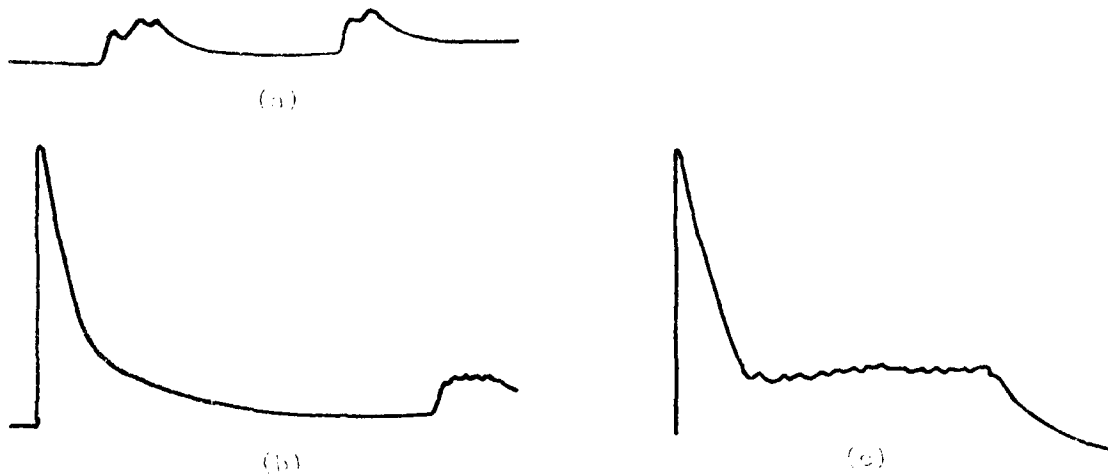


Figure 8-8: Forms of positive point corona observed by Kip with an oscilloscope: (a) two bursts; (b) a streamer followed by a short burst; (c) streamer followed by a long burst. The decay of the streamers was dragged out by the oscilloscope time constant (Loeb, 1965, p.80).

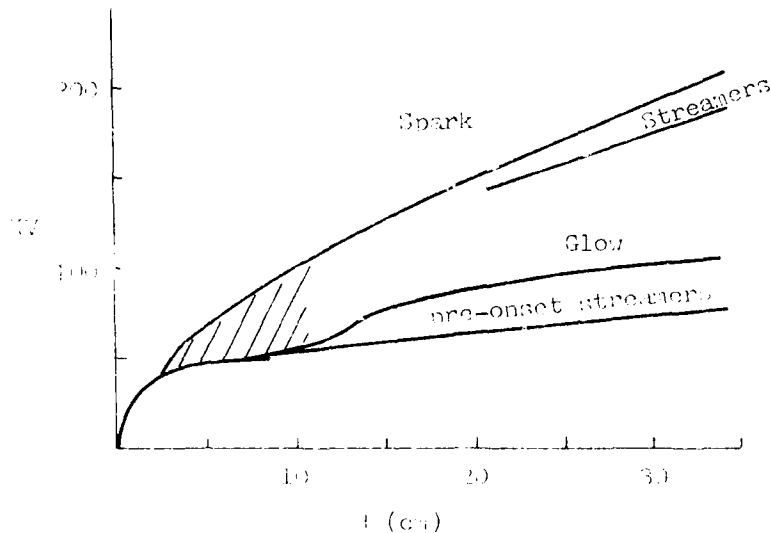


Figure 8-9: Positive point corona modes as a function of voltage and electrode separation (after Loeb, 1965, p. 94).

for  $d$  less than about 3 cm, the gap breaks down without any corona. At longer gap lengths, transitions through pre-onset streamers, steady glow, and pre-breakdown streamers are possible. The cross-hatched region was found to be achievable only by indirect means. For example, raising the voltage above 50 KV at  $d=7.5$  cm results in immediate gap breakdown. However, if a 15 cm gap is raised to 75 KV, the gap can be closed down to 7.5 cm and the steady corona will be maintained (Loeb, 1965, p.94).

#### 8.3.1 Theory of Positive Corona

Loeb and Kip proposed an explanation for the streamers and bursts and the steady corona. They believed the positive space charge left in the gap by an incomplete streamer would prevent the growth of a new streamer, while allowing smaller bursts to form. Once developed, the burst pulses precluded a streamer, but eventually, the space charge became so strong that bursts could no longer form. After the space charge cleared, the streamer-burst cycle could repeat itself. As the voltage was increased above onset, the frequency and duration of the bursts increased. When the voltage reached about 10% over  $V_0$ , they believed the space charge was cleared as fast as it formed. Then, the steady burst corona began. (Kip, 1939)

This theory was accepted until 1960 when Hermstein proposed a modification to it (Loeb, 1965, p.78). In retrospect Loeb (1965, p.100) realized,

...it was unreasonable to believe that such a glow corona once established could extend from an onset potential over a range of two the three times that potential before breakdown streamers and a spark mater-

ialized. The illogical element arises in that it had been assumed that in a range of some 10% or less above the threshold potential, the anode field could clear burst pulse space charge so as to permit onset of steady corona. In light of this assumption, it seems strange that a 200% increase in point potential should be needed to clear the same sort of charge for breakdown streamer appearance.

What Loeb and Kip had failed to consider was the formation of negative ions by electron attachment.

A streamer which does not cross the gap terminates in a low field region. The streamer consists of electrons and positive ions. Some additional electron-ion pairs are created photoelectrically. However, in the weak field, the electrons cannot ionize gas molecules. They are drawn to the anode by the electric field, but become attached to  $O_2$  molecules, forming a slow moving negative space charge.

The negative space charge reduces the electric field between itself and the positive space charge, which remains behind in the low field region, and increases the field at the anode. The enhanced field region, however, is shorter than the high field region which began the streamer, so further streamers are inhibited. Less intense pulses do form which create new electrons, beyond the negative space charge, by photoelectric action. These electrons attach and replenish the negative space charge which is constantly being neutralized at the anode. The result is a glow type discharge at the anode (Loeb, 1965, pgs. 90-92).

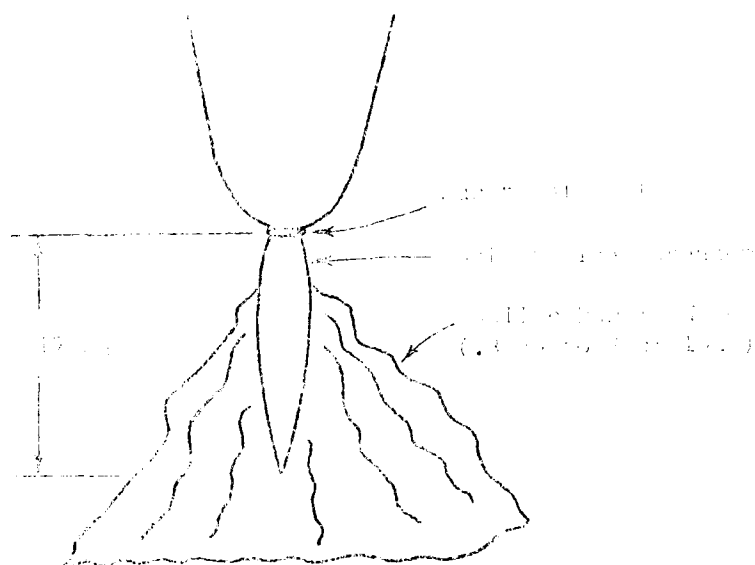


Figure 8-10. Physical appearance of pre-onset streamers in positive point corona. Dimensions are for 760 torr (after Loeb, 1948).

#### 4-2 Appearance of Positive Point Corona

Fig. 8-10 shows the dimensions and appearance of the pre-onset point corona. It is characterized by a bright blue streamer cone projecting from the anode. Near the point, the streamer is straight, but it flares out as the streamer branches. The streamer cone has a dusky purple coloring. The burst pulse produces a glow that is a velvety glow on the point surface. The glow is not uniform, but it spreads over the point.

#### 8.4 Detection and Control of Corona

Corona may be detected by any of its characteristics. As we have seen, corona is accompanied by a visual display. However, the light is usually observable only when the surrounding environment is dark. In some cases, the smell of ozone or nitrous oxides may be detected. Corona also creates audible and radio frequency noise.

The noise created by corona is due to its pulsing nature. Audible noise results from pressure waves in air which are produced by the varying intensity of the corona. In power systems, this noise is composed of 60 Hz harmonic components, with 120 Hz being the most prevalent. This noise increases when it is rainy or foggy. Radio noise is produced by corona and is also amplified by the presence of water vapor. Most readers have probably experienced this phenomenon while driving under a transmission line with an AM radio playing. (Miller, 1977)

Finally, the electrical current due to corona may be measured with a sensitive ammeter or an oscilloscope. Several companies manufacture special corona detection equipment. Kuffel and Abdullah (1970, ch.6) and Gallagher and Pearmain (1983, ch.7) cover some of the detection techniques in detail.

The primary technique for reducing corona is to avoid high field intensification factors, wherever possible. Sharp edges, points, and scratches should be eliminated by design or by careful construction. When single conductors are used, the diameter may have to be increased to reduce corona. Power transmission lines



generally use bundled conductors to increase the effective diameter of the conductor. High voltage equipment often uses large, toroidal shaped metal surfaces to grade out the electric field.

#### 8.5 Partial Discharge in Solids and Liquids

Corona-like discharges can occur in solid and liquid dielectrics, as well as in gases. The discharge occurs in microscopic voids or bubbles within the solid or liquid, but these voids or bubbles may be formed as a result of the high electric field in the immediate vicinity of a sharply curved or pointed electrode. When the voltage across the void becomes excessive, a partial breakdown of the dielectric occurs. Thus, this type of discharge is known as partial discharge.

A void in a liquid or solid is usually gas-filled and has a lower dielectric constant than the surrounding medium. In chapter 2, we saw that the region with the lower dielectric constant is the more highly stressed. As a result, the void may breakdown at a much lower voltage than would the solid or liquid. When the void breaks down, a small amount of charge (picocoulombs) is transferred in the form of a pulse. The continued repetition of such pulses may eventually expand the void, leading to total breakdown. This process is known as treeing.

Treeing has become a very significant problem for the electric utilities, since they began the extensive use of underground residential distribution (URD). The cables for URD use polyethylene (PE) or cross-linked polyethylene (XLPE) as the dielectric. Fortunately, PE and XLPE have proven to be quite resistant to

treeing, and the presence of water accentuates the problem (Banji, et al, 1983). As a result, considerable research is being conducted on these types of insulation.

The voltage at which partial discharge begins is known as the partial discharge inception voltage (PDIV). Once partial discharge has begun, the voltage must be lowered to the partial discharge extinction voltage (PDEV) to stop the discharge (that is,  $PDEV < PDIV$ ). It is extremely important for the normal operating voltage to be below the PDEV. If the operating voltage was above the PDEV, a voltage surge could initiate a partial discharge which would not stop when the voltage returned to normal.

#### 8.6 Summary

In this chapter, we have looked at the corona discharge. Although it occurs in most gases over a wide range of pressures, we have primarily considered corona in air at sea-level pressure. The phenomena exhibited by positive and negative corona are very different, but in both cases, the formation of negative ions in the low field region has a strong influence on the discharge behavior. Also, both types are visible and audible. Thus, corona may be detected by visual, audio, or electrical methods. Corona can also occur in voids or bubbles in solids and liquids; then, it is known as partial discharge. Partial discharge may result in deterioration and failure of the dielectric over time.

## REFERENCES :

- Bamji, S., et al (1983). IEEE Transactions on Electrical Insulation. V. EI-18, p. 32.
- Dunbar, W.G. (1966). Corona Onset Voltage of Insulated and Bare Electrodes in Rarefied Air and Other Gases. US Air Force Aero-Propulsion Laboratory Technical Report 65-122, Wright-Patterson AFB, OH 45433. DTIC AD# 483820.
- Gallagher, T.J. and Pearmain, A.J. (1983). High Voltage Measurement, Testing and Design. John Wiley & Sons, Chichester.
- Kip, A.F. (1938). Physical Review. V. 54, p.139.
- Kip, A.F. (1939). Physical Review. V. 55. p.549.
- Kuffel, E. and Abdullah, M. (1971). High Voltage Engineering. Pergamon Press, Oxford.
- Kunhardt, E.E. and Luessen, L.H. (ed.) (1983). Electrical Breakdown and Discharge in Gases (2 vols.). Plenum Press, New York.
- Loeb, L.B. (1948). Journal of Applied Physics. V. 19, p.882.
- Loeb, L.B. (1965). Electrical Coronas. University of California Press, Berkeley.
- Loeb, L.B., et al (1941). Physical Review. V. 60, p.714.
- Miller, D.B. (1977). High Voltage Engineering. Unpublished course notes. Purdue University, West Lafayette, Indiana.
- Trichel, G.W. (1938). Physical Review. V. 54, p. 1078.

## CHAPTER 9

### THE ARC DISCHARGE

#### Introduction

Virtually everyone has witnessed the arc discharge in the form of lightning. Because of the large currents carried by arcs and the potential for severe damage to equipment, the arc is often regarded as the ultimate form of the electrical discharge. The arc exhibits several features which separate it from other forms of electrical discharges. First, the current density in the arc column is very high. It may be as high as  $100 \text{ A/cm}^2$  versus 1 to  $10 \text{ mA/cm}^2$  for a normal glow discharge. It is even higher at the electrodes.

Second, the cathode fall in an arc is usually about 100 V, which is far lower than the normal or abnormal glow discharge. Finally, the arc column provides much more light than a glow discharge. (Hirsh and Oskam, 1978, p.294)

Several different techniques may be used to establish an arc discharge. The first way is to slowly increase the supply voltage and follow the voltage-current characteristic which was shown in figure 7-1. Realistically, this is only practical for a large tube at a pressure of a few torr. A second way to establish an arc is to suddenly apply a voltage which is well above the breakdown voltage. In this case, the transitions between different types of discharges are compressed in time.

Figure 9-1 (Brown, 1966, p.234) shows the variation of current

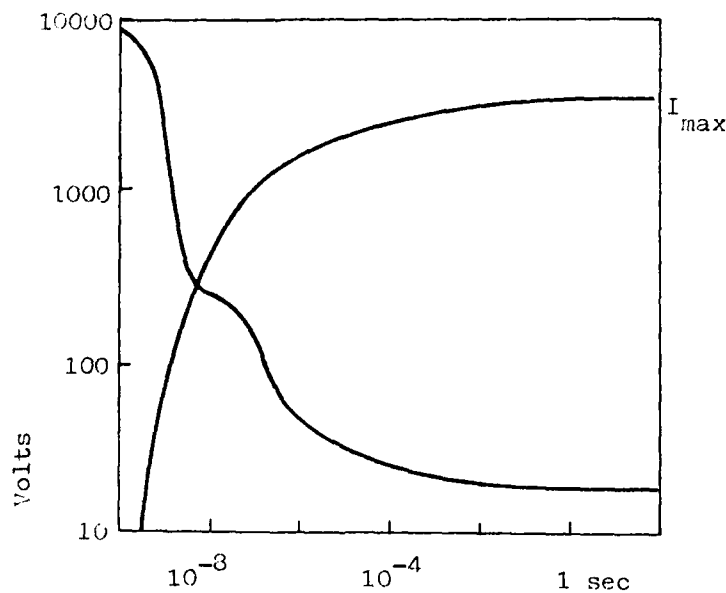


Figure 9-1: Variation of voltage and current for a sudden application of a voltage above the breakdown voltage.

and voltage as a function of time for a suddenly overvolted gap. Since the breakdown voltage is somewhat statistical in nature, it is sometimes desirable to cause breakdown by pre-ionizing the gap. This can be done with UV light, x-rays, electron beams, or lasers. A fourth method is to draw apart two current carrying electrodes which were initially in contact. If the current is high enough, localized heating causes thermionic emission at the cathode, and the arc develops.

While the arc is often thought of as a catastrophic event, it has significant commercial applications. It is used in a variety of lighting applications. An example is the high pressure sodium lamp (often known by the General Electric trademark, Lucalox), which provides the intense yellow light seen over large

parking lots. The arc is also used to manufacture stainless steel and to process other materials in electric furnaces. Several types of pulsed power switches utilize an arc discharge. Finally, power circuit breakers must be able to interrupt an arc when they open under load or short circuit conditions.

Although the arc has been studied since 1808, many of its phenomena are still in basic dispute. The arc typically exists in a mixture of gases--some from the electrodes, some from the surrounding medium, and some from chemical reactions. The characteristics of the arc seem to vary with minor changes in the gas composition, electrode surface, and geometry. Thus, the theoretical descriptions of the arc are not complete. Several good references are Hirsh and Oskam (1978, ch.5), VonEngel (1965, ch. 9), Brown (1966, ch.15), Cobine (1957, ch.9), and Hoyaux (1968).

In this chapter, we will look primarily at the DC arc. The next section will present the general characteristics of the arc. Then, each region of the arc will be considered separately. The final two sections will cover oscillations in DC arcs and AC arcs.

## 9.2 General Characteristics

The most noticeable characteristic of the arc is its luminous column structure. At atmospheric pressure, the column consists of a brilliant core which is so hot that all the gases are largely dissociated. The core is surrounded by a cooler region of flaming gases. When the arc burns horizontally, the center is drawn up by the rising hot gases, causing the column to arch. This effect

probably resulted in the name of the discharge (Cobine, 1957, pgs.290-292).

At low pressure, the discharge may be luminous if the discharge is constricted by the tube. The temperature of the positive column is very different, however. Figure 9-2 shows a schematic diagram of the variation of the temperature with pressure for the various components of the positive column plasma. Note, above 20 torr, or so, the temperature of the ions, electrons, and gas is very high--5000°K to 6000°K. This is known as local thermal equilibrium. At very low pressures, the gas and ion temperatures drop to a few hundred degrees, while the electron temperature soars to as much as 40,000°K.<sup>1</sup> This major difference in the condition of the plasma requires completely different analysis techniques. Most of the discussion in this chapter will pertain to high pressure arcs.

The form of a high pressure arc is illustrated in figure 9-3a. The positive column appears between the two electrodes. It is constricted at both electrodes, with the constriction being much more severe at the cathode. Since the same current must flow throughout the discharge, the current density is higher at the anode, and much higher at the cathode, than in the column. Figure 9-2b shows the potential distribution across the discharge. Basically, it consists of three parts: the cathode fall, the anode fall, and the positive column. The first two

---

<sup>1</sup>The reader should recall, from chapter 2, the temperature of a species is simply a measure of the kinetic energy of a particle having the most probable velocity.

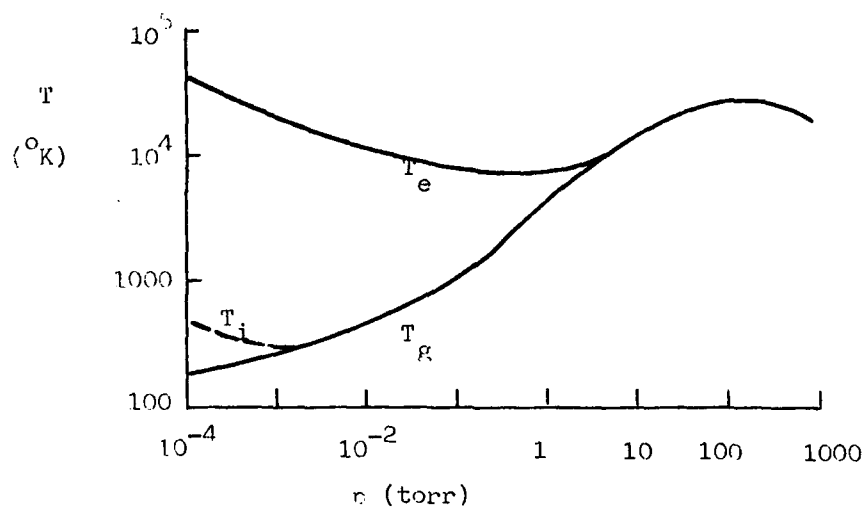
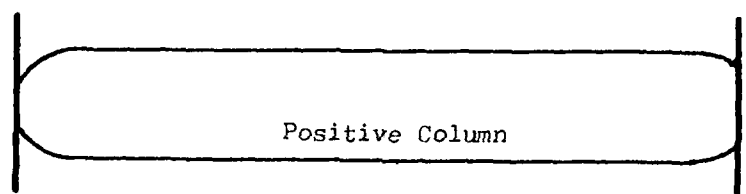
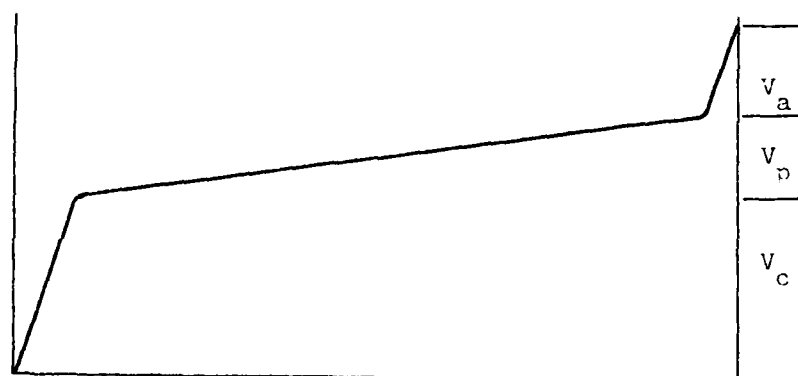


Figure 9-2: Temperature variation with pressure of the positive column plasma components.



(a)



(b)

Figure 9-3: Regions of the arc discharge: (a) typical visual appearance; (b) potential distribution.



are actually about as thick as one mean free path of an electron and are approximately 10 volts, while the positive column drop is a function of its length.

The variation of the arc voltage with current is shown schematically in figure 9-4. At first, the voltage drops with increasing current, but eventually it becomes almost constant. At very large currents (thousands of amperes), the voltage may begin to increase with current. (Cobine, 1957, p.299)

### 9.3 The Regions of the Arc

For current to flow in an arc, three things must happen. First, the neutral gas must be made into a conducting medium by the creation of charged particles. Second, currents must be transferred across the cathode-gas junction, and third, current must be transferred across the anode-gas junction. In this section, we will look at each of the three regions.

#### 9.3.1 The Cathode

Cathode processes are believed to dominate the characteristics of the arc; however, much of the phenomena are still largely unexplained. In the abnormal glow, the discharge covers the entire cathode, and current increases are provided by increased current density. Eventually, the current density reaches a level at which it heats the cathode, and the transition to the arc begins. Self-sustained arcs<sup>2</sup> can be divided into two categories: those with refractory cathodes and those with "cold" cathodes.

---

<sup>2</sup>A non-self-sustained arc can be formed with an externally heated, thermionically emitting cathode.

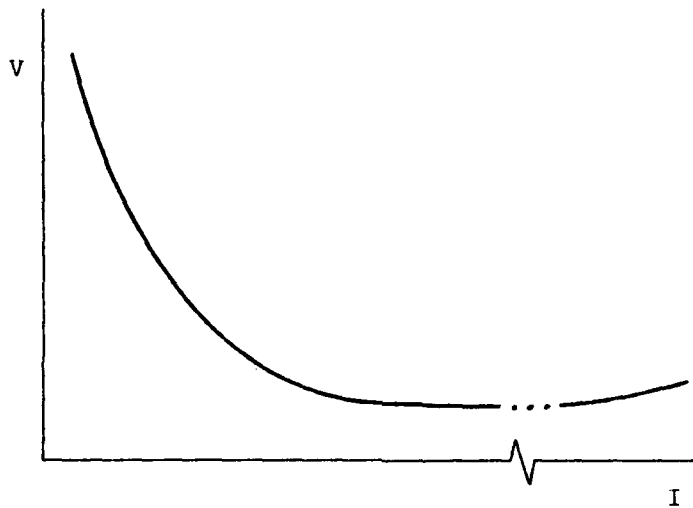


Figure 9-4: Schematic illustration of the variation of arc voltage with current.

It is the latter type which has proven to be very mysterious (Von Engel, 1965, p.273). In both cases, the cathode fall is on the order of 10 volts, but the similarity ends there.

Refractory cathodes are composed of materials, such as tungsten and carbon, which can attain temperatures high enough to thermionically emit a copious supply of electrons without vaporizing. Cold cathode materials include copper, silver, mercury, and many other metals. These metals all vaporize before they reach a temperature which provides enough thermionic emission to maintain the arc.

The refractory cathodes are usually characterized by a "low" current density and an incandescent cathode spot, which can only be moved very slowly. However, there are variations in the behavior of refractory cathodes. At relatively low currents (10 A),

the column is tightly constricted at the cathode, resulting in current densities of up to  $10^5$  A/cm<sup>2</sup>. This is known as the "burning spot" arc. Increasing the current frequently results in a sudden transition to a larger cathode spot with a current density of  $10^3$  A/cm<sup>2</sup>. This is known as the "burning spot free" arc.<sup>3</sup> Most observations of refractory cathodes appear to be consistent with thermionic emission being the source of cathode electrons.

In contrast to the refractory cathodes, cold cathodes exhibit very small cathode spots with current densities of  $10^6$  to  $10^8$  A/cm<sup>2</sup> (Hirsh and Oskam, 1978, p.332). In some cases, several spots have been observed. Thermionic emission does not account for the current. Field emission has been proposed as the source of electrons, but it is not entirely satisfactory. Still others have proposed some type of localized pressure effects at the cathode as the cause.

Considerable material may be lost from a cold cathode by vaporization, by melting, or by simply being "blasted" off the surface. If the entire cathode current were carried by electrons, the loss of material would amount to one atom for each eight electrons (Cobine, 1957, p.301). Actually, 15% to 50% of the cathode current is carried by ions (Hirsh and Oskam, 1978, p.334).

The cathode spot for cold cathodes typically exhibits a random motion over the cathode surface with velocities as high as 10 m/sec on mercury. This motion has resulted in one of the most

---

<sup>3</sup>These names apparently come from literal translations of the German words used to describe the phenomena.

perplexing problems in physics, today. If a magnetic field is applied, as shown in figure 9-5, the Lorentz force should cause the spot to move down. Experimentally, however, it is observed to move up. This phenomenon is called "retrograde motion", and numerous theories (all beyond the scope of this text) have been put forth to explain it (Howatson, 1976, p.96).

### 9.3.2 The Positive Column

The positive column represents the body of the arc since the electrode regions are only a fraction of a millimeter at atmospheric pressure. The name derives from the net positive charge in the center of the column, which results from the outward diffusion of the the electrons.

At high pressures, the plasma is maintained by thermal ionization. The electrical heat input to the column is  $V_p I_a$ , where  $V_p$  is the voltage drop across the positive column and  $I_a$  is the arc current. The electrical heat input causes the temperature of the gas to rise until heat losses balance the input. Heat losses may take the form of heat conduction or radiation of heat and light. The boundaries of the positive column are well defined, so the radial temperature gradient may be several thousand degrees Kelvin per millimeter.

Modeling of the positive column involves developing terms to express the input and the losses and, then, equating the two. This becomes very complicated, since both the thermal and electrical conductivities are functions of position. Simplifying assumptions must be made, but closed form solutions are generally

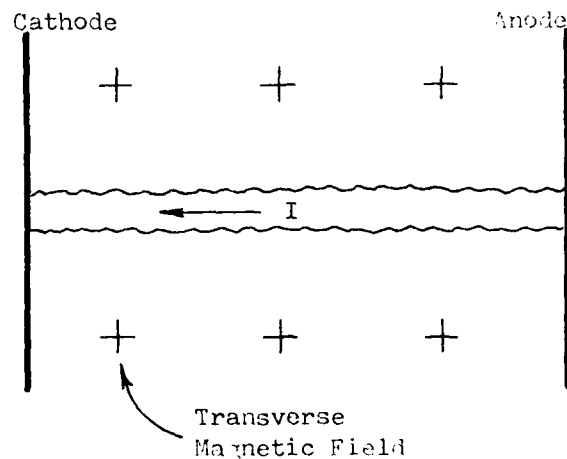


Figure 9-5: Retrograde motion of the cathode spot due to a transverse magnetic field.

not possible. Figure 9-6 shows a schematic representation of the variation of the current density, temperature, and illumination across the diameter of a cylindrical arc.

At low pressure, the positive column of the arc is similar to that of the glow discharge. Since the gas temperature is only a few hundred degrees, thermal ionization is no longer a factor. Instead, the ionization is due to electron collisions.

### 9.3.3 The Anode Region

The arc anode region is very similar to the glow discharge anode region. As electrons are drawn toward the anode, the electric field is intensified, and the anode fall is established. Typically, the anode fall ranges from 2 to 12 volts, but measurements are difficult and uncertain. Like the cathode fall, the anode fall occurs over the length of the mean free path of an

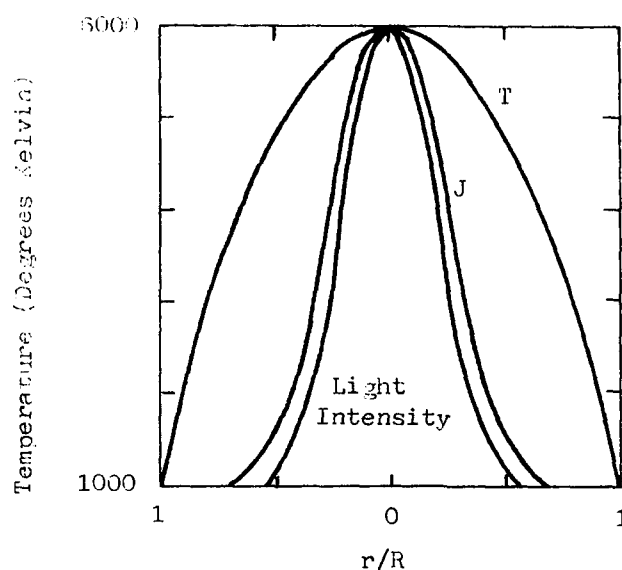


Figure 9-6: Variation of temperature, illumination, and current density across the diameter of the positive column (after Brown, 1966, p.241).

electron. As electrons are accelerated through the anode fall, they may ionize gas molecules, providing an input of positive ions to the positive column to replace ions lost at the cathode (Hirsh and Oskam, 1978, p.342).

The temperature of the anode may be greater than or equal to that of the cathode, at high pressure, but is limited by the melting point of the metal or its oxides. However, the anodes can be water cooled with no effect on the operation of the arc, other than the absence of anode material in the plasma. This indicates the high temperature of the anode is not required (Cobine, 1957, p.343).

The anode spot is larger than the cathode spot, resulting in a lower current density. Howatson (1976, p.98) reports the anode spot is less prone to random motion, while Hirsh and Oskam (1978, p.342) report it may travel randomly over the anode surface with "appreciable" velocities. Although the anode is less complicated than the cathode, in some respects there are less reliable data concerning it than the cathode.

#### 9.4 Oscillations in DC Arcs

Until now, we have been considering steady state DC arcs. In this section, we will consider the effects of an oscillation in the arc current. In particular, let the arc current be described by

$$I_a = I_{dc} + I_{ac}\sin(\omega t) \quad (9.1)$$

Curve 1 in figure 9-7 shows the downward sloping voltage-current characteristic for an arc in the vicinity of  $I_{dc}$ . Superimposed on it are several other curves.

First, consider a very low frequency oscillation. If the current change very slowly, the voltage will adjust and follow the DC characteristic. If, however, the current changes at a faster rate, the ionization of the column will be insufficient when the current is increasing. More voltage will be required to increase the ionization. Conversely, when the current is decreasing, the ionization will be too high, and the voltage will drop below the static characteristic. The dynamic characteristic takes on an elliptical shape, as shown by the ellipse number 2. The ellipses are traversed in the clockwise direction. As the

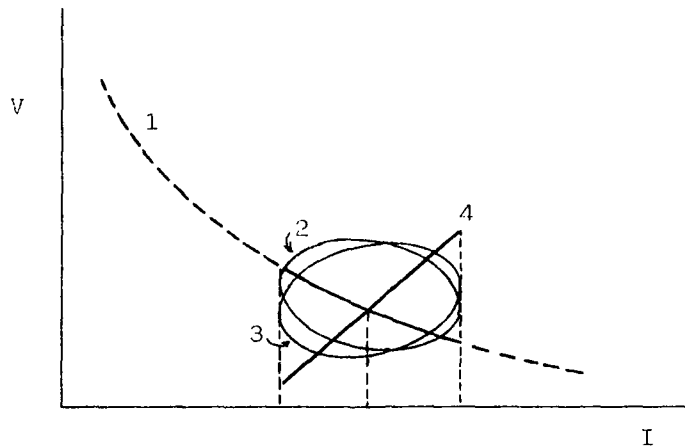


Figure 9-7: Illustration of the dynamic characteristics of a DC arc subjected to sinusoidal perturbations of varying frequencies (after Cobine, 1957, p. 345).

frequency of the variation increases, the ends of the ellipse move further from the static characteristic, effectively rotating the ellipse. In the figure, ellipse 3 is the dynamic characteristic at a higher frequency than ellipse 2. At very high frequencies, the ionization is unable to change during a cycle, and the positive column behaves like a resistor. Curve 4 shows the dynamic relation between current and voltage in that case.

The negative sloping characteristic of the arc literally corresponds to a negative resistance. If an arc forms in a circuit containing capacitance and inductance, it is possible for the arc to cancel out the circuit resistance, resulting in current oscillations. Fortunately, the curvature of the arc



characteristic only allows one point on it to exactly cancel the resistance, so the current will be bounded. For example, an arc on the primary of a transformer will cause oscillations in the secondary due to the inductance and distributed capacitance of the windings.

### 9.5 AC Arcs

We have seen that the positive column reaches very high temperatures at high pressures. Clearly, we would not expect the gas to cool down as soon as the arc was extinguished. Thus, if voltage were quickly reapplied, breakdown would reoccur. At low frequencies ( $<100$  Hz), the characteristic for an AC discharge is similar to that of the DC arc, except that reignition must occur every half-cycle. The characteristics of AC arcs are strongly dependent on the nature of the electrodes, the length of the arc, and the values of impedances in the external circuit.

Figure 9-8 shows typical voltage and current waveforms of a resistive circuit for the positive half-cycle. The arc voltage is characterized by three values: the reignition voltage,  $V_r$ ; the burning voltage,  $V_b$ ; and the extinguishing voltage,  $V_e$ . After the current has gone to zero in the negative half-cycle preceding figure 9-8, gas deionization and electrode cooling begin. Thus, a high voltage is required to reignite the arc. Inductance in the circuit may lower  $V_r$ . The arc voltage tends to be higher than the DC characteristic while the current is increasing, and lower when the current is decreasing. The AC volt-ampere characteristic is shown in figure 9-9.

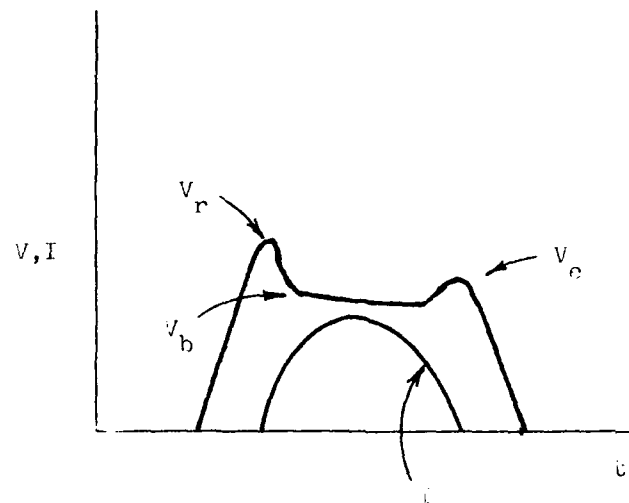


Figure 9-8: Current and voltage waveforms for the positive half-cycle of an AC arc (after Cobine, 1957, p. 348).

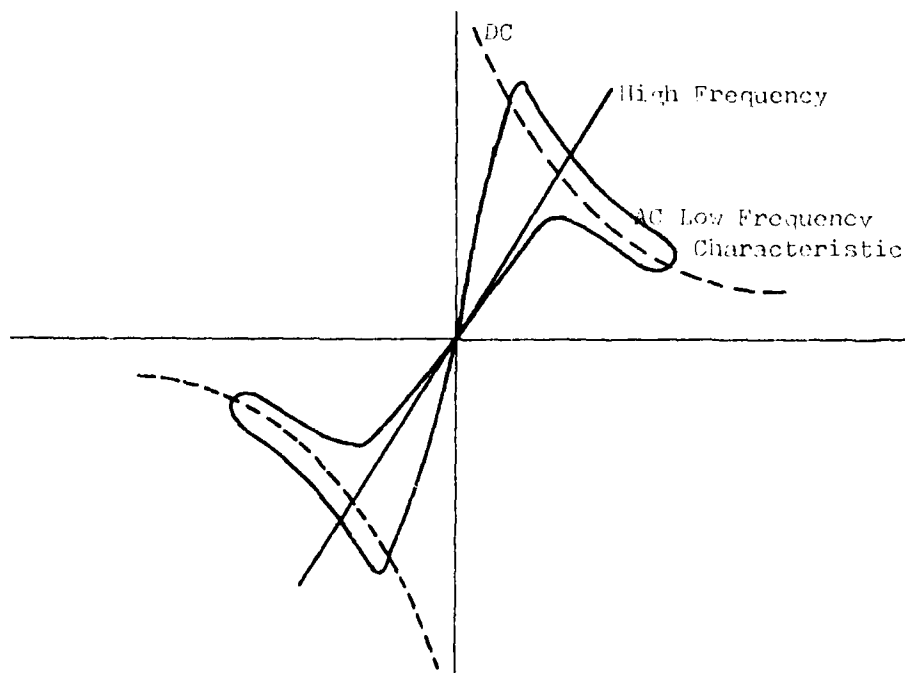


Figure 9-9: Voltage-current characteristic of an AC arc (after Cobine, 1957, p. 349).

The process of reignition is essentially a race between the deionization processes and the increasing circuit voltage. The deionization process is different for short and long arcs. In a short arc, the cathode and anode falls account for substantially all of the arc voltage. Also, cooling processes at the electrodes are important. For long arcs, the electrodes are less important, and the deionization of the column is more important. A short arc with refractory electrodes may reignite at the burning voltage, while the reignition between low boiling point electrodes may be relatively high. Obviously, if the cathode and anode are of different materials, successive half-cycles will be asymmetric.

#### 9.6 Summary

The arc discharge is characterized by high current density, a low cathode fall, and, at atmospheric pressure, an intense luminous display. Much of the basic understanding of arc phenomena is still lacking, and often only qualitative observations (some of them contradictory) are available. The cathode processes are the most important to the arc discharge, as the cathode must become a very good electron emitter for the discharge to form. The positive column dominates the appearance of the discharge, and temperatures of several thousand degrees Kelvin are achieved at atmospheric pressure. The anode seems to be a passive part of the arc, although the anode fall region is necessary to supply some positive ions. Finally, the characteristics of transient disturbances and AC arcs are largely a function of the frequency.

## REFERENCES :

- Brown, S.C. (1966). Introduction to Electrical Discharges in Gases. John Wiley & Sons, New York.
- Cobine, J.D. (1957). Gaseous Conductors. Dover Publications, New York.
- Hirsh M.N. and Oskam, H.J. (ed) (1978). Gaseous Electronics. Academic Press, New York.
- Howatson, A.M. (1976). An Introduction to Gas Discharges (2nd edition). Pergamon Press, Oxford.
- Hoyaux, M.F. (1968). Arc Physics. Springer-Verlag, Berlin and New York.
- VonEngel, A. (1965). Ionized Gases. Clarendon Press, Oxford.

THIS PAGE INTENTIONALLY BLANK

## CHAPTER 10

### BREAKDOWN IN VACUUM

#### 10.1 Introduction

Until now, we have been primarily interested in gas breakdown. In chapter 6, Paschen's law stated the breakdown voltage would increase as the product of gas pressure and electrode spacing was reduced below the value at the Paschen minimum. Eventually, a point is reached where electron collision becomes unable to cause electrical breakdown. Typically, this happens when the electron mean free path becomes longer than the distance between the electrodes. When that happens, the system is at the upper end of the vacuum regime.

Theoretically, vacuum breakdown should only be limited by field emission. The Fowler-Nordheim equation predicts field emission will be insignificant below an electric field strength of  $10^7$  V/cm. In reality, field emission currents appear at average field strengths of  $10^5$  V/cm, indicating a field enhancement factor of 100. Complete breakdown into a luminous arc may even occur because there are adsorbed gases in the electrodes and oil vapors from the vacuum pump.

Contamination of the electrodes may result in the formation of a small gas cloud, if the electrode becomes heated by the field emission. Electrons passing through such a cloud may ionize some of the molecules, forming an avalanche, and low pressure gas

breakdown follows. The breakdown voltage is influenced by a number of factors, and the nature of the breakdown is not thoroughly understood.

Because of the difficulties associated with obtaining a good vacuum and uncertainty in the breakdown voltage, vacuum is usually used only where it is essential. Some of its more important applications include: high power or high voltage vacuum tubes, particle accelerators and separators, microwave tubes, nuclear fusion experiments, low loss capacitors, power circuit breakers, and space systems.

There are several good sources of information on vacuum breakdown. Among them are Latham (1980), Alston (1968, ch.4), Meek and Craggs (1978, ch.2), Denholm, et al (1973, section 7), and Mulcahy and Bolin (1971). The last two are DOD technical reports and are available from the Defense Technical Information Center. In addition, there has been a series of International Symposiums on Discharges and Electrical Insulation in Vacuum. The eleventh was held in September, 1984. Papers from the tenth were published in special issues of the IEEE Transactions on Electrical Insulation (June, 1983, V. EI-18, no. 3) and Plasma Science (Sept, 1983, V. PS-11, no. 3).

In this chapter, we will first discuss the pre-breakdown phenomena in vacuum and some of the factors which affect vacuum breakdown. Since many factors influence vacuum breakdown, no one theory is able to fully explain it. Thus, the understanding

of vacuum is somewhat incomplete, and a number of theories have evolved. The chapter concludes by presenting several of them.

## 10.2 Pre-Breakdown Conduction

The breakdown of a vacuum gap is always preceded by a measurable current, which may take the form of a steady current or pulses, or both. As the voltage is raised, a small gap produces a relatively steady current. The steady current has generally been attributed to field emission at isolated microprotrusions or whiskers. Figure 10-1 shows a sketch of a whisker found by workers using an electron microscope at the U.S. Naval Research Laboratory (Little and Whitney, 1963). Whiskers are not merely surface irregularities; they are much smaller and may cause local fields as high as  $3 \times 10^7$  V/cm (Latham, 1983). The formation of whiskers seems to be the result of applying a high electric field to the electrode surface. Recently, Latham (1983) has proposed an alternative emission mechanism, associated with insulating microinclusions in the cathode surface.

Larger gaps produce small pulses (microdischarges) of current which may transfer microcoulombs of charge and last from 50  $\mu$ sec to several msec. As the gap voltage is increased, the microdischarges may occur by themselves, or they may be superimposed on a steady current. In either case, if the voltage is raised beyond a certain point, the pulses disappear and a steady current is observed (Alston, 1968, p. 60).

The presence of microdischarges is associated with adsorbed material on the cathode surface. Chatterton has shown the



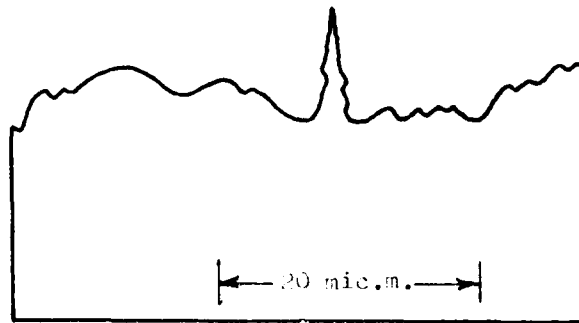


Figure 10-1: Sketch of a cathode whisker formed by a high electric field at the cathode surface.

threshold voltage increases with conditioning of the electrode, which verifies the importance of electrode contamination (Meek and Craggs, 1978, p.151). The frequency of the pulses increases with voltage. Alston (1968, p. 61) reports of an experiment conducted with uniform field, copper electrodes spaced 2 mm apart in a  $10^{-5}$  torr vacuum. The voltage was increased at the rate of 5 KV/minute. At 20 KV, a  $1\mu\text{A}$  current was observed, but at slightly higher voltages, pulses with 200  $\mu\text{A}$  peaks and 50 msec duration occurred. Finally, complete breakdown occurred at 100 KV. Figure 10-2 shows a typical current waveform for a microdischarge between steel electrodes spaced 1.0 mm apart. Also shown is the voltage dip which accompanies the pulse.

The cause of microdischarges is generally agreed to be an exchange of positive and negative ions between the electrodes. However, several possibilities have been suggested as the source of the ions. The theory is similar to the particle exchange theory of breakdown which will be discussed in section 10.4.1.

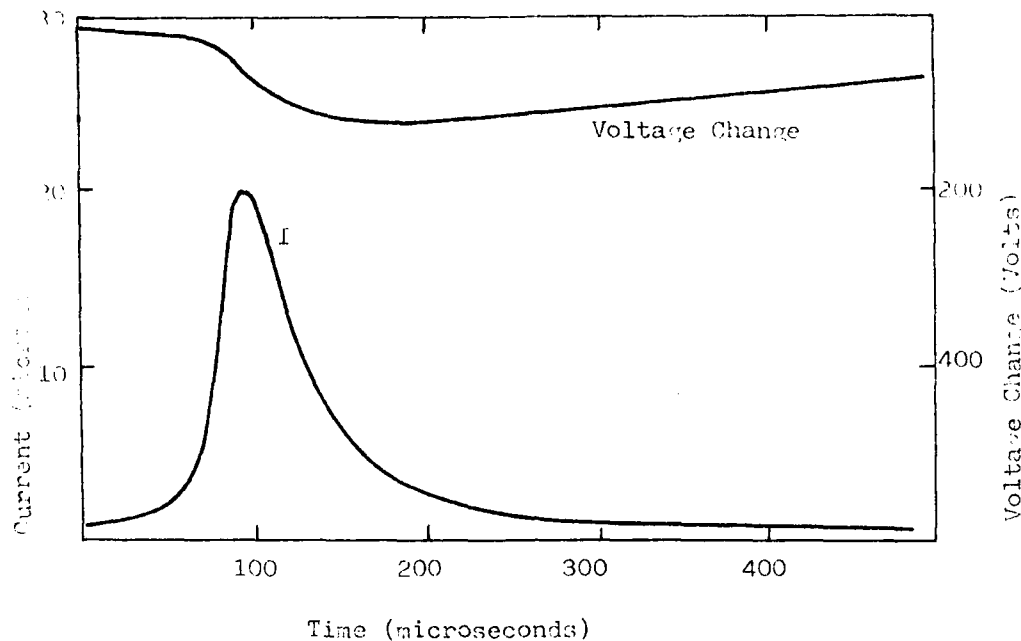


Figure 10-2: Current and voltage waveforms for a 1.0 mm vacuum gap between steel electrodes (after Mulcahy and Bolin, 1971, p. 3-6).

### 10.3 Factors Affecting the Breakdown Voltage

Before examining some of the factors which affect the breakdown voltage, we should define what is meant by breakdown voltage. Ideally, it could be defined, "...as that voltage which, when increased by a small amount, will cause the breakdown of a vacuum gap that has held that voltage for an infinite time" (Alston, 1968, p.69). Actually, conditioning of the electrodes has a significant effect on the breakdown voltage. Some equipment, such as vacuum switchgear, would be rated below the lowest voltage at which breakdown could occur because any breakdown would be disruptive. Other equipment, such as a linear accelerator, may be able to withstand the sparking during the conditioning

process. In those cases, the higher conditioned breakdown rating would be used.

Several factors which influence breakdown will be considered; however, these factors are interdependent. The effect of any one factor is often influenced by the state or condition of other factors. This makes it impossible to establish a simple set of rules which will guarantee a high breakdown voltage. (Mulcahy and Bolin, 1971, p. 4-13)

#### 10.3.1 Electrode Separation

The spacing between electrodes is one of the easiest factors to vary and has been extensively investigated. Research has shown the breakdown voltage is proportional to the gap length for short gaps; that is

$$V_S = Kd \quad (10.1)$$

where  $d$  is the gap length and  $k$  is a constant. For long gaps, however, the voltage is more nearly related to the gap length by

$$V_S = K_1 d^\alpha \quad (10.2)$$

where  $\alpha$  has a value between 0.4 and 0.7 (Mulcahy and Bolin, 1971, p.4-13).<sup>1</sup> Taking the common logarithm of both sides yields

$$\log_{10} V_S = \log_{10} K_1 + \alpha \log_{10} d \quad (10.3)$$

Equation 10.3 is of the form  $y=ax+b$ . Thus, if the breakdown voltage is plotted against the gap length on log-log coordinates, a straight line of slope  $\alpha$  should result. Figure 10-3 shows such a plot for copper and aluminum. In both cases, there is a change

---

<sup>1</sup>This  $\alpha$  should not be confused with Townsend's first ionization coefficient.

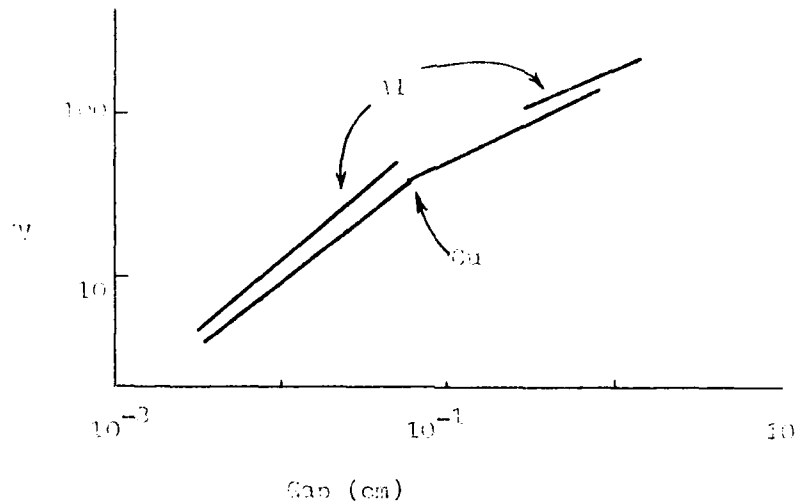


Figure 10-3: Vacuum breakdown voltage as a function of gap length for copper and aluminum electrodes (after Meek and Craggs, 1978, p.130)

in slope in the vicinity of  $d=1$  mm. Denholm, et al (1971, p.361) and Alston (1968, p.65) both put the dividing line between short and long gaps at 1 mm. However, Mulcahy and Bolin (1971, p.4-34) indicate equation 10.1 is valid until  $d=7.5$  mm. In either event, a longer gap tends to breakdown at a lower value of electric field strength than a shorter gap.

#### 10.3.2 Electrode Material, Finish, and Conditioning

As previously mentioned, repeated sparking of a gap will condition the electrodes, resulting in a higher breakdown voltage. Apparently, the sparking results in surface melting and smoothing, as well as the removal of impurities (Meek and Craggs, 1978, p.130). Figure 10-4 shows the change in breakdown voltage

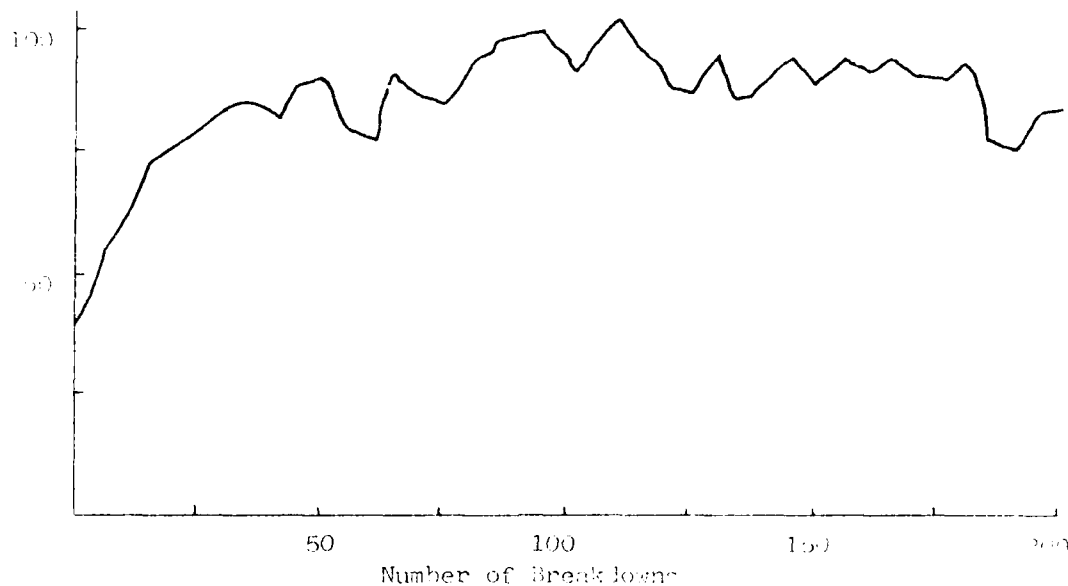


Figure 10-4: Variation of breakdown voltage with the number of breakdowns (Mulcahy and Bolin, 1971, p.4-14)

as a function of the number of breakdowns for a 3/32 inch gap. Note, the average breakdown voltage for shots 50 to 175 is about twice the initial breakdown voltage. Conditioning may take anywhere from 10 to 10,000 sparks depending on the material and other variables (Alston, 1968, p.67).

Not surprisingly, the electrode material has a significant effect on the breakdown voltage. As will be seen in the next section, electrical breakdown in a vacuum depends on phenomena at both electrodes. Thus, the anode material has a greater influence than in gas breakdown. Table 10-1 shows breakdown voltages at  $10^{-5}$  torr for a 1 mm gap between uniform field electrodes of several different materials. These values were obtained after the electrodes were cleaned with a hydrogen glow discharge and

Table 10-1: Vacuum Breakdown Voltages for Several Electrode Materials (Anderson, 1935)

Material	Breakdown Voltage in KV
Steel	122
Stainless Steel	120
Nickel	96
Monel Metal	60
Aluminum	41
Copper	37

spark conditioned. The values in table 10-1 are frequently quoted in texts or articles, sometimes without reference and sometimes referenced to other sources. Anderson (1935) is the original source for these numbers. An approximate ranking of electrode materials from lowest to highest breakdown voltage is: C, Be, Pb, Al, Cu, Ni, Fe, Stainless Steel, Ti, Ta, Mo, and W (Mulcahy and Bolin, 1971, p.4-3). Differences in material used by different investigators probably account for the reversed order of copper and aluminum in this list and table 10-1.

The surface condition and finish of the electrodes may also influence the breakdown voltage in vacuum. It is generally agreed surface contamination may reduce the standoff voltage of a vacuum gap. Contamination may be in the form of oxides, dust, polishing materials, or other organic materials. When copper electrodes are used, oxidation is always present since it forms in 60 msec at  $10^{-5}$  torr and even faster at higher pressures (Alston, 1968,

p.69). If the electrodes are polished, microscopic polishing compound particles may be imbedded in the electrodes. Other organic materials may result if oil diffusion pumps, rubber O-rings, and vacuum grease are used. Figure 10-5 gives an indication of how significant contamination can be. The figure shows the breakdown voltage for dusty electrodes and for electrodes which were wiped with lens paper before pumpdown.

The effects of surface finish are less well established than the effects of contamination. Denholm, et al (1973, p.364) suggest the electrode surfaces should be given a very fine polish to achieve high breakdown strength. Table 10-2 shows breakdown values for three electrodes, of the same material, with different finishes. On the other hand, Mulcahy and Bolin (1971, p.4-3) report breakdown values for electrodes cleaned with 600 grit abrasive paper were indistinguishable from those of electrodes with a 1.0 micron finish. Thus, they conclude, "Surface finish is in itself of minor importance, but can appreciably affect the degree of cleanliness that is achieved."

Table 10-2: Breakdown Voltage for Different Surface Finishes  
(Denholm, et al, 1973, p. 365)

Surface Finish	Breakdown in KV
Electrolytic Polish (8 $\mu$ in rms)	52
Buff Polish (8 $\mu$ in rms)	60
Metallographic (2 $\mu$ in rms)	75

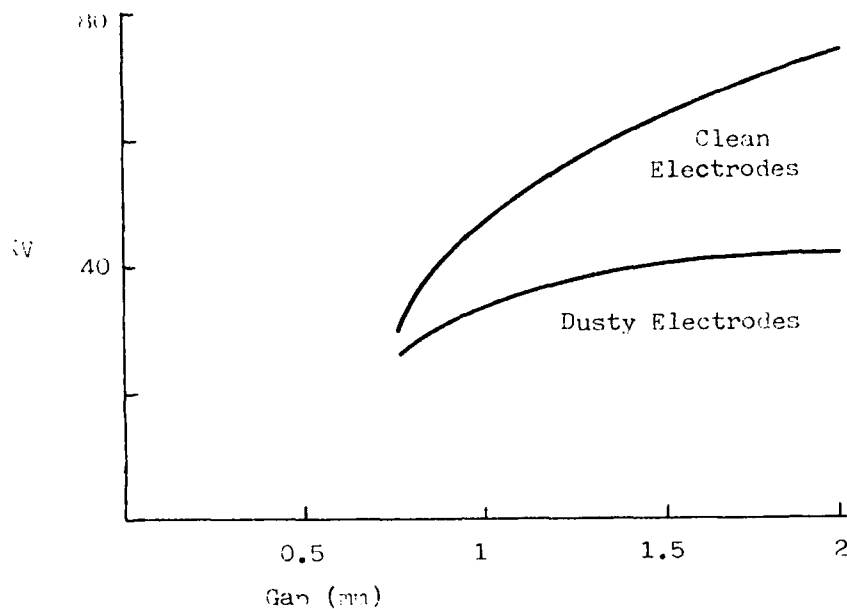


Figure 10-5: Effect of surface contamination on vacuum breakdown voltage (after Denholm, et al, 1973 p. 363).

### 10.3.3 Electrode Area

For reasons which are not yet understood, the breakdown voltage is dependent on the area of the gap. Figure 10-6 (Denholm, et al, 1973, p.371) shows the breakdown voltage as a function of electrode area for stainless steel electrodes, separated by 1 mm. While a 20 cm<sup>2</sup> electrode breaks down at 40 KV, a 1000 cm<sup>2</sup> electrode only withstands 25 KV. The area effect can produce some seemingly anomalous results. In gases, we saw the breakdown voltage was higher for uniform fields than for non-uniform fields. Because of area effects, the opposite can be true in vacuum. When spherical electrodes are used, the breakdown voltage



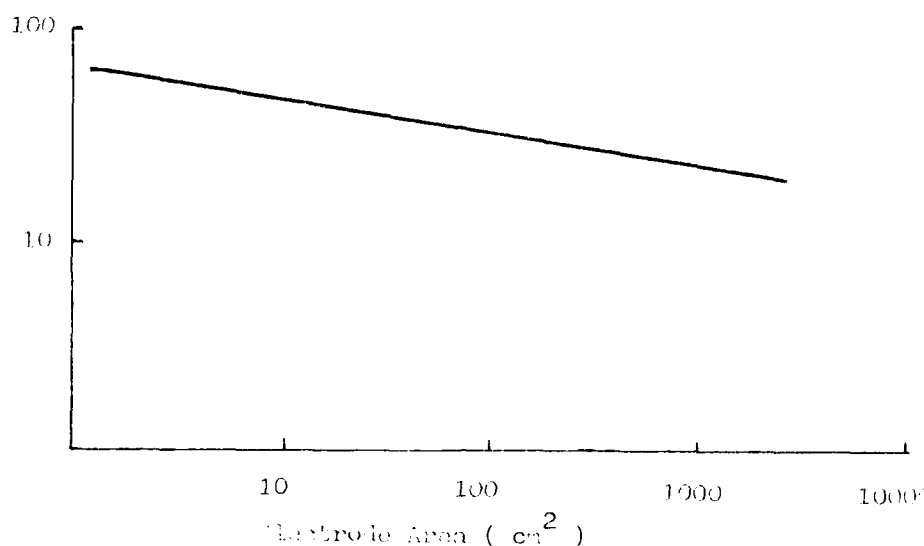


Figure 10-6: Breakdown Voltage vs Electrode Area

increases as the diameter decreases, even though the field becomes more non-uniform. Apparently, the smaller spheres have a smaller effective area, yielding a higher breakdown (Mulcahy and Bolin, 1971, p.4-17).

#### 10.3.4 Time Effects

Most vacuum breakdown studies have been for DC voltages. However, Denholm (1958) studied the impulse and AC breakdown strengths of small gaps with steel electrodes. He reported the breakdown field for DC, AC (50 hz), and 1.2/50 impulse voltages<sup>2</sup>. His field strengths have been converted to breakdown voltages in figure 10-7. The breakdown strength of a gap is seen to be

---

<sup>2</sup>Impulse voltages are characterized by two numbers. The first is the time in usecs for the voltage to reach its peak value; the second is the time in usecs for the voltage to return to 50% of the peak value. See, for example, Greenwood (1971, p.511).

# BREAKDOWN IN VACUUM

207

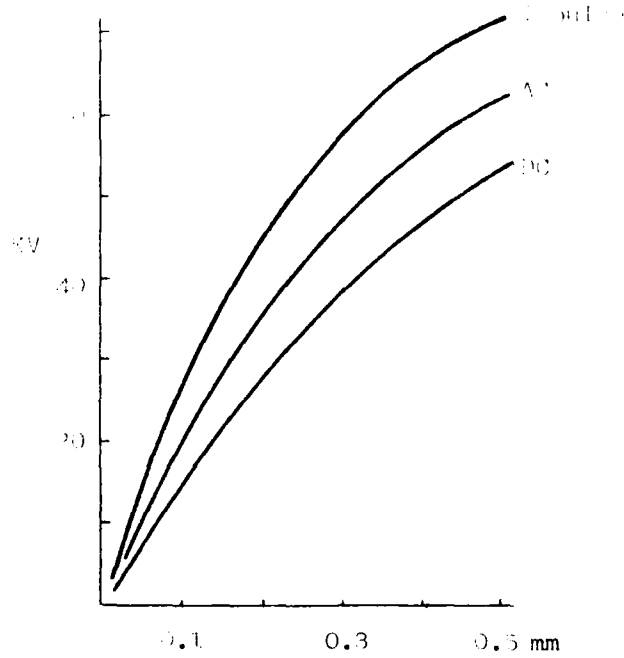


Figure 10-7: Vacuum breakdown voltage as a function of gap length for AC, DC, and 1.2/50 impulse voltages (after Denholm, 1958).

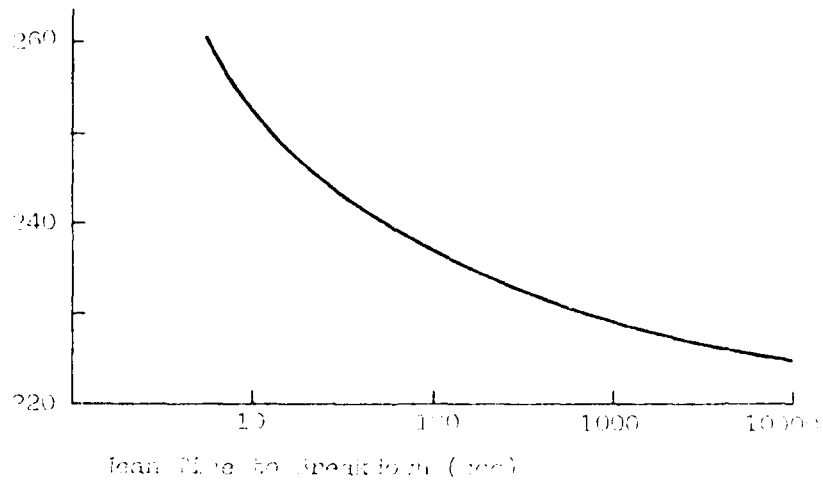


Figure 10-8: Time required for a 7.5 mm vacuum gap to breakdown for a range of applied voltages (after Mulcahy and Bolin, 1971, p. 4-20).

greatest for the impulse and lowest for the DC voltage. This seems to imply a relationship between the breakdown voltage and the amount of time the voltage is applied. Mulcahy and Bolin (1971, p.4-20) investigated the time required for a 7.5 mm gap, with nickel electrodes, to breakdown at various voltages. Their results are shown in figure 10-8. Clearly, the less time the voltage is applied, the higher will be the breakdown voltage.

#### 10.3.4 Other Effects

Under an experimental program sponsored by the Defense Advanced Research Projects Agency and the Army Electronics Command, a variety of factors which influence vacuum breakdown were studied. The results of the study were summarized in a table by Mulcahy and Bolin (1971, pgs. 4-34 to 4-36), which is reproduced here as table 10-3. As previously mentioned, their comments concerning the effects of gap length and electrode surface finish disagree with other published reports.

Table 10-3: Factors and Effects in Vacuum Insulation (after Mulcahy and Bolin, 1971 p. 4-36)

FACTOR	EFFECT ON BREAK-DOWN VOLTAGE (BDV)	INTERACTS WITH	RECOMMENDATIONS
ANODE MATERIAL	Refractory metals have higher BDVs than non-refractory metals.	Conditioning, discharge energy, gas content.	Use refractory metals especially when high energy discharges are to be endured.
CATHODE MATERIAL	Cu better than Al. No significant difference between Ni, Ti, & stainless steel.	Gas content, Anode mat'l. Cathode may become covered with layer of anode material with moderate & high energy discharges.	Some improvement can be obtained with high strength cathode mat'ls.
CONDITIONING	Increases BDV by more than a factor of 2 in most cases.	Discharge energy, anode material.	Conditioning technique is very important. If high-energy discharges are possible, use them. Use good anode mat'l.
GAP	BDV $\propto$ to gap below 0.75 cm, to $\sqrt{\text{gap}}$ above 0.75 cm.	Gas content, polarity.	When appropriate, break a large gap into a series of small gaps.
GEOMETRY OF ELECTRODES	Spherical or curved surfaces better than flat ones. Small area better than large area.	Gas content, polarity.	Use geometries which minimize highly stressed area, even if it increases the maximum E field.

Table 10-3, Continued

FACTOR	EFFECT ON BREAK-DOWN VOLTAGE (BDV)	INTERACTS WITH	RECOMMENDATIONS
SURFACE FINISH	Not significant if surface is reasonably smooth and clean.	contamination	Do not expend effort beyond that which produces a clean and reasonably smooth surface.
GAS CONTAMINATION	Pure gases have a negligible effect, but gases with dust and organic contamination reduce the BDV.	Conditioning. Exposure seldom reduces BDV below unconditioned level.	Avoid exposure to contaminated gases.
MAGNETIC FIELD	Lowers BDV for gaps < 7.5 mm, raises BDV for gaps > 7.5 mm	Gap.	Avoid magnetic field in highly stressed regions.
PROCESSING BAKEOUT	Bakeout increases BDV, improves consistency.	Electrode material and geometry.	Hydrogen or vacuum firing of electrodes can be beneficial. Complete system bakeout is useful
TIME	The longer the period of application of stress the more likely a low breakdown voltage	Conditioning, contamination	Minimize time at highest stress, but do not leave without stress or deconditioning may occur.

Table 10-3, Continued

FACTOR	EFFECT ON BREAK-DOWN VOLTAGE (BDV)	INTERACTS WITH	RECOMMENDATIONS
PREBREAK-DOWN CURRENT	High prebreakdown currents can heat anode & lead to breakdown.	Gap, magnetic field, conditioning, electrode material.	When possible, condition to produce low prebreakdown currents.
DIELECTRIC COATINGS	Cathode coatings can raise BDV significantly.	Polarity--anode coatings usually detrimental; conditioning.	Apply a thin dielectric film to the anode when possible.
PRESSURE	As the glow discharge pressure range is approached, the BDV goes through a maximum.	Geometry, conditioning.	When possible, use "high pressure" operation or conditioning.
ELECTRODE TEMPERATURE	Heated cathodes may raise BDV; heated anodes lower BDV; cryogenic cooling may raise BDV.	Polarity, contamination	More investigation of this factor is required.

#### 10.4 Breakdown Hypotheses

Many hypotheses have been proposed to explain the mechanics of vacuum breakdown. Basically, the mechanisms fall into three categories which will be discussed in this section.

##### 10.4.1 Particle Exchange Hypotheses

This category assumes secondary emission processes result in an exchange of particles (electrons, positive ions, and negative ions) between the electrodes. When the secondary processes become cumulative, breakdown follows. Figure 10-9 shows an electron (in the center) striking the anode. The electron may cause a photon or a positive ion to be released from the anode. Photons and positive ions may strike the cathode, causing secondary electrons, etc. If we let:

- A = number of + ions produced per electron
- B = number of secondary electrons per + ion
- C = number of photons produced per electron
- D = number of electrons per photon

then breakdown would occur when every electron managed to replace itself, or when

$$AB + CD \geq 1 \quad (10.4)$$

Researchers found the product AB was at most about 0.04 and photon effects were unable to make up the difference. Thus, the theory had to be modified.

The theory was modified by assuming negative ions could be ejected from the cathode by positive ion bombardment. This effect was put into the formula by neglecting photons and letting

- G = number of - ions produced per + ion
- H = number of + ions produced per - ion

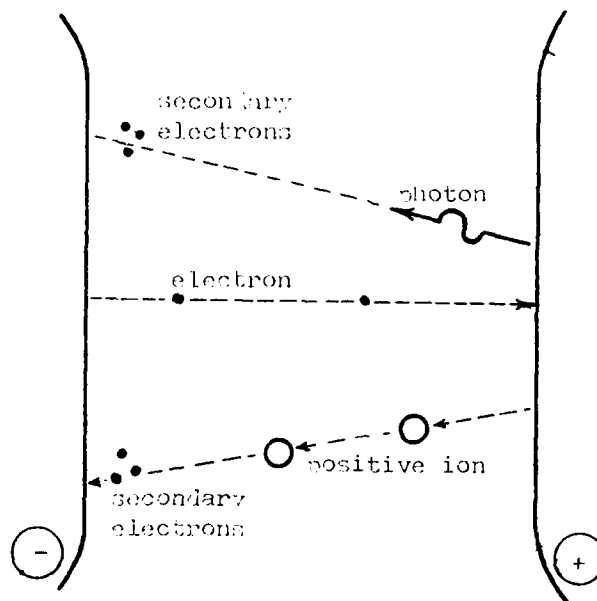


Figure 10-9: Particle exchange mechanism of vacuum breakdown (after Alston, 1968, p. 76).

Breakdown was then assumed to occur when

$$AB + GH \geq 1 \quad (10.5)$$

The modified theory appears to be plausible at voltages above 250 KV (Alston, 1968, p.76).

#### 10.4.2 Electron Beam Hypotheses

These theories assume localized field emission causes heating at one of the electrodes. The heat causes embedded gas molecules to escape, and low pressure gas breakdown follows. The field emission is assumed to be from a whisker like the one shown in figure 10-1. Figure 10-10a shows the electron beam striking the anode, causing heating and vapor release. In figure 10-10b, the current density causes the whisker to heat, releasing gas molecules. Eventually, the whisker melts or explodes. Whether the



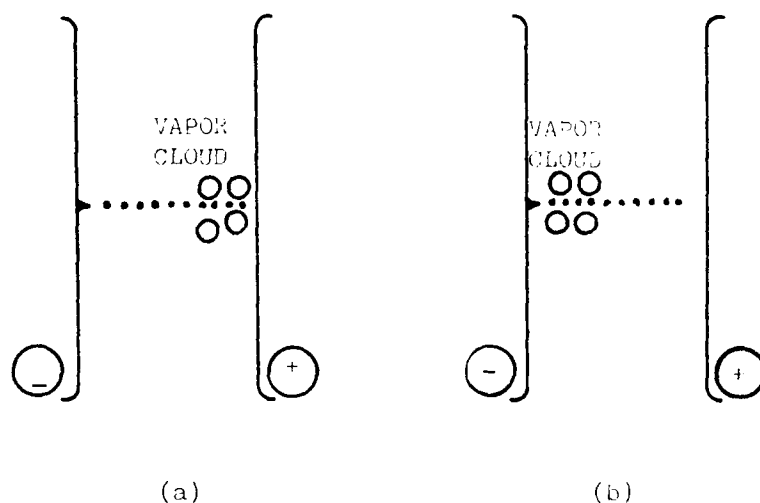


Figure 10-10: Electron beam theory of vacuum breakdown  
 (a) vaporization at the anode  
 (b) vaporization at the cathode  
 (after Alston, 1968 pgs. 77-81)

vapor cloud forms at the anode or the cathode, additional electrons may cause ionization in the gas cloud. The resulting positive space charge may enhance the field, increasing the field emission, and it may cause secondary electron emission by positive ion bombardment.

#### 10.4.3 Clump Hypothesis

This theory assumes a "clump" or aggregate of material could be torn away from an electrode by electrostatic forces. It would then fly across the gap and crash into the opposite electrode as shown in figure 10-11. Upon impact, the clump could break apart or cause gas molecules to be released, forming a vapor cloud. This theory was formulated as early as 1931, and had the

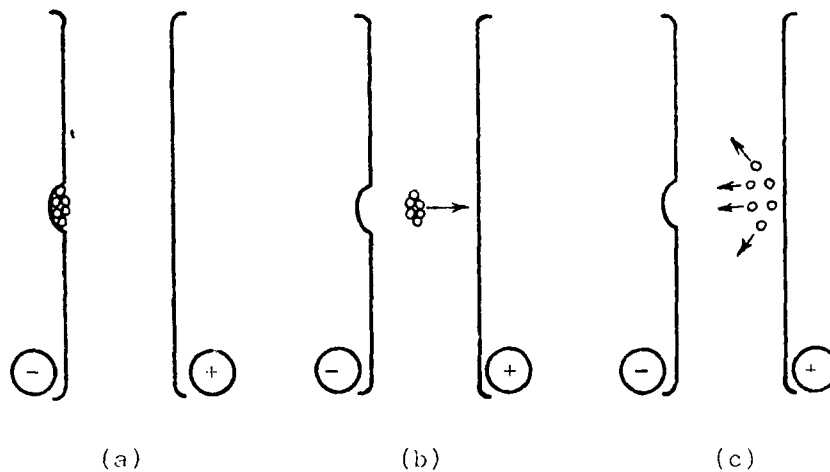


Figure 10-11: Clump hypothesis of vacuum breakdown  
 (a) clump in the anode surface  
 (b) clump flying across the gap  
 (c) clump exploding at cathode surface  
 (after Alston, 1968, p. 82).

advantage of predicting a breakdown voltage proportional to the square root of the gap length (equation 10.2 with  $\alpha=0.5$ ). However, it was 1960 before several Russian researchers actually observed clumps. Even then, breakdown did not occur when the clump was torn away. Further research showed breakdown could be induced by positively charged clumps striking the cathode (Alston, 1968, pgs. 82-85).

#### 10.4.4 Discussion of the Hypotheses

All three theories have some experimental support, and none can explain all the available experimental results. It may be that all the phenomena occur in a given gap, but the exact cause of breakdown is determined by the factors which were summarized

in table 10-3. In particular, there seems to be a change in breakdown mechanism at a critical gap length which varies from 2.0 to 20 mm, depending on the material (Alston, 1968, p.86). Alternatively, combinations of the theories may be required (Mulcahy and Bolin, 1971, p.3-13).

#### 10.5 Summary

Theoretically, vacuum breakdown should be limited only by field emission, but breakdown generally occurs at field levels well below that required for field emission. Breakdown is always preceded by a pre-breakdown current which may be level or pulsing in nature. The breakdown is strongly influenced by many factors including: gap length, electrode material, surface finish and contamination, electrode area and shape, and the nature of the applied voltage.

These factors cause vacuum breakdown to be very different than gas breakdown. For example, the maximum electric field drops as the vacuum gap gets longer, and non-uniform electrodes may breakdown at a higher voltage than uniform electrodes with the same spacing. A number of theories have been proposed to account for vacuum breakdown, and they fall into three general categories. Each has supporting evidence, and each fails to explain some of the available experimental observations. Thus, further research is required to determine when each theory is valid or if a combination of them is required.

## REFERENCES :

- Alston, L.L. (ed.) (1968). High-Voltage Technology. Oxford University Press, London.
- Anderson, H.W. (1935). Electrical Engineering. V. 54, p. 1315.
- Denholm, A.S. (1958). Canadian Journal of Physics. V. 36, p. 476.
- Denholm, A.S., et al (1973). Review of Dielectrics and Switching. US Air Force Weapons Laboratory Technical Report 72-88, Kirtland AFB, NM 87117. DTIC AD# 907739L.
- Greenwood, A. (1971). Electrical Transients in Power Systems. John Wiley & Sons, New York.
- Latham, R.V. (1980). High Voltage Vacuum Insulation. Academic Press, London.
- Latham, R.V. (1983). IEEE Transactions on Electrical Insulation. V. EI-18, p. 194.
- Little, R.L. and Whitney, W.T. (1963). Journal of Applied Physics. V. 34, p. 2430.
- Meek, J.M. and Craggs, J.D. (ed) (1978). Electrical Breakdown of Gases. John Wiley & Sons, Chichester.
- Mulcahy, M.J. and Bolin, P.C. (1971). High Voltage Breakdown Study--Handbook of Vacuum Insulation. US Army Electronics Command Technical Report ECOM-00394-20, Fort Monmouth, New Jersey. DTIC AD # 723107.

THIS PAGE INTENTIONALLY BLANK

## CHAPTER 11

### BREAKDOWN IN LIQUIDS

#### 11.1 Introduction

Liquid dielectrics are frequently used both in pulsed power systems and in power transmission and distribution equipment. They possess certain advantages over other dielectrics. They are much denser than gases, which gives them a higher electric strength. Liquids, being pourable, fill the space to be insulated much more readily than a solid, and they are self-healing, if a discharge does occur. On the negative side, liquids are easily contaminated by condensation, dissolved gases, and by-products of electric discharges.

The understanding of the breakdown process in liquids lags behind that of gases or solids. There are several reasons for this. First, the liquid state is not as simple as the gaseous state, nor is it as ordered as the solid state. Second, there is an immense volume of experimental results available, many of which are conflicting. Often, the experiments were not controlled enough to allow the results to be used in formulating a general theory. For example, many reports and papers deal with various properties of transformer oil, but too often, the transformer oil is an ill-defined mixture of liquids, solids, and gases. Finally, there are as many as one hundred different

liquids which are of possible interest to electrical engineers. Because of the variation in their physical and chemical properties, it is very difficult to develop any general theory. (Schmidt, 1982)

This chapter will provide a brief description of conduction in liquids and an introduction to some of the breakdown theories. Additional sources of information include: Alston (1968, ch. 6 & 7), Kuffel and Abdullah (1971, pgs. 90-96), Denholm, et al (1973, section 5), and Schwinkendorf (1976 a & b). Each of these includes extensive references to the literature.

### 11.2 Conduction in Liquids

If a voltage is applied to a liquid, the current-field characteristic exhibits three regions, as shown schematically in figure 11-1. At low fields (region 1), the current is largely due to dissociation of molecules by cosmic radiation. This current may be of the order of picoamperes. The ionic current reaches a saturation level at intermediate field levels (region 2). At high fields (region 3), the current begins to increase rapidly, by several orders of magnitude. This current increase is due to electron emission from the cathode and possibly some dissociation of the liquid molecules by the electric field. (Alston, 1968, p.114)

Electron emission may be due to field emission or Schottky emission. Near breakdown, experimental evidence seems to indicate that a Schottky-type emission is more plausible (Schwinkendorf, 1976b, p.8). If electron emission is important for

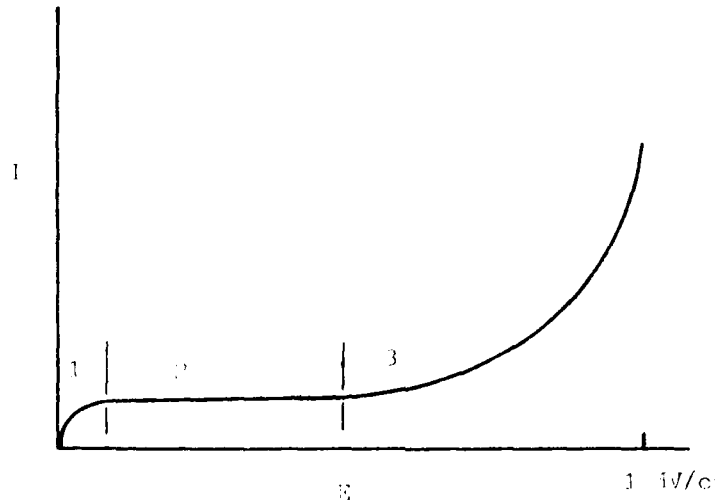


Figure 11-1: Schematic illustration of the increase in current with electric field for a liquid (after Alston, 1968, p. 115).

breakdown, then we would expect the nature of the cathode to be important also.

While the cathode is probably important in the breakdown process, the metal-liquid interface is extremely complex and cannot be easily altered in a controlled manner. Thus, there is a lack of experimental results which demonstrate the effect of the cathode on the breakdown process (Alston, 1968, p.114). There is evidence, however, that the emission process may be very localized. A positive ion or positively charged dust particle may enhance the field as it approaches the cathode. Before being neutralized, one ion or particle may cause an intense stream of electrons to be emitted. The electron



emission, in turn, causes localized heating, vaporization, and bubble formation. The importance of bubbles will be discussed in the next section. (Alston, 1968, p.119)

### 11.3 Breakdown Theories

Electrical breakdown in a liquid involves a transition from a highly insulating liquid in which a small current flows to a spark or arc in a vapor column. When an arc forms in a liquid, several things occur (Alston, 1968, p.129):

1. A relatively large quantity of electricity flows, the exact amount being determined by the external circuit.
2. A bright, luminous path forms between the electrodes.
3. Bubbles are formed by vaporization of the liquid, and solid by-products may form, depending on the chemical nature of the liquid.
4. Small pits form on the electrodes at the site of the arc.
5. A shockwave is transmitted through the liquid and is accompanied by an explosive sound.

The shockwave, mentioned above, is no small concern. The equipment enclosure must have enough structural strength to withstand it. Many a researcher has had to mop up an oil spill because an enclosure was ruptured by the shockwave.

While the general characteristics of liquid breakdown are known, only the insulating oils have been extensively studied. With extremely pure, degassed oil and clean electrodes,

breakdown strengths of about 1 MV/cm have been obtained. In highly purified oil, the breakdown strength shows a small, but definite, dependence on electrode material, and it decreases as the electrode spacing increases. If the oil is degassed, there is no variation of breakdown strength with pressure. However, when gases, like  $N_2$  or  $O_2$ , are in solution, the breakdown strength increases with pressure. (Alston, 1968, p.130)

In a real working environment, elaborate purifying techniques cannot be used on insulating liquids. Thus, there will be impurities in the liquid, and these impurities may determine the breakdown strength more than the liquid itself. These impurities may be gaseous, liquid, or solid in nature, and each type leads to a breakdown theory.

#### 11.3.1 Bubble Breakdown

Gas filled bubbles may form in a liquid for several different reasons, including: gas filled pockets at the electrodes, changes in temperature or pressure, agitation, dissociation by electron collision, and corona type discharges at irregularities on the cathode. Once a bubble forms, two factors are of concern. First, the dielectric constant of the gas will be lower; thus, the gas will be more highly stressed than the liquid (recall equation 2.8). This may result in breakdown (partial discharge) of the bubble which may cause more gas to form (Alston, 1968, p.130). Second, a bubble will tend to elongate in the direction of the field. As it does so, it may reach a point where its dimensions and pressure result in break-

down (Kuffel and Abdullah, 1971, p.93). Eventually, the bubble may bridge the gap, in which case breakdown will occur quickly.

Alston, (1968, p.131) has shown photographic evidence of a bubble forming and growing until breakdown occurred. Theoretical expressions have been derived for the breakdown strength of bubbles, but the values calculated do not agree very well with experimental results (Kuffel and Abdullah, 1971, p.93).

#### 11.3.2 Liquid Globule Breakdown

If a globule of another liquid, such as water, is in suspension in the insulating liquid, breakdown may be caused by instability of the globule in the electric field. The effect is similar to that of the gas bubble. The electric field causes the globule to elongate in the direction of the field. Eventually, it may provide a low conductivity path leading to complete breakdown. Alston (1968, p.135) suggests, at a field strength of 1 MV/cm, about  $10^7$  molecules would be required for the elongation to occur. That number of molecules would occupy a sphere with a radius of about 0.05  $\mu\text{m}$ . He also shows photographs of breakdown in silicone due to a water globule.

#### 11.3.3 Solid Particle Breakdown

Solid particles may be in suspension in a liquid insulator. If the dielectric constant of the solid,  $\epsilon_s$ , is different than that of the liquid,  $\epsilon_l$ , the particle will become polarized, and will experience a force in a non-uniform field. Usually,  $\epsilon_s > \epsilon_l$ , and the force will move the solid toward the maximum field region. Thus, particles may become aligned, forming a

bridge across the gap. Breakdown may then occur along the liquid-solid interface.

These three theories all assume the presence of impurities in the liquid. A fourth theory--electronic breakdown--postulates breakdown by collisional processes.

#### 11.3.4 Electronic Breakdown

Once an electron has been emitted from the cathode, it will be accelerated by the electric field. The electronic breakdown theory assumes some of the electrons gain enough energy to ionize a liquid molecule by collision. If the field is high enough, then an avalanche or streamer might form. This theory accounts for the emission of light before breakdown and predicts the branching of the arc which is often observed (Budenstein, 1974, p.34). However, it predicts a formative time lag which is much shorter than is normally observed (Kuffel and Abdullah, 1971, p.92).

#### 11.4 Summary

Liquid dielectrics are frequently used in pulsed power and power systems equipment. Liquids are relatively easy to work with, offer fairly high breakdown strengths, and are self-healing when a discharge does occur. However, due to the complexity of the liquid state and the metal-liquid interface, the theoretical understanding of liquid breakdown lags behind that of the other types of dielectrics. The theories of breakdown fall into two areas--formation of a streamer by electron collisions and breakdown due to impurities in the liquid.

Impurities may dominate the performance of the liquid, so it is possible that electronic breakdown can only be observed in very pure liquids.

#### REFERENCES :

- Alston, L.L. (ed.) (1968). High-Voltage Technology. Oxford University Press, London.
- Budenstein, P.P. (1974). Impulse Breakdown in Vacuum, Gases, Liquids, and Solids with Large Electrode Separation. US Army Missile Command Technical Report RG-75-32, Redstone Arsenal, Alabama. DTIC AD # B003478L.
- Denholm, A.S., et al (1973). Review of Dielectrics and Switching. US Air Force Weapons Laboratory Technical Report 72-88, Kirtland AFB, NM 87117. DTIC AD# 907739L.
- Kuffel, E. and Abdullah, M. (1971). High Voltage Engineering. Pergamon Press, Oxford.
- Schmidt, W.F. (1982). IEEE Transactions on Electrical Insulation. V. EI-17, p. 478.
- Schwinkendorf, W.E. (1976a). Review of Electrical Breakdown Processes in Water. US Air Force Weapons Laboratory Technical Report 76-110, Kirtland AFB, New Mexico. DTIC AD # B015794L.
- Schwinkendorf, W.E. (1976b). Study of Conduction and Electrical Breakdown of Dielectric Liquids. US Air Force Weapons Laboratory Technical Report 76-112, Kirtland AFB, New Mexico. DTIC AD # B016014L.

## CHAPTER 12

### BREAKDOWN IN SOLIDS

#### 12.1 Introduction

Solid dielectrics offer very high electric breakdown strengths as well as structural strength. However, they are more expensive, and they are not self-healing--breakdown through a solid is catastrophic. Thus, solid insulation is used where the conductors or electrodes must be close together or must be supported. Examples include underground transmission and distribution lines, which are usually used only in cities; energy storage capacitors, where a thin dielectric is required to obtain a high value of capacitance; and transformers. Because there is a wide range of applications for solid dielectrics, a great deal of research into their properties has been conducted over the past 60 years, or so. While this research has resulted in a basic understanding of the breakdown processes in solids, there are a number of theories, and none explain all the phenomena.

An ideal solid insulator has no conductive elements, no voids or cracks, and has uniform dielectric properties. Practical materials have conductive inclusions, voids, and thickness variations; and their composition may vary from batch to batch (Dunbar and Seabrook, 1976, p.38). Several properties of interest for solid insulators are shown in table 12-1. Some

Table 12-1: Properties of interest for solid insulation  
(after Denholm, et al, 1973, p.301)

ELECTRICAL PROPERTIES	MECHANICAL PROPERTIES	THERMAL PROPERTIES
Electric strength	Tensile, shearing, compressive, and bending strengths	Conductivity
Surface breakdown strength	Elastic moduli	Expansion
Tracking resistance	Hardness	Primary creep
Volume and surface resistivities	Impact and tearing strengths	Thermal decomposition
Permittivity	Viscosity	Plastic flow
Loss angle	Extensibility	Spark, arc, and flame resistance
Insulation resistance	Flexibility	Temperature coefficients
Frequency effect	Machinability	Melting point
Discharge resistance	Fatigue	Pour point
	Abrasion resistance	Vapor pressure
	Stress crazing	
	Bonding ability	
	Processing tech- niques available	

Table 12-1, Continued

CHEMICAL PROPERTIES	MISCELLANEOUS PROPERTIES
Electrochemical stability	Density
Solubility	Refractive index
Solvent crazing	Transparency
Resistance to reagents	Color
Compatibility with other materials	Porosity
Aging and oxidation stability	Permeability
	Moisture sorption
	Surface absorption of water
	Resistance to fungi
	Resistance to light and fungi
	Cost
	Radiation resistance
	Consistency



of these properties may be more important than the breakdown strength for a particular application, and table 12-1 could serve as a checklist when comparing different materials.

Denholm, et al (1973, p.340) expressed the difficulties which may be encountered when working with solid insulators:

...the design of solid insulation in systems is not a straightforward matter. The starting point is normally the technical requirements and constraints. These include some of the following: working voltage and waveshapes, dimensions, life, weight, temperature, environment, and cost. Many materials will be ruled out at this point by difficulties either in mechanical support or lack of availability in the required geometry....The next step is perhaps to examine which materials can operate at the necessary stress to give the required life. This is difficult since seldom will appropriate data be available....Thus one must search the literature for test data obtained under conditions near to those of the problem and then make intelligent adjustments....There is a marked absence of high-voltage solid dielectric information in the literature...the most useful data to the pulse power designer is that contained in the unpublished work<sup>1</sup> of J.C.Martin et al, at the U.K. Atomic Weapons Research Establishment, Aldermaston, England. His memoranda include much information on several plastics (mylar, polyethylene, lucite, polypropylene) at high voltages and stresses for volumes up to tens of liters.

In this chapter, we will look briefly at the mechanisms of breakdown in solids and some of the factors which affect it. Sources of additional information include the two references cited above, two books by O'Dwyer (1964, 1973), and Alston (1968, ch. 8 & 9).

---

<sup>1</sup>Author's Note: several of these reports are contained in the Air Force Weapons Laboratory Pulsed Electric Power notes, which are available from DTIC

## 12.2 Breakdown Mechanisms

The breakdown strength of a solid varies with the amount of time the voltage is applied. Figure 12-1 shows this relationship in schematic form. The time axis is logarithmic and runs from nanoseconds to many years. As indicated on the figure, different regions of the curve are associated with different types of breakdown. We will briefly consider each type of breakdown in this section.

### 12.2.1 Intrinsic Breakdown

The intrinsic electrical strength of a solid is something of an ideal concept--breakdown will normally occur well below it. Early attempts to measure the intrinsic strength gave misleading results due to secondary effects. Typical values of intrinsic strength for some of the plastics and synthetic insulators range from 5 to 10 MV/cm (Denholm, et al, 1971, p.305). O'Dwyer (1964, p.3) characterizes intrinsic breakdown as:

1. Occurring at low temperatures, often at or below room temperature
2. Being independent of the size and shape of the sample and of the material and configuration of the electrodes
3. Occurring in a time of  $10^{-8}$  to  $10^{-6}$  seconds.

The intrinsic breakdown is related to the physical structure and temperature of the material. Because it occurs so quickly, intrinsic breakdown is generally assumed to be electronic in nature. There will be some free electrons in an

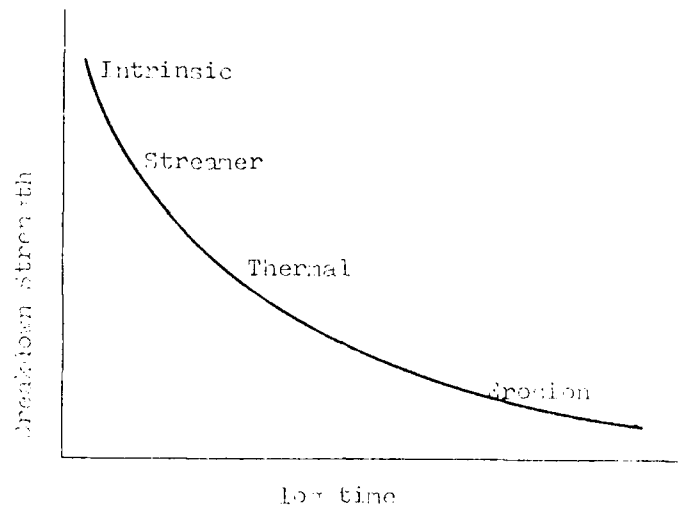


Figure 12-1: Schematic illustration of the variation of the breakdown strength of a solid as a function of the time the voltage is applied (after Kuffel and Abdullah, 1971 p.79).

insulator due to impurities, vacant lattice positions, thermal excitation, etc. These electrons will be accelerated by an external electric field, and will collide with molecules in the lattice. If the field is high enough, a large number of electrons may move across the forbidden gap from the valence band to the conduction band (Denhom, et al, 1973, p. 303). This process happens very suddenly, and causes breakdown (O'Dwyer, 1964, p.59).

#### 12.2.2 Electromechanical Breakdown

If a solid insulator supports a pair of electrodes, surface charges will form at the boundaries when an electric field is applied. These surface charges cause an electrostatic force

which compresses the dielectric. If the compression is too high, the dielectric may fail mechanically. Alternatively, the thinning of the dielectric may cause the electric field to increase beyond the failure point. This effect worsens as the material heats up and becomes soft. Polyethylene, for example, may fail mechanically around 40°C.

### 12.2.3 Avalanche or Streamer Breakdown

Avalanche or streamer breakdown is related to intrinsic breakdown. The theory is similar to gas breakdown--a single electron can be accelerated to cause ionization by collision, resulting in an exponential buildup of electrons. O'Dwyer (1964, p.4) characterizes avalanche breakdown as:

1. Occurring at low temperatures
2. Occurring only in thin slabs of dielectrics having very low electrical conductivities and very high breakdown strengths
3. Occurring at an electric field strength which changes with slab thickness
4. Producing noisy pre-breakdown currents when the voltage is slowly applied, and having considerable statistical variation of breakdown time when sudden overvoltages are applied

The avalanche theories combine some of the aspects of intrinsic breakdown with some of those of thermal breakdown.

#### 12.2.4 Thermal Breakdown

Some current flows in a dielectric when an electric field is applied. This current causes heat, some of which is dissipated and some of which raises the temperature of the material. There are also other heat sources, such as partial discharges and hot metal conductors in the vicinity. The heating causes more free electrons and more current. If the heat builds up at some point in the dielectric, a condition of thermal runaway can occur. For gradually applied voltages, O'Dwyer characterizes thermal breakdown as:

1. Occurring at high temperatures
2. Being dependent on the dielectric size and shape and the geometry and thermal properties of the electrodes
3. Requiring a time to develop of at least a few milliseconds, but usually much longer
4. Exhibiting lower breakdown strength for AC than DC, due to hysteresis losses in the dielectric.

Calculations have shown the maximum field strength for thermal breakdown drops with increasing material thickness, and thicknesses greater than 10 cm are of little electrical benefit (Denholm, et al, 1973, p. 314).

#### 12.2.5 Erosion Breakdown

As previously discussed in section 8.5, there will usually be small voids in a solid dielectric. These voids are typically filled with gas, which has a lower dielectric strength than the solid. Thus, the void receives a disproportionate share

of the voltage drop and may actually breakdown. Continued breakdown of the void may result in local heating and deterioration of the solid. This can cause the void to expand, and eventually, breakdown of the complete dielectric occurs. This can be accentuated in an AC system, because the void may breakdown several times during each cycle of voltage.

### 12.3 Factors Affecting Breakdown

Table 12-2 (Denholm, 1973, p.317) lists several factors which affect the breakdown voltage of solids. Further discussion of these effects and a variety of data for specific materials are available in the reference.

Table 12-2: Factors Affecting The Breakdown Voltage of Solids

FACTOR	COMMENT
Time at Stress	Small reduction in stress often increases life considerably
Insulation Thickness	In practice, operating stress is usually decreased for thicker sections.
Area and Volume	An increase in area (or volume) by $10^3$ reduces stress by factor 2 (typically)
Environment	Can result in failure by tracking, chemical deterioration, thermal breakdown, radiation effects
Waveform	Peak to peak voltage important
Polarity	Point to plane: negative breakdown voltage greater than positive for most solids

12.4 Summary

Solid dielectrics are used where the space for the dielectric is limited. Although they are capable of withstanding very high voltages, solids are not self-healing. The breakdown process in solids is a function of the amount of voltage which is applied and the time for which it is applied.

This chapter has presented only the basics of the areas which were covered, but hopefully, it has inspired the reader to delve more deeply into some of them.

**REFERENCES :**

- Alston, L.L. (ed.) (1968). High-Voltage Technology. Oxford University Press, London.
- Denholm, A.S., et al (1973). Review of Dielectrics and Switching. US Air Force Weapons Laboratory Technical Report 72-88, Kirtland AFB, NM 87117. DTIC AD# 907739L.
- Dunbar, W.G. and Seabrook, J.W. (1976). High Voltage Design Guide for Airborne Equipment. US Air Force Aero-Propulsion Laboratory Technical Report 76-41, Wright-Patterson AFB, OH 45433.
- O'Dwyer, J.J. (1964). The Theory of Dielectric Breakdown of Solids. Clarendon Press, Oxford.
- O'Dwyer, J.J. (1973). The Theory of Electrical Conduction and Breakdown in Solid Dielectrics. Clarendon Press, Oxford.
- US Air Force Weapons Laboratory. (1973) Pulsed Electrical Power Dielectric Strength Notes, PEP 5-1. AFWL-TR-73-167. Kirtland AFB, New Mexico. DTIC AD# 921128L.

## APPENDIX

## USEFUL CONSTANTS AND CONVERSION FACTORS

Constants

Avogadro's number:	$6.023 \times 10^{23}$ molecules/gr-mole
Boltzmann constant (k):	$1.381 \times 10^{-23}$ J/°K
Electron charge:	$-1.602 \times 10^{-19}$ coulomb
Electron mass:	$9.110 \times 10^{-31}$ kg
Gas volume:	22.414 liters/mole (760 torr, 0°C)
Loschmidt number:	$2.687 \times 10^{25}$ molecules/m <sup>3</sup> (at 760 torr, 0°C)
Permittivity of free space ( $\epsilon_0$ )	$8.854 \times 10^{-12}$ F/m
Permeability of free space ( $\mu_0$ )	$4\pi \times 10^{-7}$ H/m
Plank constant (h)	$6.624 \times 10^{-34}$ J-sec
Proton mass	$1.673 \times 10^{-27}$ kg
Stefan-Boltzmann constant ( $\sigma$ )	$5.67 \times 10^{-8}$ W/m <sup>2</sup> (°K) <sup>4</sup>
Universal gas constant (R)	8.314 J/(mole-°K)



Conversion FactorsEnergy

$$1 \text{ eV} = 1.602 \times 10^{-19} \text{ J}$$

$$1 \text{ calorie} = 4.18 \text{ J}$$

Length

$$1 \text{ Angstrom (A)} = 10^{-10} \text{ m}$$

Power

$$1 \text{ Hp} = 746 \text{ watts}$$

Pressure

$$1 \text{ torr} = 1 \text{ mm Hg}$$

$$1 \text{ atmosphere} = 760 \text{ torr}$$

$$1 \text{ atmosphere} = 1.013 \times 10^5 \text{ Nt/m}^2$$

## INDEX

- Abnormal glow 142, 150, 153
- Absorption coefficient 64
- Ambipolar diffusion 77, 78, 147
- Anode dark space 145
- Anode directed streamer 130
- Anode drop, arc 180
  - glow 147
- Anode glow 145, 147
- Anode phenomena, arc 186-188
  - glow 147
- Arc 143, 177-194
  - AC 190-192
    - anode drop 180
    - anode phenomena 186-188
    - cathode 182-185
      - current density 177
      - emission 184
      - fall 177, 183
      - phenomena 185
      - spot 183, 184
    - formation in liquid 222
    - high pressure 179, 180
    - low pressure 180
    - methods of formation 177, 178
    - positive column 177, 179, 185, 186
    - reignition 190
    - temperature characteristic 181
    - volt-ampere characteristic 182
- Area effect, vacuum breakdown 205
- Aston dark space 145, 148
- Atom-atom collisions 60
- Attachment 46, 58, 62, 162-165, 170, 171
- Avalanche, electron 108-110, 117, 119
- Average velocity 31
- Balmer series 3, 37, 38
- Bohr theory 36
- Boltzmann equation 30
- Brackett series 37, 38
- Breakdown voltage 107, 114, 120-125, 136
- Bubble breakdown 174, 223
- Burst corona 167-169
- Capacitive energy storage 10-12
- Cathode 182-185
  - arc current density 177, 180, 184
  - dark space 145
  - directed streamer 128
  - effect on gas breakdown 124
  - effect on liquid breakdown 221
  - fall
    - arc 177, 180, 183
    - glow 150-153
  - glow 145, 146
  - phenomena 182-185
  - spot 183, 184
- Collisions 45, 114
  - cross-section 48, 51
  - elastic 46
  - exciting 46
  - frequency 54, 58
  - inelastic 46
  - ionizing 46, 62, 113, 186
  - molecular 59, 127
  - probability of 49, 50, 53
  - radiative 46
  - superelastic 46
- Column, positive
  - arc 177, 185, 186
    - high pressure 179, 180
    - low-pressure 180
  - drop 180
- Concentration gradient 75
- Conditioning of electrodes 199, 201
- Corona 46, 136, 143, 157-176
  - audio phenomena 157, 173
  - burst pulses 167-169
  - control 173
  - detection 173
  - negative 157, 159-165
  - offset voltage 158, 166, 168
  - onset voltage 158, 168

- Corona
  - partial discharge 174, 175, 223
  - positive 157, 166-172
  - radio interference 157, 173
  - space charge 162-165, 170, 171
  - streamers 168, 171
  - Trichel pulses 159, 171
  - visual phenomena 157, 165, 172
- Crookes dark space 145, 146
- Cross section
  - attachment 58
  - elastic 49
  - exciting 56
  - inelastic 49
  - photoabsorption 64, 65
  - total collision 48, 51
- Current density
  - arc 177, 180, 184
  - glow 150-153
- Dark discharge 107
- Dark space
  - anode 145
  - Aston 145, 145
  - cathode 145
  - Crookes 145, 146
  - Faraday 145, 146, 148
  - Hittorf 145
- Deionization 66
- Diffusion 75, 76, 146
  - Ambipolar 77, 78, 147
  - coefficient 75, 76
  - deionization by 66
- Discharge
  - appearance 144, 165, 172
  - non-self-sustained 105, 107
  - self-sustained 102, 105, 107, 110, 116
  - Townsend 107, 108, 141
- Distortion, space charge 22, 23, 110, 162-165, 170, 171
- Distribution function
  - Fermi-Dirac 82-84
  - Maxwell-Boltzmann 27, 30-32, 61, 82
- Drift velocity 71-74, 76, 108, 147
- Einstein
  - photoelectric equation 97
  - relation 76
- Elastic collisions 46
- Electrodes 69, 108, 141
  - Conditioning 199, 201
- Electron
  - attachment 46, 58, 62, 162-165, 170, 171
  - avalanche 108-110, 117, 119
  - bombardment 82, 99
  - diffusion 75, 76, 146
  - emission--see emission, electron
  - field intensified ionization 109, 166
  - mobility 59, 69-75, 110
  - temperature 180
- Electronegative gases 58
- Emission, electron
  - electron bombardment 82, 99
  - field 81, 94, 95, 184, 195, 213, 220
  - ion bombardment 82, 101, 116, 127
  - photoelectric 82, 95-97
  - Schottky 81, 92, 93, 220
  - secondary 98, 107, 116, 127, 212
  - thermionic 81, 91-93, 177, 184
- Energy 5-7
- Energy level diagrams
  - hydrogen atom 39
  - solids 87, 89
- Excitation 54, 55
- Exclusion principle 83, 84, 105
- Faraday dark space 145, 146, 148
- Fermi-Dirac distribution 82-84
- Fermi level 84, 86, 91
- Field distortion, space charge 22, 23, 110, 162-165, 170, 171
- Field emission 81, 94, 95, 184, 195, 213, 220
- Flashover 136, 137
- Forbidden band 87
- Formative time lag 127, 130, 225

- Fowler-Nordheim equation 94, 195  
Free path 52  
  distribution 52  
  mean 53, 60, 113, 114, 195  
Gap length 111, 150, 200  
Gas 44, 108, 141  
  density 28  
  pressure 33-35, 44, 108, 148  
  temperature 33, 44, 61  
Geiger counter regime 167  
Glow discharge 141-156  
  abnormal 142, 150, 153  
  anode 147  
  cathode 150-153  
  dark spaces 144-148  
  normal 142, 150, 153  
  positive column 145, 147, 150  
  visual appearance 2, 143  
Grid electrode 153-155  
Heat loss, arc 185  
Heisenberg uncertainty principle 83  
Hittorf dark space 145  
Hydrogen  
  energy levels 39  
  spectral series 37, 38  
Inductive energy storage 12, 13  
Inelastic collisions 46  
Ion attachment 46, 58, 62, 162-165, 170, 171  
Ionization 54  
  electron collision 46, 62, 113, 186  
  energy 41, 62, 124  
  field intensified 109, 166  
  multiple 57  
  photo-ionization 62, 64, 97, 105, 129, 130, 171  
  potential 40, 41, 61, 62, 113  
  probability of 55, 114  
  strongly 62  
  thermal 61, 185  
  weakly 62  
Kinetic theory 26  
Liquid breakdown 219-226  
  electronic 225  
  gas bubbles 223  
  liquid globules 224  
  saturation current 220  
  solid particles 224  
Losses, positive column 185  
Lyman series 37, 38  
Maxwell-Boltzmann distribution 27, 30-32, 61, 82  
Mean free path 53, 195  
  electrons 53, 113, 114  
  molecules 60  
Metastable atoms 116, 124  
Mobility  
  electrons 59, 69-76, 110  
  ions 59, 76, 110  
Multiple dielectrics 23-25  
Multiplication of electrons in fields 109  
Multiply charged ions 57  
Negative corona 159-165  
Negative glow 145, 146, 148  
Negative ions 46, 58, 62, 162-165, 170, 171  
Non-uniform field breakdown 133, 136  
Normal cathode fall 150-153  
Orbits, hydrogen 38  
Overvoltage, determines applicable breakdown mechanism 131  
Oxide layer on electrodes 203  
Partial discharge 174, 175, 223  
Particle density 28  
Paschen's law 120, 122, 130, 151, 154, 195  
Paschen series 37, 38  
Pauli exclusion principle 83-85  
Penning effect 124, 125  
Pfund series 37, 38  
Photoelectric emission 82, 95, 105  
Photoelectric work function 86, 90, 97  
Photo-ionization 62, 64, 97, 105, 129, 130, 171  
Plasma 147  
Point gap, breakdown curve 135

- Polarity effects, breakdown 133, 134
- Positive column
  - arc 177, 185, 186
  - glow 145, 147-150
- Positive corona 166-172
- Positive ion bombardment 82, 101, 116, 127
- Potential barrier 88, 90
  - energy diagram 89
- Power 7-9
- Pressure 33-35, 44, 108, 48
- Probability of
  - collision 49, 50, 53
  - excitation 55
  - ionization 55, 56, 114
- Quantum of energy 37, 62, 97
- Radial temperature distribution 187
- Radiation 105
- Ramsauer effect 51
- Recombination 66
- Recovery voltage 190
- Reduced pressure 53
- Refractory electrodes 183, 184
- Reignition voltage 190
- Richardson-Dushman equation 91
- RMS velocity 33
- Rod gap, breakdown curve 135
- Saha's equation 61
- Saturation current 92, 107, 117, 220
- Schottky
  - emission 81, 92, 220
  - equation 92
- Series, hydrogen atom 37, 38
- Solid breakdown 227-236
  - factors affecting (table) 235
  - mechanisms
    - avalanche 233
    - electromechanical 232
    - erosion 234
    - intrinsic 231
    - thermal 234
  - properties (table) 228-229
- Space charge effects 22, 23, 110, 162-165, 170, 171
- Spark 107, 141
- Sparking potential 107, 108, 120-125
- Sphere gap 136, 205
- Sputtering 101
- Statistical time lag 127
- Streamer 128
  - anode directed 130
  - cathode directed 128
  - in positive corona 168-171
- Surface flashover 136, 137
- Switch
  - closing 12
  - opening 13
- Temperature 33
  - arc column 180, 187
  - electrode 183, 184
  - electron 78, 180
  - gas 44, 61, 180
  - ion 78, 180
- Thermal equilibrium 185
- Thermal ionization 61, 185
- Thermionic emission 81, 91-93, 177, 184
- Thermionic work function 86, 90
- Townsend
  - discharge 107, 108, 141
  - first ionization coefficient 108, 109, 124, 132
  - second ionization coefficient 115-119, 132
- Trichel pulses 159-165
- Ultraviolet light, irradiation 98, 105
- Uncertainty principle 83
- Vacuum applications 196
- Vacuum breakdown 195-217
  - breakdown hypotheses
    - clump 214
    - electron beam 213
    - particle exchange 212
  - conditioning effect 199, 201
  - electrode effects
    - area 205
    - finish 203
    - material 202
  - formation of whiskers 197
  - gap length effect 199
  - pre-breakdown current 197

Vacuum breakdown  
  table of factors affecting  
    209-211  
  time effect 206  
Velocity  
  distribution 28  
  mean 31  
  most probable 31  
  RMS 33  
  
Work function 88  
  photoelectric 86, 90, 97  
  thermionic 86, 90  
  
X-rays 97